

Stellingen

behorende bij het proefschrift

*Estimation of Detector Responses
by Midway Forward and Adjoint Monte Carlo Coupling
in Nuclear Systems*

door Igor V. Serov

1. Vergroting van het aantal detectoren, waarvan de responsie moet worden bepaald, leidt alleen tot vermindering van de efficiëntie van de midway Monte-Carlomethode, als de bovengenoemde detectoren zich in verschillende omgevingen bevinden.

Dit proefschrift, hoofdstuk 6 en hoofdstuk 7

2. Accurate informatieanalisten zouden voorkeur voor de Monte-Carlomethode moeten hebben, aangezien deze naast nauwkeurige resultaten ook de onzekerheden ervan levert. Voor verdere analyses en gevolgtrekkingen zijn de laatste even belangrijk als de eerste.

Dit proefschrift, hoofdstuk 1

3. Integralen van diverse eigenfuncties van de transportvergelijking worden in nodale reactorfysische methodes¹ als parameters gebruikt. Eén Monte-Carloberekening is voldoende om alle benodigde integralen in één reactornode te bepalen. Daarvoor moet men verschillende scoringsalgoritmen gebruiken.

¹ R.D. Lawrence, "Progress in Nodal Methods for the Solution of the Neutron Diffusion and Transport Equations," *Prog. Nucl. Energy*, **17**, 3, 271 (1986)

4. Monte-Carlosimulaties waarbij pseudodeeltjestransport wordt toegepast voor zo genoemde "next-event"-schaters^{2,3} maken deze methode van variantiereductie inefficiënt in problemen, waar meer dan één detectorresponsie bepaald moet worden.

² M.H.Kalos, "On the estimation of flux at a point by Monte Carlo", *Nucl. Sci. Eng.*, **16**, 111, (1963)

³ T.M.Booth, "A Sample Problem for Variance Reduction in MCNP", LA-103363-MS, (1985)

5. Zonder twijfel verlengt de beschaving het menselijke leven. Maar zij creëert ook nieuwe gevaarbronnen. Middelen worden niet alleen direct aan verlenging van menselijke leven besteed, maar ook aan ontwikkeling van beschermende maatregelen tegen nadelige gevolgen van de gevaarbronnen, welke maatregelen onvervreemdbare elementen van de beschaving worden⁴. Hier dient het worden toegevoegd, dat een beschermende maatregel optimaal is, wanneer iedere verandering meer levens kost dan zij redt.

⁴ A.H.Holi, "Population and Society" in "Problems of Population", *Progress*, p.229, (1977)

6. Succesvolle verspreiding van vervalsingen en onzinnigheden gepubliceerd⁵ door "one of the first nuclear physicists" en "a medical doctor" over straling en behandeling van stralingsziekten zoals:

- "a 16-foot wall cannot stop a gamma ray but a body, that is to say human, can";
- "the danger in the world today in my opinion is not the atomic radiation which may or may not be floating through the atmosphere but the hysteria occasioned by that question";
- "radiation is more of a mental than a physical problem";
- "dianazene⁶ runs out radiation - or what appears to be radiation; it also protects a person against radiation in some degree; it also turns on and runs out incipient cancer";

kan gevaarlijke consequenties hebben. Het lezen en navolgen van zijn ideeën creëert een vals veiligheidsgevoel en leidt tot een verkeerde kijk op de werkelijkheid.

⁵ L.Ron Hubbard, "All about Radiation", Church of Scientology International, Los Angeles, (1996).

⁶ medicijn, voorgesteld door L.Ron Hubbard in Ref. (5)

7. De BCG (Boston Consulting Groep) businessportfoliomatrix⁷ kan aanzienlijk verbeterd worden door beschouwing van een derde dimensie, namelijk het relatieve groeitempo van een marktaandeel ten opzichte van het relatieve groeitempo van de gehele markt.

⁷ R.G. Dyson, "Strategic Planning: Models and Analytical Techniques", Wiley, Chapter 4, (1990)

8. De Engelse omschrijving "Monte Carlo Modeling of a Nuclear Oil Well Logging Tool⁸" kan met één Nederlands woord "sjoelen⁹" verduidelijkt worden.

⁸ Dit proefschrift, hoofdstuk 6

⁹ Van Dale, Groot Woordenboek der Nederlandse Taal, door G. Geerts en H. Heestermans, Van Dale Lexicografie: 12 de herziene dr., Utrecht/Antwerpen, (1992)

9. De definitie van Communisme¹⁰ als "Sowjetmacht plus elektrificatie van het hele land" is niet correct, daar thans blijkt dat Communisme minus Sowjetmacht meer is dan alleen elektrificatie van het hele ex-Sowjetland.

¹⁰ V.I. Lenin, "State and Revolution", Chapter 4, (1919)

**Estimation of Detector Responses by
Midway Forward and Adjoint
Monte Carlo Coupling
in Nuclear Systems**

**TR diss
2853**

Igor V. Serov

Interfaculty Reactor Institute
Delft University of Technology
December 1996

CIP-GEGEVENS KONINKLIJKE BIBLIOTHEEK, DEN HAAG

Serov, Igor Valerievich

Estimation of Detector Responses by Midway Forward and Adjoint
Monte Carlo Coupling in Nuclear Systems /

Igor V. Serov. - Delft: Interfacultair Reactor Instituut,
Technische Universiteit Delft. - With ref.

ISBN 90-73861-45-4

NUGI 812

Subject headings: Monte Carlo methods / variance reduction.

Copyright © 1996 by Igor V. Serov

All rights reserved.

Printed in the Netherlands.

Estimation of Detector Responses by Midway Forward and Adjoint Monte Carlo Coupling in Nuclear Systems

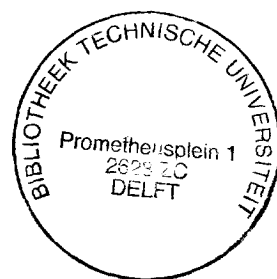
PROEFSCHRIFT

ter verkrijging van de graad van doctor
aan de Technische Universiteit Delft,
op gezag van de Rector Magnificus Prof.ir. K.F. Wakker,
in het openbaar te verdedigen ten overstaan van een commissie,
door het College van Dekanen aangewezen,
op dinsdag 3 december 1996 om 16.00 uur
door

Igor Valerievich SEROV

Physics Engineer,
Moscow Physics Engineering Institute

geboren te Smolensk, Rusland



Dit proefschrift is goedgekeurd door de promotor:

Prof. dr.ir.H. van Dam

Samenstelling promotiecommissie:

Rector Magnificus,	voorzitter
Prof.dr.ir.H. van Dam,	Technische Universiteit Delft, promotor
Dr.ir. J.E. Hoogenboom,	Technische Universiteit Delft, toegevoegde promotor
Prof.ir. M. Peeters,	Technische Universiteit Delft
Prof.dr. M.S. Keane,	Technische Universiteit Delft
	Centrum voor Wiskunde en Informatica Amsterdam
Prof.dr.ir. M. de Bruin,	Technische Universiteit Delft
Prof.dr.ir. W. Lourens,	Universiteit Utrecht
Prof.dr. S.W. de Leeuw,	Technische Universiteit Delft

The research described in this thesis was performed at the Reactor Physics Department of the Interfaculty Reactor Institute, Delft University of Technology, Mekelweg 15, Delft, The Netherlands

*"Ook bij het modelleren van nucleaire problemen loont het
om de gulden middenweg te bewandelen"*

Prof.ir Max Peeters

TU Delft (1996)

Aan mijn ouders

Aan Lenoesje en Ninoesje

Contents

1. General Introduction	9
2. Midway Theory of Detector Response Determination	15
2.1 Purpose	15
2.2 Two Traditional Approaches - Forward and Adjoint - to Determination of a Detector Response	16
2.3 The Third Form - Midway Response Functional.....	18
2.4 Virtual Boundary Conditions, Sources and Three Forms of Detector Response	25
2.5 Midway Response Perturbation Theory	28
2.6 Midway Response Criticality Theory	31
2.7 Midway Detection of Photons Generated at Neutron Generated at Neutron Interactions	33
3. Midway Monte Carlo Response Estimation	37
3.1 Midway Monte Carlo	37
3.2 New Midway Option in the MCNP Monte Carlo Code	41
4. Analytical and Numerical Optimization of Midway Monte Carlo	47
4.1 Introduction	47
4.2 Symmetric Problem with δ -scattering; Analog Midway Monte Carlo	48
4.3 Symmetric Forward-Scattering Problem; Black Absorber Technique	55
4.4 Unsymmetric Problem with Isotropic Scattering	62
5. Examples of Applicability and Efficiency of the Midway Monte Carlo	71
5.1 Introduction	71
5.2 A Difficult Neutron Problem	71
5.3 A Difficult Photon Problem	75
5.4 Two Point Detectors	79
6. Validation of the Midway MCNP Option against Neutron and Photon Benchmarks	81
6.1 Introduction	81
6.2 Sky-shine MCNP Benchmark	81
6.2.1 The reference MCNP model	82
6.2.2 The midway MCNP model	83
6.2.3 Comparison of Results and Discussion	84

6.3 The Nuclear Oil Well Logging Tool MCNP Benchmark	87
6.3.1 The reference MCNP Model	90
6.3.2 The midway MCNP Model	90
6.3.3 Comparison of Results	91
6.3.4 Discussion	91
7. Midway Applications to Interpretation of Experimental Data	95
7.1 Introduction	95
7.2 Motivation for utilization of the midway Monte Carlo Method for Power Distribution Determination in a Nuclear Reactor	96
7.3 HOR research reactor	99
7.3.1 In-core Foil Activation Rate Determination	101
7.3.2 Out-of-core Foil Activation Rate Determination	105
7.4 A Boron Neutron Capture Therapy Facility	107
7.4.1 Introduction	107
7.4.2 Application	108
7.4.3 Comparison of Results and Discussion	111
8. General conclusions	115
References	119
List of Publications	125
Samenvatting	127
Dankwoord	129
Curriculum Vitae	131

Chapter 1

General Introduction

"Do you suppose I could buy back my introduction to you?"

S.J.Perelman, Will B.Johnstone, and Arthur Sheekman

Monkey Business (1931 film)

Monte Carlo methods are widely used to solve many radiation transport problems: reactor design (both fission and fusion), nuclear criticality safety, radiation shielding, nuclear safeguards, detector design and analysis, nuclear well logging, personal dosimetry and health physics, accelerator target design, medical physics and radiotherapy, aerospace applications, defense applications, radiography, waste disposal, and decontamination and decommissioning.

The idea behind all these applications of Monte Carlo is to duplicate numerically the statistical process of nuclear particles transport and interaction with materials. The individual particles and corresponding probabilistic events that comprise the process are simulated sequentially on a digital computer. Some aspects of their average behavior are recorded. The average behavior of particles in the modeled physical system is then inferred from the average behavior of the simulated particles.

In contrast to Monte Carlo methods, deterministic methods, the most common of which is the discrete ordinates method, solve the transport equation for the average particle behavior. The discrete ordinates method visualizes the phase space to be divided into many small boxes, and the particles move from one box to another. In the limit as the boxes get progressively smaller, particles moving from box to box take a differential amount of time to move a differential distance in space. In the limit this approaches the integro-differential transport equation, which has derivatives in space and time. In practice, utilization of the deterministic methods implies use of the finite element or finite difference approaches, which in turn inherently requires discretization of geometry. In many cases proper description of the geometry may not be possible because of a large number of required meshes or because of the nonconformity of region boundaries to the basic co-ordinate system.

By contrast, Monte Carlo "solves" a transport problem by simulating particle histories rather than by solving an equation. No transport equation need even to be written down to solve a transport problem by Monte Carlo. Nonetheless, one can derive an equation that describes the probability density of particles in phase space; this equation turns out to be the same as the integral transport equation. Monte Carlo transports particles between events (for example, collisions) that are separated in space and time. Differential space and time are no longer the inherent parameter of Monte Carlo transport. The integral equation does not have time or space derivatives. Monte Carlo, therefore, does not use phase space boxes, and there is no inherent need for any approximations in space, energy, direction and time. For these reasons, the very important potential of Monte Carlo lies in the possibility to include with relative ease all desired variables, as position, energy, direction and time without discretization, and to accurately incorporate practically any model for particle scattering, cross-section data, and geometry detail.

For the above reasons, Monte Carlo methods are often preferred to deterministic ones to solve complicated problems which involve complex functional dependences of the transport model parameters and particle densities from position in the phase space. Finally, and again for the above reasons, Monte Carlo is often found to be the only method accurate enough for use in benchmarking.

A particular group of radiation transport applications, which are very difficult or impossible to solve with required accuracy by means of the deterministic methods are radiation transport problems, which involve estimation of reaction rates or fluxes at detectors which are small or remote from the radiation source (Laky *et al.*, 1995; Lee *et al.*, 1995; Redmond *et al.*, 1994; Harrington *et al.*, 1995; Liu, 1995). For many of the applications from this group Monte Carlo is the only choice.

For this group of applications, however, Monte Carlo methods can be associated with a problem of taking large computer time to generate statistically converged results to sufficient precision¹.

The direct or analog simulation of Monte Carlo particles in a radiation transport calculation is governed by probability laws, which are given by the physics of the particle source and the interaction mechanisms of the

¹ Following the MCNP manual (Briesmeister, 1993) we distinguish between precision and accuracy of estimation. Precision of the estimated quantity is the statistical uncertainty of a Monte Carlo estimation of its expected value. Accuracy is a measure of the systematic error, which measures the difference between the expected value and the true physical quantity being estimated.

particles with matter. Numerical tracking of even a large number of source particles in a large system in accordance with this physical probability laws will result in only few contributions to remote or small detectors and, correspondingly, with large statistical uncertainties of the results.

This difficulty of the analog Monte Carlo is especially pronounced in problems which involve point or small detection volumes, optically thick materials, complicated streaming paths or combinations of these cases. Monte Carlo would not be practical for many applications were it not for numerous variance reduction methods (Booth, 1985; Booth 1988; Hendricks, 1985; Burn, 1992) that enhance the sampling of those particle histories that contribute to a detector response. The statistical sampling laws are modified in such a way that the statistical uncertainty in the desired quantity is reduced. At the same time the estimation procedure is also altered as to remove any bias from the estimator. Applicability of a particular technique depends strongly on each individual case and often requires substantial effort (Burn, 1992; Booth, 1983; Mickael, 1995; Wagner *et al.*, 1994).

For a certain classes of these difficult problems, in addition to the variance reduction methods, the precision of a Monte Carlo calculation can be improved by solving an adjoint transport equation (Hoogenboom, 1977) instead of the forward one. In the reversed world of adjoint Monte Carlo particles, these particles originate in the detector, fly backwards in time, and upscatter in energy towards the physical source. In a sense, tracking adjoint particles is like backtracking forward particles.

The choice of a forward versus an adjoint Monte Carlo calculation depends upon the relative size of the source and detector regions. It is much easier to transport particles from a small region to a large region than it is to transport particles from a large region to a small region. Adjoint Monte Carlo can be preferred to forward in case of small detection volumes or point detectors (Hoogenboom, 1977).

The solution of the adjoint transport equation is an adjoint function, which describes the importance of physical particles for contribution to the detector response. For multiplying systems detector response was determined by Hoogenboom (1977) by adjoint Monte Carlo as some functional of the adjoint function, but the method was shown to be associated with a disadvantage (Hoogenboom, 1977). Practically, the detector response is calculated in the adjoint mode by integrating the adjoint or importance function, weighted with the source density over energy, direction and space in the source domain.

However, particularly in Monte Carlo reactor calculations, particularly, the source is not a pre-given analytical function, but rather a statistical distri-

bution available from a prior forward eigenfunction Monte Carlo calculation at discrete values of space coordinates, energies, directions and weights of particles created at fission events. It is very easy to sample from such a set, but it is practically impossible to use it as a scoring function in case of an adjoint simulation. A method to overcome this difficulty is to step towards deterministic discretization of the scoring (source) domain into a number of energy, position and direction meshes. The average source density and the adjoint flux can be accumulated for each mesh. The approximation is that within a mesh interval the source and the adjoint flux are assumed to be constant. The sum of their products over all meshes gives the expected approximate value of the detector response. In a limit of infinite small scoring meshes the adjoint Monte Carlo simulation remains unbiased.

If the system is large, however, it can be very unwieldy and may require much computer and human resources to subdivide the whole volume of the source domain into small meshes in space, direction and energy and also the score in such small meshes are prone to large variances. Moreover, large number of meshes can seriously decelerate the Monte Carlo calculation and the gain in efficiency expected from substituting forward simulation by the adjoint one, may turn into a loss. From this we can conclude, that a large domain is not always attractive for scoring purposes and that in certain (i.e. reactor) problems it may be desired to reduce its size.

Another drawback of the adjoint approach arises in problems involving deep penetration. The choice of a forward versus an adjoint Monte Carlo calculations becomes less important as both source and detector domains appear small when viewed from the other. Because either of the particles needs to penetrate up to the remote scoring domain, both choices may become almost equally poor in practical deep penetration calculations, if not supplemented with something else.

In the scope of this research we present a relatively simple scheme of efficient coupling of forward and adjoint calculations at an intermediate scoring domain.

The forward-adjoint midway coupling method originates when

- the physical source is replaced with a virtual surface source somewhere midway between the genuine source and the detector, and
- the forward transport from the surface to the detector is beneficially replaced by adjoint transport from the detector to the surface.

The principal possibility of the midway coupling is based on the general reciprocity equation (Williams, 1977) and has been shown, for example, by

Marcuk and Orlov (1961) and Hensen and Sandmeier (1965). It was further developed for deterministic methods by Korobeinikov and Usanov (1994). Kawai *et al.*, (1990) proposed to apply a forward-adjoint Monte Carlo coupling technique to neutron streaming calculations in complex geometries and doubled the efficiency of a Monte Carlo simulation for a single detector system design.

The author initiated a broader study of possible benefits provided by forward-adjoint Monte Carlo coupling in 1994 and developed the midway Monte Carlo coupling method (Serov *et al.*, 1996b). The theory behind the midway method is presented in Chapter 2.

The method was practically implemented (Serov *et al.*, 1995) in the local version of the MCNP code (Briesmeister, 1993). Chapter 3 is dedicated to the specifics of the midway Monte Carlo method and its implementation in the MCNP code. According to the midway Monte Carlo method the scoring takes place at the medium-size surface in both the forward and adjoint calculation and carries the following benefits. Firstly, for problems involving small detectors in large reactor systems it allows to overcome the practical limitations of the adjoint Monte Carlo advantages by reducing the size of the scoring domain. Secondly, in deep penetration problems (which also can be reactor problems with small detectors), it allows to predict fluxes with a much higher efficiency than forward or adjoint Monte Carlo separately.

Chapter 4 contains an analyses of the midway method application to an academic sample problem. For this example the position of the midway surface and the relative forward to adjoint workload are optimized to achieve the highest efficiency of the coupled calculation. With the help of this example the author wanted to demonstrate the inherent possibilities of the midway Monte Carlo method to provide significant efficiency increase for solutions of deep-penetration problems.

Starting from this point the research was directed towards wide-ranging tests, benchmarks and applications of the midway Monte Carlo method and the corresponding MCNP option aiming to promote the method in the community of nuclear Monte Carlo users.

Within the scope of this research the midway option was used to model a number of streaming and deep neutron and photon penetration problems, described in a MCNP report (Wagner *et al.*, 1994). Two of these problems were chosen for demonstration in this dissertation because they are relatively simple in description. These examples were also chosen because they pose a difficult variance reduction challenge. The results of the calculations

and their analyses are presented in the corresponding sections of Chapter 5.

Further on, the midway method has also been tested (Serov *et al.*, 1996c; Serov *et al.*, 1996d) against a number of MCNP neutron and photon benchmarks. These are the nuclear well logging porosity tool (Brockhoff *et al.*, 1994) and the photon sky-shine experiment (Whalen *et al.*, 1991). The results of the calculations are presented in Chapter 6. The calculations were also performed for the published models (Brockhoff *et al.*, 1994; Whalen *et al.*, 1991) of these benchmarks. The results of the comparative analyses are presented.

Chapter 7 deals with the applications of the midway method to interpretation of experimental data. In-core and out-of-core neutron detector response calculations for the Hoger Onderwijs Reactor, IRI, Delft were performed by means of standard options of MCNP and the new midway options. Neutron and photon deep penetration studies using the midway option (Serov *et al.*, 1996e) were repeated for the Boron Neutron Capture Facility at the Lower Flux Reactor, ECN, Petten.

Concluding remarks are in the Chapter 8.

Chapter 2

Midway Response Determination Theory

*"Movies should have a beginning, a middle and an end,"
harrumphed French Film Maker Georges Franju
at a symposium some years back.
'Certainly,' replied Jean-Luc Godard.
'But not necessary in that order.'"*

Jean-Luc Godard

Time (14 September 1981)

2.1 Purpose

Many practical problems of particle radiation transport requires a quantitative determination of radiation influence upon an object, or, differently, the object's influence upon the radiation field. Detector response to radiation is determined as an integral of functions, characterizing the radiation source, penetrability of the medium and the detector itself. Complex geometrical heterogeneity of systems considered, various scales of sources, detectors and penetration media make it imperative to investigate the possibilities to choose the most suitable integration domain for a particular problem. This section deals with formulation of the available possibilities. To one of this possibilities, namely to the integration within a so called midway surface domain, located somewhere midway between the source and the detector we give the most attention.

2.2 Two traditional approaches - forward and adjoint - to the determination of a detector response

The steady-state neutral particle *forward transport equation* in a multiplying medium is given by (Bell, 1970)

$$\begin{aligned} & \nabla \cdot \underline{\Omega} \Psi(\underline{r}, E, \underline{\Omega}) + \Sigma_t(\underline{r}, E) \Psi(\underline{r}, E, \underline{\Omega}) \\ &= \int_E \int_{4\pi} \Sigma(\underline{r}, E', \underline{\Omega}' \rightarrow E, \underline{\Omega}) \Psi(\underline{r}, E', \underline{\Omega}') d\Omega' dE' + S(\underline{r}, E, \underline{\Omega}). \end{aligned} \quad (2.2.1)$$

where $\Psi(\underline{r}, E, \underline{\Omega})$ is the *forward flux density*; $\Sigma_t(\underline{r}, E)$ is a total cross section for particles interaction of energy E with nuclei of the medium at the spatial point \underline{r} ; $\Sigma(\underline{r}, E', \underline{\Omega}' \rightarrow E, \underline{\Omega})$ is a reproduction cross section and $S(\underline{r}, E, \underline{\Omega})$ is a *forward source function* which is non-zero in the source domain V_s . The latter cross section can present a sum of partial components of cross sections of various processes leading to particle procreation. For neutrons, for example, these are scattering reactions, fission, $(n, 2n)$, etc. Often it becomes necessary to isolate the fission process:

$$\Sigma(\underline{r}, E' \underline{\Omega}' \rightarrow E \underline{\Omega}) = \frac{\chi(E) \nu \Sigma_f(\underline{r}, E')}{4\pi} + \Sigma_s(\underline{r}, E' \underline{\Omega}' \rightarrow E \underline{\Omega}), \quad (2.2.2)$$

where $\chi(E)$ is a normalized spectrum of fission neutrons; ν - average number of neutrons emitted by fission; $\Sigma_f(\underline{r}, E)$ - fission cross section; $\Sigma_s(\underline{r}, E', \underline{\Omega}' \rightarrow E, \underline{\Omega})$ - differential scattering cross section.

To find a solution of the Eq.(2.2.1) in a domain V bounded by a surface A_V it is necessary to specify the boundary conditions for the density of the particle entering the domain V through the surface A_V . The volume V is chosen such that there are no sources outside V . The boundary condition for the flux density $\Psi(\underline{r}, E, \underline{\Omega})$ is then:

$$\Psi(\underline{r}, E, \underline{\Omega}) = 0 \text{ for } \underline{r} \in A_V \text{ and } \underline{n} \cdot \underline{\Omega} < 0. \quad (2.2.3)$$

Here and further in the text \underline{n} is the outward normal vector to the considered surface.

It is convenient to write the transport equation in operator notation as

$$\nabla \cdot \underline{\Omega} \Psi + B \Psi = S, \quad (2.2.4)$$

where B is the Boltzman operator without the divergence term.

Response observed per unit time by a detector is a linear functional of the forward flux density is defined by:

$$R = \langle S^*, \Psi \rangle_V, \quad (2.2.5)$$

where $S^*(\underline{r}, E, \underline{\Omega})$ is a given *forward detector response function*, which is non-zero in the detector domain V_d . Eq.(2.2.5) will be referred as the *forward response determination form*. The angle brackets indicate an inner product that effectively integrates over the space, energy, and direction variables and the subscript behind the right bracket indicate the domain of the spatial integration.

Although Eq.(2.2.5) is generally used in overwhelming majority of cases, already in 1950-s due to the development of adjoint functions theory (Ussachoff, 1955) it has been accepted that this way is not the only one. The alternative is to determine the same response as a linear functional

$$R = \langle \Psi^*, S \rangle_V \quad (2.2.6)$$

of the adjoint function $\Psi^*(\underline{r}, E, \underline{\Omega})$. Eq.(2.2.6) will be referred to as the *adjoint response determination form*.

The adjoint function obeys the *adjoint transport equation* (Lewins, 1970)

$$\begin{aligned} & - \nabla \cdot \underline{\Omega} \Psi^*(\underline{r}, E, \underline{\Omega}) + \Sigma_t(\underline{r}, E) \Psi^*(\underline{r}, E, \underline{\Omega}) \\ & = \int_E \int_{4\pi} \Sigma(\underline{r}, E, \underline{\Omega} \rightarrow E', \underline{\Omega}') \Psi^*(\underline{r}, E', \underline{\Omega}') d\Omega' dE' + S^*(\underline{r}, E, \underline{\Omega}), \end{aligned} \quad (2.2.7)$$

where the detector response function serves as the source term and therefore can also be called an *adjoint source function*. The same considerations allow us to refer to the source function $S(\underline{r}, E, \underline{\Omega})$ as to the *adjoint detector function*, to the physical source as to the *adjoint detector*, and to the physical detector as to the *adjoint source*. Later on, we will use this freedom in nomenclature for formulation of generalized statements.

The adjoint transport equation in operator notation is

$$-\nabla \cdot \underline{\Omega} \Psi^* + B^* \Psi^* = S^*, \quad (2.2.8)$$

where B^* is the operator adjoint to B .

The boundary condition for the adjoint flux density is the condition adjoint to Eq.(2.2.3):

$$\Psi^*(\underline{r}, E, \underline{\Omega}) = 0 \text{ for } \underline{r} \in A_v \text{ and } \underline{n} \cdot \underline{\Omega} > 0. \quad (2.2.9)$$

The introduction of the adjoint detector response determination form Eq.(2.2.6) is based on the fundamental interconnection between the forward flux density and adjoint function (Ussachoff, 1955; Lewins, 1970):

$$R = \langle S^*, \Psi \rangle_V = \langle \Psi^*, S \rangle_V. \quad (2.2.10)$$

We note here, that the detector response R can be determined not only in the domain where the detector is actually placed, but also in the source domain which is located in some other place.

One can question, whether there exist other domains inside V , where the detector response can also be determined. This question will be dealt with in the next Section.

2.3 The Third Form: Midway Response Functional

To answer the above question we bring into consideration an arbitrary midway domain V_m , bounded by the surface A_m within a system domain V as shown in Fig.(2.3.1).

Let us subtract the forward transport equation (2.2.4) multiplied by the adjoint function $\Psi^*(\underline{r}, E, \underline{\Omega})$ from Eq.(2.2.8) multiplied by the forward flux density $\Psi(\underline{r}, E, \underline{\Omega})$ and integrate over energy, direction and space within the domain V_m . After some algebraic transforms we obtain:

$$\langle \nabla \cdot \underline{\Omega} \Psi \Psi^* \rangle_{V_m} = \langle \Psi^*, S \rangle_{V_m} - \langle S^*, \Psi \rangle_{V_m}. \quad (2.3.1)$$

Applying the Gauss theorem to the divergence term we have:

$$[\underline{n} \cdot \underline{\Omega} \Psi \Psi^*]_{A_m} = \langle \Psi^*, S \rangle_{V_m} - \langle S^*, \Psi \rangle_{V_m}, \quad (2.3.2)$$

where the square brackets in difference with the angle ones indicate the integration in space takes place on the surface, which encloses the corresponding volume domain.

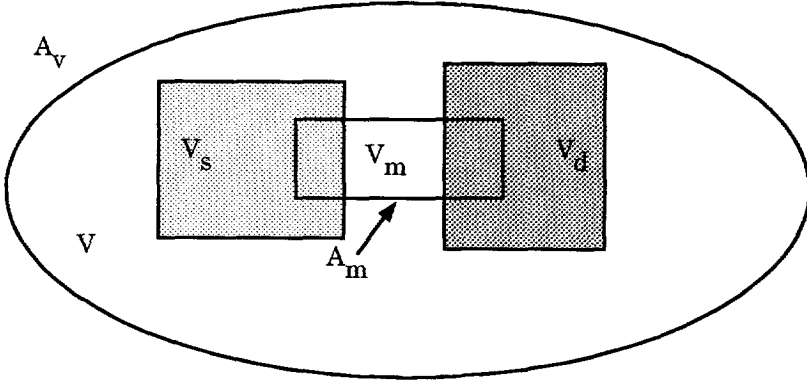


Figure 2.3.1 Integration Domain for Detector Response Determination

Eq.(2.3.2) is usually referred to as the *general reciprocity theorem* (Williams and Engle, 1977). Because of the arbitrary nature of the midway domain V_m , this equation can be effectively used in any subdomain of the system V . It is difficult, however, to assign any physical meaning to the involved integrals in the general case considered above. The difficulty is caused by the fact that in general the integration involves only the portions of the source and detector located within the midway domain. At the same time the forward and adjoint flux densities involved in the integration are due to the entire source and detector, respectively.

In order to overcome this difficulty and arrive to an interpretable form of Eq.(2.3.2) we split the original problem into four subproblems a,b,c and d. These subproblems are equivalent to the original problem in everything except that the source and detector functions are set to zero everywhere except in the following subdomains:

- a. source in $V_m \cap V_s$ and detector in $V_m \cap V_d$;
- b. source in $V_m \cap V_s$ and detector in $V_m - (V_m \cap V_d)$;
- c. source in $V_m - (V_m \cap V_s)$ and detector in $V_m \cap V_d$;
- d. source in $V_m - (V_m \cap V_s)$ and detector in $V_m - (V_m \cap V_d)$.

The corresponding Fig.(2.3.2.a-2.3.2.d) can be used as visual aid for the four subproblem definitions:

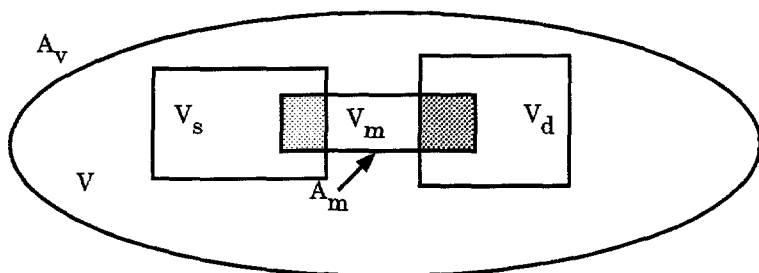


Figure 2.3.2.a Integration Domains for Subproblem a

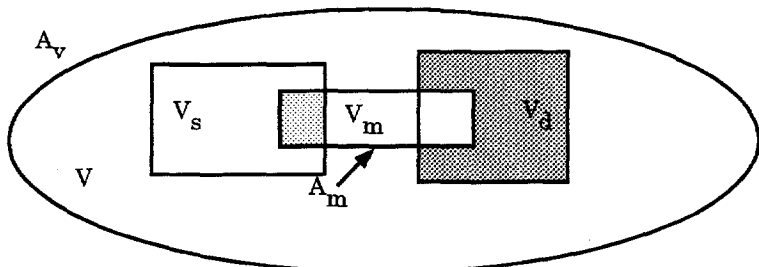


Figure 2.3.2.b Integration Domains for Subproblem b

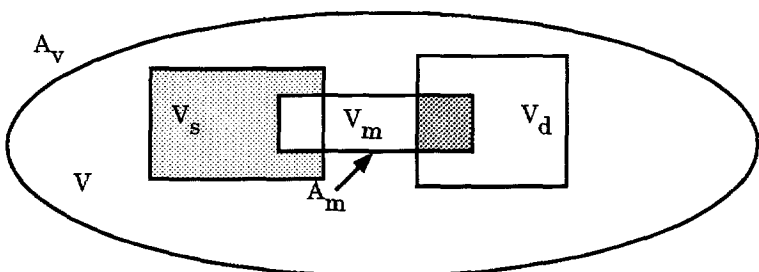


Figure 2.3.2.c Integration Domains for Subproblem c

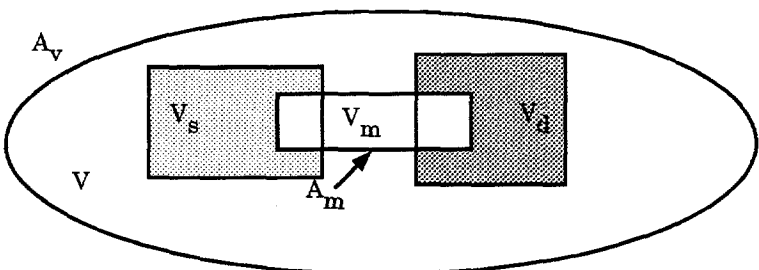


Figure 2.3.2.d Integration Domains for Subproblem d

Applying the definition of the detector response Eq.(2.2.5) supplemented by the equivalence expression Eq.(2.2.10) to the subproblems a and d we obtain:

$$R_a \equiv \langle S^*, \Psi_i \rangle_V = \langle \Psi_i^*, S \rangle_V ; \quad (2.3.3)$$

$$R_d \equiv \langle S^*, \Psi_o \rangle_V = \langle \Psi_o^*, S \rangle_V ; \quad (2.3.4)$$

Here $\Psi_i(\underline{r}, E, \underline{\Omega})$ and $\Psi_o(\underline{r}, E, \underline{\Omega})$ are forward flux densities due to the corresponding parts of the forward source in V_m and $V-V_m$;

$\Psi_i^*(\underline{r}, E, \underline{\Omega})$ and $\Psi_o^*(\underline{r}, E, \underline{\Omega})$ are adjoint functions due the corresponding parts of the adjoint source in V_m and $V-V_m$.

Taking into account the specifics of the source and detector description for these subproblems it follows then from the general reciprocity theorem, that

$$[\underline{n} \cdot \underline{\Omega} \Psi_i \Psi_i^*]_{A_m} = 0 \quad (2.3.5)$$

for the subproblem a and

$$[\underline{n} \cdot \underline{\Omega} \Psi_o \Psi_o^*]_{A_m} = 0 \quad (2.3.6)$$

for the subproblem d.

Applying now the general reciprocity theorem for the subproblems b and c inside and outside the midway domain and taking into account the definition of the detector response Eq.(2.2.5) supplemented by the equivalence equation (2.2.10) we come to:

$$R_b \equiv \langle S^*, \Psi_i \rangle_{V-V_m} = \langle \Psi_o^*, S \rangle_{V_m} = [\underline{n} \cdot \underline{\Omega} \Psi_o \Psi_o^*]_{A_m} ; \quad (2.3.7)$$

$$R_c \equiv \langle S^*, \Psi_o \rangle_{V_m} = \langle \Psi_i^*, S \rangle_{V-V_m} = -[\underline{n} \cdot \underline{\Omega} \Psi_o \Psi_i^*]_{A_m}; \quad (2.3.8)$$

It is easy to see that because of the linearity of the transport models involved, the total response of the system is an additive quantity and can be expressed as the sum of the solutions of the four subproblems:

$$R = R_a + R_b + R_c + R_d. \quad (2.3.9)$$

Now we observe, that the left hand side type quantities of the general reciprocity equation Eq.(2.3.2) appearing in Eq.(2.3.7) and Eq.(2.3.8) can be interpreted as parts of the total system response. This suggests the following

Definition of Midway Response:

The midway response is that part of the total system response, which originates by the part of the source at one side of the midway surface and contributes and sinks in the part of the detector at the other side of the midway surface:

$$R_m = R_b + R_c \quad (2.3.10)$$

In accordance with Eq.(2.3.7) and Eq.(2.3.8) the midway response can be expressed as the surface integral:

$$R_m = [\underline{n} \cdot \underline{\Omega} \Psi_i \Psi_o^*]_{A_m} - [\underline{n} \cdot \underline{\Omega} \Psi_o \Psi_i^*]_{A_m}. \quad (2.3.11)$$

In this general form the midway response R_m has little practical use for the determination of the total system response R .

However, taking into account the arbitrariness of the midway domain, we can obtain a more advantageous expression for the midway response by requesting the midway domain to enclose exclusively either the source or the detector domain. In these and only these two cases the midway response

becomes equal to the total system response and the latter can be determined using the *midway response form*:

$$R = \left[\underline{n} \cdot \underline{\Omega} \Psi \Psi^* \right]_{A_m} \quad (2.3.12)$$

in case of the source enclosed by the midway subdomain, because $\Psi_0(\underline{r}, \underline{E}, \underline{\Omega}) = 0$ and $\Psi_1^*(\underline{r}, \underline{E}, \underline{\Omega}) = 0$ and

$$R = - \left[\underline{n} \cdot \underline{\Omega} \Psi \Psi^* \right]_{A_m} \quad (2.3.13)$$

in case of the detector enclosed by the midway subdomain, because $\Psi_1(\underline{r}, \underline{E}, \underline{\Omega}) = 0$ and $\Psi_0^*(\underline{r}, \underline{E}, \underline{\Omega}) = 0$. The midway domain containing the source exclusively or the detector exclusively will be referred to as the *midway source enclosure* or *midway detector enclosure*, respectively. Using notations of Section (2.2) we recognize, that the midway source enclosure can also be called the *midway forward source enclosure* or the *midway adjoint detector enclosure*. Analogously the midway detector enclosure can also be called the *midway forward detector enclosure* or the *midway adjoint source enclosure*. Later on, we will use this freedom in nomenclature for formulation of generalized statements.

The midway response Eq.(2.3.11) defines the net integral flow of response through the surface. The part $R_a + R_d$ of the total system response R does not stream through the midway surface. Therefore the total response R cannot be determined by the midway response in a general case. In order to apply the reduced midway response formula (2.3.12) or (2.3.13) to the determination of the total response R , it is necessary to detach the source and detector domains by the midway surface so that the entire response necessarily crosses the surface and therefore is taken care of by one of the reduced midway response formulae.

The reduced forms of the midway response can also easily be obtained from the general reciprocity theorem Eq.(2.3.2) by applying the above rule for the midway subdomain selection, although in that case the definition and the status of the midway response remain hidden.

It is worthy to note, that the midway formalism is intimately tied together with a *generalized contributon response theory* (Williams, 1991). The latter is an extension of the *spatial channel theory* published much earlier (Williams and Engle, 1977). In accordance with the contributon theory the response is transferred between a particle source and the detector by pseudo particles called *contributons*. Unlike the usual particles which may be absorbed anywhere the contributon particle possess an exclusive feature of necessarily contributing to the detector response. Also the contributons

never escape out of the system, but get sank in the detector and contribute to the response. The transport of contributons is described by the *generalized contributon transport equation* (Williams, 1991). The solution of this equation is the *angular response flux*:

$$C(\underline{r}, E, \underline{\Omega}) = \Psi(\underline{r}, E, \underline{\Omega}) \Psi^*(\underline{r}, E, \underline{\Omega}). \quad (2.3.14)$$

This function has fundamental meaning for the definition of the midway response Eq.(2.3.11), Eq.(2.3.12) and Eq.(2.3.13). Integration of the contributon equation over the entire system domain leads to the traditional forward and adjoint forms Eq.(2.2.5) and Eq.(2.2.6). Integration over an arbitrary midway domain leads to the general reciprocity theorem Eq.(2.3.2). Integration over an arbitrary midway source enclosure or midway detector enclosure leads to the corresponding midway response form Eq.(2.3.12) or Eq.(2.3.13). Equivalence of forward, adjoint and midway response forms is a demonstration of the fact, that the total number of contributons crossing the surface of any midway enclosure equals the number of contributons originated in the source and sank in the detector.

The different signs in the formulae Eq.(2.3.12) and Eq.(2.3.13) have certain physical sense. The angular response current is a vector that points in the direction of the net response flow. Positiveness of the integral at the right hand side of the Eq.(2.3.12) or Eq.(2.3.13) means predominance of the contribution flow in the direction of the positive normal \underline{n} to the midway surface. In case of the detector enclosure the integral of the angular response current projection onto the normal vector \underline{n} is negative, which demonstrates that the contributons flow from the source into the midway detector domain towards the detector.

Furthermore, if not stated otherwise, we will assume that the midway surface surrounds exclusively the detector domain and use the Eq.(2.3.13) referring to the detector enclosure as to the midway enclosure.

We have demonstrated that for a total system response determination, a correctly chosen midway surface can serve as the integration domain different from the source and detector for a total system response determination. Utilization of midway bilinear surface integration can be considered as the cornerstone of the *midway response determination method* as opposed to linear volumetrical integration of *forward or adjoint response determination methods*.

2.4 Virtual Boundary Conditions, Sources and Three Forms of Detector Response

In this section we develop other forms of a particle transport problem described by equations (2.2.4) and (2.2.3), which can be advantageous in applications and show the interconnections between these different forms.

Consider a *virtual forward source*:

$$S_v(\underline{r}, E, \underline{\Omega}) = -\underline{n} \cdot \underline{\Omega} \Psi(\underline{r}, E, \underline{\Omega}), \quad \underline{r} \in A_m, \quad (2.4.1)$$

where A_m is a midway surface surrounding exclusively the detector, and replace the physical source $S(\underline{r}, E, \underline{\Omega})$ in the transport equation Eq.(2.2.4) by this virtual source:

$$\nabla \cdot \underline{\Omega} \tilde{\Psi} + B \tilde{\Psi} = S_v, \quad (2.4.2)$$

and the boundary condition similar to Eq.(2.2.3):

$$\tilde{\Psi}(\underline{r}, E, \underline{\Omega}) = 0 \text{ for } \underline{r} \in A_v \text{ and } \underline{n} \cdot \underline{\Omega} < 0. \quad (2.4.3)$$

The transport operator is not changed and the problem determined by Eq.(2.2.8) together with the boundary condition Eq.(2.2.9) remains adjoint to the problem of Eq.(2.4.2) with Eq.(2.4.3).

Following the usual procedure we derive the general reciprocity theorem for the problem Eq.(2.4.2) with Eq.(2.4.3) in the system domain V:

$$\langle S^*, \tilde{\Psi} \rangle_V = - [\underline{n} \cdot \underline{\Omega} \Psi^* \tilde{\Psi}]_{A_m}. \quad (2.4.4)$$

The right hand side integral is nothing else but the midway response R_m of the original problem through the detector enclosure A_m , which equals to the total system response in accordance with Eq.(2.3.13). It follows then from Eq.(2.4.4) and Eq.(2.2.5), that

$$\langle S^*, (\tilde{\Psi} - \Psi) \rangle_{V_m} = 0, \quad (2.4.5)$$

and because of the arbitrariness of the detector response $S^*(\underline{r}, E, \underline{\Omega})$ within the midway domain we obtain:

$$\tilde{\Psi}(\underline{r}, E, \underline{\Omega}) = \Psi(\underline{r}, E, \underline{\Omega}), \text{ for all } \underline{r} \in V_m. \quad (2.4.6)$$

This proves that the problem of Eq.(2.4.2) and Eq.(2.4.3) is equivalent to the original problem Eq.(2.2.4) and Eq.(2.2.3) from the point of view of flux or response determination within the domain bounded by the surface of the virtual source. It should be noted, that the possibility of replacing the physical source with a virtual surface source is well known (Case and Zweifel, 1967).

By means of the above clarification it is possible to demonstrate the close interrelation between the virtual surface source, regular forward, adjoint and midway forms of response. Indeed, two different approaches of the detector response determination are possible when the virtual source is given. Firstly, the total system response R can be determined by the formula similar to Eq.(2.2.5):

$$R = \langle S^*, \tilde{\Psi} \rangle_V, \quad (2.4.7)$$

if the solution of the particle transport problem Eq.(2.4.2) and Eq.(2.4.3) is available Secondly, if the solution of the adjoint transport problem Eq.(2.2.8) and Eq.(2.2.9) is available, then the response R can be calculated by the formula similar to Eq.(2.2.6):

$$R = [\Psi^* S_v]_{A_m}, \quad (2.4.8)$$

or by force of Eq.(2.4.1) by the equivalent midway formula Eq.(2.3.13). This suggests an alternative

Interpretation of the Midway Method:

According to the midway response method the forward problem with the virtual forward surface source is replaced by the corresponding adjoint problem and subsequent adjoint response determination with this virtual source.

The original forward problem Eq.(2.2.4) and Eq.(2.2.3) is to be specified in the entire forward domain for determination of the virtual source. For the

determination of the adjoint function at the midway surface the adjoint problem should also be specified in the entire system.

Third form of the problem setup equivalent to the problems of Eq.(2.2.4) with the boundary condition Eq.(2.2.3) and Eq.(2.4.2) with the boundary condition Eq.(2.4.3) in the sense of response or flux determination within the midway domain can be derived using a *virtual forward boundary condition*:

$$\tilde{\Psi}(\underline{r}, E, \underline{\Omega}) = \Psi(\underline{r}, E, \underline{\Omega}) \text{ for } \underline{r} \in A_m. \quad (2.4.9)$$

which is considered jointly with Eq.(2.4.2) considered only within the enclosure. The adjoint problem is given by Eq.(2.2.8), but also restricted to the interior of the enclosure by the *virtual adjoint boundary condition*

$$\tilde{\Psi}^*(\underline{r}, E, \underline{\Omega}) = \Psi^*(\underline{r}, E, \underline{\Omega}) \text{ for } \underline{r} \in A_m. \quad (2.4.10)$$

Again by implying the standard procedure we come to the following form of the general reciprocity theorem for the midway enclosure V_m :

$$[\underline{n} \cdot \underline{\Omega} \Psi \Psi^*]_{A_m} = - \langle S^*, \tilde{\Psi} \rangle_V, \quad (2.4.11)$$

from which we come again by the equality expressions Eq.(2.4.5) and Eq.(2.4.6).

Similar argumentation can be repeated using the *virtual adjoint source*:

$$S_v^*(\underline{r}, E, \underline{\Omega}) = \underline{n} \cdot \underline{\Omega} \Psi(\underline{r}, E, \underline{\Omega}) \text{ for } \underline{r} \in A_m \quad (2.4.12)$$

on the midway enclosure of the source or with the virtual adjoint boundary condition Eq.(2.4.10) and leads to the equations (2.4.5) and (2.4.6), where V_m denotes now the midway source enclosure.

The above argumentation can be summarized in the following

Statement of Equivalent Virtuality:

The detector response in a given system due to the actual (forward or adjoint) source equals the detector response due to the virtual (forward or ad-

joint) source or virtual (forward or adjoint) boundary condition specified at the surface of the corresponding (forward or adjoint) midway detector enclosure as the solution of the corresponding (forward or adjoint) transport problem.

Due to the recognized symmetry between forward and adjoint transport problems and different forms of the midway sources and boundary fluxes it becomes evident, that the forward and adjoint procedures leading to the determination of the midway response are generally independent from each other. This signifies also, that for the solution of these counterpart transport problems different methods can be employed.

2.5 Midway Response Perturbation Theory

Gertsl suggested (1977), that constructive use of the midway formulae for the determination of detector responses is possible if an explicit equation for the angular response flux is obtained. This equation has been derived (Gertsl, 1976; Gertsl, 1977). Later it has been presented within a generalized contribution response theory (Williams, 1991) and carries great theoretical value. The equation appeared to be extremely difficult to solve even for very simple problems, which made the utilization of this approach very problematic for applications (Williams, 1980). Moreover, the knowledge of either exact forward flux density $\Psi(\underline{r}, E, \underline{\Omega})$ or adjoint function $\Psi^*(\underline{r}, E, \underline{\Omega})$ is required to generate the contribution scattering kernel (Williams, 1991) and response term of the generalized contribution transport equation (Williams, 1991). If they are known, however, as it is emphasized in (Williams, 1991), there is no need to solve the contribution equation and the response can be calculated from Eq.(2.2.5) or Eq.(2.2.6).

An alternative is to search the response flux on the midway surface as the product of forward flux density and adjoint function as solutions of the equations Eq.(2.2.4) and Eq.(2.2.8). Yet, it is at least strange to search for two exact solutions for midway integration instead of using Eq.(2.2.5) or Eq.(2.2.6), which require only one of them (although in a different spatial domain).

Intuitively it is plausible to suggest, that the exact knowledge of both the forward and adjoint densities is superfluous and that at least some part of this knowledge may not be as mandatory as stated above. An alternative direction for practicing the midway integration is to replace the exact solutions $\Psi(\underline{r}, E, \underline{\Omega})$ and $\Psi^*(\underline{r}, E, \underline{\Omega})$ with some approximate functions $\phi(\underline{r}, E, \underline{\Omega})$ and $\phi^*(\underline{r}, E, \underline{\Omega})$, found as solutions of some simplified transport equations which are set in such a way that the detector response R is not altered.

One of the fundamental results of the perturbation theory (Lewins, 1970) is that the detector response can be generally determined exactly using an exact solution of either forward or adjoint transport problem. The second solution can be either exact or approximate being obtained from the simplified model of the original problem. Williams (1991) has applied perturbation theory to prove that if a perturbation domain of the adjoint problem is located outside the midway detector enclosure then the exact value of response can be determined by midway integration Eq.(2.3.13) of the correspondingly perturbed angular response flux. Consistent and well-founded review of independent forward and adjoint transport problem perturbations is given by Korobeinikov and Usanov (1994).

Consider an arbitrary midway detector domain V_m bounded by the surface A_m . Let the perturbation domain for the adjoint problem to be located outside the midway detector enclosure and describe the altered adjoint problem is described by:

$$-\nabla \cdot \underline{\Omega} \varphi^* + B^* \varphi^* = S^*; \quad B^* = B \text{ for } \underline{r} \in V_m. \quad (2.5.1)$$

Let the forward transport problem remain unperturbed and described by Eqs.(2.2.4) and (2.2.3).

Using the procedure which lead us to the general reciprocity theorem Eq.(2.3.2) for a combination of the unperturbed forward and perturbed adjoint problems for integration inside the midway detector domain (where the adjoint operator remains unperturbed) we obtain:

$$[\underline{n} \cdot \underline{\Omega} \Psi \varphi^*]_{A_m} = - \langle S^*, \Psi \rangle_{V_m}, \quad (2.5.2)$$

from which we immediately obtain the exact total system response as an integral of the unperturbed forward and perturbed adjoint flux densities product:

$$R = - [\underline{n} \cdot \underline{\Omega} \Psi \varphi^*]_{A_m}. \quad (2.5.3)$$

Naturally, the same procedure can be repeated for integration within the midway source enclosure. If the adjoint model remains unperturbed and

the perturbation domain of the forward problem is located outside the enclosure we get:

$$R = [\underline{n} \cdot \underline{\Omega} \varphi \Psi^*]_{A_m} . \quad (2.5.4)$$

where $\varphi(r, E, \Omega)$ is a solution of the perturbed forward problem. The above argumentation can be summarized in the following:

Statement of Two Exact Solutions Redundancy

The midway response is not biased by any perturbation of one (forward or adjoint) of the two transport problems performed inside the midway enclosure of the corresponding (forward or adjoint) detector.

To give a practical example of the usefulness of the proved statement we distinguish

The Black Absorber Technique for Midway Monte Carlo Calculations

One (forward or adjoint) of the two Monte Carlo simulations required for the midway coupling can be ignored inside the midway enclosure of the corresponding (forward or adjoint) detector.

or equivalently

Materials outside the midway enclosure of the (forward or adjoint) source can be substituted with an absolutely black absorber in a corresponding (forward or adjoint) Monte Carlo simulation required for the midway determination of the physical detector response.

2.6 Midway Response Criticality Theory

The forward criticality eigenfunction equation is written as:

$$\begin{aligned} & \nabla \cdot \underline{\Omega} \Psi_{\text{eig}}(\underline{r}, E, \underline{\Omega}) + \Sigma_t(\underline{r}, E) \Psi_{\text{eig}}(\underline{r}, E, \underline{\Omega}) \\ = & \int_{E'} \int_{4\pi} \left[\frac{\chi(E) \nu \Sigma_f(\underline{r}, E')}{4 \pi k_{\text{eff}}} + \Sigma_s(\underline{r}, E', \underline{\Omega}' \rightarrow E, \underline{\Omega}) \right] \Psi_{\text{eig}}(\underline{r}, E', \underline{\Omega}') d\Omega' dE'. \end{aligned} \quad (2.6.1)$$

This equation is used to describe neutron transport in a multiplying medium of a nuclear reactor without external source. The following equation is usually formed as an adjoint equation to the above Eq.(2.6.1) and is called the *adjoint criticality eigenfunction equation*:

$$\begin{aligned} & - \nabla \cdot \underline{\Omega} \Psi_{\text{eig}}^*(\underline{r}, E, \underline{\Omega}) + \Sigma_t(\underline{r}, E) \Psi_{\text{eig}}^*(\underline{r}, E, \underline{\Omega}) \\ = & \int_{E'} \int_{4\pi} \left[\frac{\nu \Sigma_f(\underline{r}, E) \chi(E')}{4 \pi k_{\text{eff}}} + \Sigma_s(\underline{r}, E, \underline{\Omega} \rightarrow E', \underline{\Omega}') \right] \Psi_{\text{eig}}^*(\underline{r}, E', \underline{\Omega}') d\Omega' dE'. \end{aligned} \quad (2.6.2)$$

Both equations are considered to be valid within a system domain V. The following boundary conditions are satisfied:

$$\begin{aligned} \Psi_{\text{eig}}(\underline{r}, E, \underline{\Omega}) &= 0 \text{ for } \underline{r} \in A_v \text{ and } \underline{n} \cdot \underline{\Omega} < 0; \\ \Psi_{\text{eig}}^*(\underline{r}, E, \underline{\Omega}) &= 0 \text{ for } \underline{r} \in A_v \text{ and } \underline{n} \cdot \underline{\Omega} > 0. \end{aligned} \quad (2.6.3)$$

The solutions of the eigenvalue equations (2.6.1) and (2.6.2) are to be properly normalized by the reactor power level.

The adjoint Eq.(2.6.2) does not contain any source and has an adjoint eigenfunction as the solution. The eigenvalues of the two equations are proven to be identical (Bell and Glasstone, 1970). In the framework of this study we are not particularly interested in the eigenvalue, but rather in determination of the detector response, which can be directly determined by the forward response form:

$$R = \langle S^*, \Psi_{\text{eig}} \rangle. \quad (2.6.4)$$

Adjoint Eq.(2.6.2) allows neither adjoint nor midway form for the determination of the detector response, because forward Eq.(2.6.1) has no explicit source term. Therefore, the latter equation is equivalently rewritten without a fission source term:

$$\begin{aligned} & \nabla \cdot \underline{\Omega} \Psi_{\text{eig}}(\underline{r}, E, \underline{\Omega}) + \Sigma_t(\underline{r}, E) \Psi_{\text{eig}}(\underline{r}, E, \underline{\Omega}) \\ &= \int_E \int_{4\pi} \Sigma_s(\underline{r}, E' \underline{\Omega}' \rightarrow E \underline{\Omega}) \Psi_{\text{eig}}(\underline{r}, E', \underline{\Omega}') d\Omega' dE' + S_{\text{eig}}(\underline{r}, E) \end{aligned} \quad (2.6.5)$$

but with the external source in the form:

$$S_{\text{eig}}(\underline{r}, E) = \int_{E'} \int_{4\pi} \frac{\chi(E) \nu \Sigma_f(\underline{r}, E')}{4 \pi k_{\text{eff}}} \Psi_{\text{eig}}(\underline{r}, E', \underline{\Omega}') d\Omega' dE'. \quad (2.6.6)$$

An equation adjoint to Eq.(2.6.5) has a detector response source term:

$$\begin{aligned} & -\nabla \cdot \underline{\Omega} \Psi^*(\underline{r}, E, \underline{\Omega}) + \Sigma(\underline{r}, E) \Psi^*(\underline{r}, E, \underline{\Omega}) \\ &= \int_{E'} \int_{4\pi} \Sigma_s(\underline{r}, E, \underline{\Omega} \rightarrow E', \underline{\Omega}') \Psi^*(\underline{r}, E', \underline{\Omega}') d\Omega' dE' + S^*(\underline{r}, E, \underline{\Omega}), \end{aligned} \quad (2.6.7)$$

and no fission term. Eq.(2.6.2) and Eq.(2.6.7) are different and have different solutions.

Applying the procedure leading to the global reciprocity theorem for Eq.(2.6.5) and Eq.(2.6.7) within an arbitrary midway detector enclosure V_m we arrive at:

$$[\underline{n} \cdot \underline{\Omega} \Psi_{\text{eig}} \Psi^*]_{A_m} = \langle \Psi^*, S_{\text{eig}} \rangle_{V_m} - \langle S^*, \Psi_{\text{eig}} \rangle_{V_m} \quad (2.6.8)$$

where from using Eq.(2.6.4) we obtain:

$$R = \langle \Psi^*, S_{\text{eig}} \rangle_{V_m} - [\underline{n} \cdot \underline{\Omega} \Psi_{\text{eig}} \Psi^*]_{A_m} \quad (2.6.9)$$

This result can be interpreted as follows:

In the effectively critical system the total system response at a detector located within the midway enclosure can be determined as a sum of response originated by the fission source within the enclosure and the midway response streaming through the midway surface into the enclosure.

Eq.(2.6.9) and the above interpretation parallels with the results of Sections (2.3) and (2.4). Indeed, because some portion of the fission source together with the whole detector are located within the enclosure the above result corresponds to the sum $R_a + R_c$ of Section (2.3).

In case when there is no fissile material within the enclosure the above formulae reduces to the known midway expression:

$$R = - [\underline{n} \cdot \underline{\Omega} \Psi_{eig} \Psi^*]_{A_m} . \quad (2.6.10)$$

2.7 Midway Detection of Photons Generated at Neutron Interactions

Photons generated at inelastic or capture neutron interactions with a medium are ignored, if one concerns only about neutronics of the system. For several application types, however, fluxes of photons produced at neutron interactions are of importance. Experiments and transport calculations for these applications involve photon detectors, which responses are to be determined. Both the neutron and photon transport equations have the form of Eq.(2.2.4), but differ in their Boltzmann operators, flux densities and the source terms. The equations

$$\nabla \cdot \underline{\Omega} \Psi_n + B_n \Psi_n = S, \quad (2.7.1)$$

and

$$\nabla \cdot \underline{\Omega} \Psi_p + B_p \Psi_p = P, \quad (2.7.2)$$

are used in this Section to describe the neutron and photon transport respectively, denoting neutrons with the subscript n and photons with the subscript p. Here $S(\underline{r}, E, \underline{\Omega})$ is an external *forward neutron source function*,

which is non-zero in the source domain V_s . The *forward photon source function* $P(\underline{r}, E, \underline{\Omega})$ is determined by the cross section $\Sigma_{pr}(\underline{r}, E', \underline{\Omega}' \rightarrow E, \underline{\Omega})$ of photon production at neutron interactions and the forward neutron flux density $\Psi_n(\underline{r}, E, \underline{\Omega})$:

$$P(\underline{r}, E, \underline{\Omega}) = \int_E \int_{4\pi} \Sigma_{pr}(\underline{r}, E' \underline{\Omega}' \rightarrow E \underline{\Omega}) \Psi_n(\underline{r}, E', \underline{\Omega}') d\Omega' dE' . \quad (2.7.3)$$

Consider the equations, which are formally adjoint to the equations (2.7.1) and (2.7.2), correspondingly:

$$-\nabla \cdot \underline{\Omega} \Psi_n^* + B_n^* \Psi_n^* = P^* , \quad (2.7.4)$$

and

$$-\nabla \cdot \underline{\Omega} \Psi_p^* + B_p^* \Psi_p^* = S^* . \quad (2.7.5)$$

Here

$$P^*(\underline{r}, E, \underline{\Omega}) = \int_E \int_{4\pi} \Sigma_{pr}(\underline{r}, E \underline{\Omega} \rightarrow E' \underline{\Omega}') \Psi_p^*(\underline{r}, E', \underline{\Omega}') d\Omega' dE' \quad (2.7.6)$$

is the *adjoint source function of neutrons*, produced at interactions of adjoint photons with the medium. $S^*(\underline{r}, E, \underline{\Omega})$ is the *forward photon detector response function* or the *adjoint photon source function*. Possible photoneutronic sources are excluded from this consideration.

The photon detector response is defined by

$$R = \langle S^* , \Psi_p \rangle_V , \quad (2.7.7)$$

Let us subtract the forward neutron equation (2.7.1) multiplied by the adjoint function $\Psi_n^*(\underline{r}, E, \underline{\Omega})$ from the adjoint neutron equation (2.7.4) multiplied with the forward neutron flux density $\Psi_n(\underline{r}, E, \underline{\Omega})$, integrate over energy, direction and space within the arbitrary domain V_m , bounded by the

surface A_m and apply the Gauss theorem to the divergence term. After some algebraic transforms we obtain:

$$[\underline{n} \cdot \underline{\Omega} \Psi_n \Psi_n^*]_{A_m} = \langle \Psi_n^*, S \rangle_{V_m} - \langle P^*, \Psi_n \rangle_{V_m}, \quad (2.7.8)$$

Repeating the same procedure for the photon equations and functions we obtain the following equation:

$$[\underline{n} \cdot \underline{\Omega} \Psi_p \Psi_p^*]_{A_m} = \langle \Psi_p^*, P \rangle_{V_m} - \langle S^*, \Psi_p \rangle_{V_m}, \quad (2.7.9)$$

It follows from the definitions of the functions $P(\underline{r}, E, \underline{\Omega})$ and $P^*(\underline{r}, E, \underline{\Omega})$, that for every arbitrary domain V_m :

$$\langle P^*, \Psi_n \rangle_{V_m} = \langle \Psi_p^*, P \rangle_{V_m}. \quad (2.7.10)$$

Summing up Eq.(2.7.8) and Eq.(2.7.9) and using Eq.(2.7.10) we obtain:

$$[\underline{n} \cdot \underline{\Omega} \Psi_n \Psi_n^*]_{A_m} + [\underline{n} \cdot \underline{\Omega} \Psi_p \Psi_p^*]_{A_m} = \langle \Psi_n^*, S \rangle_{V_m} - \langle S^*, \Psi_p \rangle_{V_m}. \quad (2.7.11)$$

Now let the domain V_m be an arbitrary enclosure of the photon detector domain. The forward neutron source function $S(\underline{r}, E, \underline{\Omega})$ is zero within in V_m and the above equation reduces to:

$$[\underline{n} \cdot \underline{\Omega} \Psi_n \Psi_n^*]_{A_m} + [\underline{n} \cdot \underline{\Omega} \Psi_p \Psi_p^*]_{A_m} = - \langle S^*, \Psi_p \rangle_{V_m}. \quad (2.7.12)$$

Using the definition of the photon detector response Eq.(2.7.7) and the fact that the photon detector response function is zero outside the enclosure V_m we derive the

***Midway Photon Detector Response Determination Form
for a System with a Neutron Source:***

$$R = - [\underline{n} \cdot \underline{\Omega} \Psi_n \Psi_n^*]_{A_m} - [\underline{n} \cdot \underline{\Omega} \Psi_p \Psi_p^*]_{A_m}. \quad (2.7.13)$$

Chapter 3

Midway Monte Carlo Response Estimation

*"I don't like this game,
let's play another game -
let's play doctor and nurses."*

Spike Milligan (Terence Alan Milligan)

Goon Show Scripts (1972)

3.1 Midway Monte Carlo

The formalism presented in the previous Chapter is founded on the neutral particle transport theory and may be applied to midway determination of detector responses. Different methods of transport calculations can be used for estimation of the forward flux density and adjoint functions at the coupling surface. We concentrate our attention on a midway coupling of forward and adjoint Monte Carlo methods in order to decrease the calculational times required to generate the result with sufficiently low statistical uncertainty in problems where these times appear to be large.

Utilization of the midway response determination form Eq.(2.3.12) or Eq.(2.3.13) require bilinear integration, which is obviously a problem for any linear Monte Carlo method. Practically it requires that either of the two (forward or adjoint) scores is weighted with the other one, which is a statistical value sampled from a continuous distribution. In order to overcome this difficulty we follow the discretization approximation, described by Kawai (1990). The scoring domain of both the forward and adjoint calculation is subdivided in a number of energy, position and direction meshes: the energy distribution is represented with a multigroup structure; the midway surface is divided into a number of small segments; the angle distribution is represented by polar and azimuthal bin structures. A surface crossing estimator can be used for scoring in the bins defined over the midway surface.

In a limit of an infinitely large number of infinitely small angle, surface and energy meshes, the midway detector response can be estimated as the sum:

$$R = \sum_i \sum_j \sum_k \sum_m J_{ijkm} \Psi_{ijkm}^* \Delta E_i \Delta A_j \Delta \mu_k \Delta \alpha_m, \quad (3.1.1)$$

where J_{ijkm} and Ψ_{ijkm}^* are the Monte Carlo estimates of the forward current density and the adjoint functions in the azimuthal angle bin m , polar angle cosine bin k , surface segment j and energy group i , respectively. Here $\Delta \alpha_m$ is the width of the azimuthal angle bin, $\Delta \mu_k$ is the width of the polar angle cosine bin, ΔE_i is the width of the energy group and ΔA_j is the area of the midway surface segment. Practically, within a mesh interval the forward current density and adjoint function are assumed to be constant.

The surface crossing estimator is used for scoring in the bins defined over the midway surface and the forward current density is estimated after simulation of N_f forward particles by summing up the first moments of the particle weights w_{ijkm} , crossing the midway surface per unit area, per unit energy and solid angle normalized per forward source particle:

$$J_{ijkm} = \sum_{n=1, N_f} \frac{w_{ijkm}^n}{\Delta \alpha_l \Delta \mu_k \Delta E_i \Delta A_j} \quad (3.1.2)$$

Analogously, the adjoint function is estimated with the help of

$$\Psi_{ijkm}^* = \frac{J_{ijkm}^*}{\mu_k} \quad (3.1.3)$$

where J_{ijkm}^* is the estimate of the adjoint function after simulating of N_a adjoint particles:

$$J_{ijkm}^* = \sum_{n=1, N_a} \frac{w_{ijkm}^{*n}}{\Delta \alpha_l \Delta \mu_k \Delta E_i \Delta A_j} \quad (3.1.4)$$

where w_{ijkm}^* is the weight of the adjoint particle crossing the midway surface.

The relative variance of the forward current density J_{ijkn} and the adjoint function are estimated (Lux and Koblinger, 1991) by

$$r^2 [J]_{ijkn} = \frac{\sum_{n=1, N_f} (w_{ijkn})^2}{(\sum_{n=1, N_f} w_{ijkn})^2} - \frac{1}{N_f} \quad (3.1.5)$$

and

$$r^2 [\psi^*]_{ijkn} = \frac{1}{\mu_k} \left[\frac{\sum_{n=1, N_f} (w_{ijkn}^*)^2}{(\sum_{n=1, N_f} w_{ijkn}^*)^2} - \frac{1}{N_a} \right] \quad (3.1.6)$$

respectively, where $r^2[x]$ denotes the relative variance of x .

The forward current density J_{ijkn} and the adjoint function Ψ_{ijkn}^* are statistically independent from each other. Hence the sum of their relative variances gives in first order approximation the relative variance of the product for that mesh:

$$r^2 [J \Psi^*]_{ijkn} = r^2 [J]_{ijkn} + r^2 [\Psi^*]_{ijkn} \quad (3.1.7)$$

The variance of the detector response is obtained by summing the absolute variances of the products over all the meshes:

$$\sigma^2 [R_m] = \sum_i \sum_j \sum_k \sum_m r^2 [J \Psi^*]_{ijkn} J_{ijkn}^2 \Psi_{ijkn}^{*2} \quad (3.1.8)$$

The final expression for the relative statistical error of the midway response is given by:

$$r [R_m] = \frac{(\sigma^2 [R_m])^{1/2}}{R_m} \quad (3.1.9)$$

The efficiency of a forward or adjoint Monte Carlo estimation is usually measured by a Figure of Merit, defined as:

$$FOM = \frac{1}{T r^2} \quad (3.1.10)$$

where r is the relative error of the estimation and T is the computer time required to perform the calculation. T can be expressed as the product of the average computer time t required to simulate a single particle history and the number of particles

$$T = N \tau . \quad (3.1.11)$$

As $r^2[x]$ is inversely proportional to N (Lux and Koblinger, 1991), the FOM is independent of the number of particles used in the Monte Carlo calculation and is a suitable quantity to compare the efficiencies of different Monte Carlo estimations of a certain quantity on the same computer. A higher value of FOM shows the superior efficiency of the simulation.

In case of the midway estimation, the total calculational time is the sum $T_f + T_a$ of the forward and adjoint calculational times, and FOM is:

$$FOM = \frac{1}{(N_f \tau_f + N_a \tau_a) r^2[R_m]} \quad (3.1.12)$$

where computer times per forward and adjoint history τ_f and τ_a are inherently determined by geometry and physics of a particular problem. They generally differ from each other, because of different treatment of the forward and adjoint collisions. Both times τ_f and τ_a and the relative statistical error of the midway response $r[R_m]$ can be influenced by supplementary utilization of one or another variance reduction technique in forward or adjoint calculation.

Obviously, the midway surface itself is the user-defined parameter of the midway Monte Carlo method, which influences the FOM number determined by Eq.(3.6.12). In the analog calculation this influence will be transferred through the relative error only. Indeed, modeling of the midway surfaces will hardly influence the time required for the computer to model a particle history. It can be different, however, if variance reduction techniques are applied. Truncation variance reduction techniques, for example, speed up calculations by truncating parts of phase space that do not contribute significantly to the solution. The simplest example is geometry truncation in which unimportant parts of the geometry are simply not modeled.

The black absorber techniques, developed in Section (2.5) can be regarded as *fully unbiased* geometry truncation variance reduction techniques designed specifically for extra acceleration of midway Monte Carlo. If the adjoint black absorption technique is applied, for example, then the adjoint particles are transported only up to the midway surface. The computer time τ_a consumed by an average adjoint particle to reach the midway surface may depend on the distance between the source and the midway surface. Varying the midway surface position, the user varies the computer time τ_a and the FOM in correspondence with Eq.(3.6.12). If the forward black absorber technique is in use, then the FOM depends on the midway position through the relative error $r[R_m]$ and computer time per forward history τ_f .

Thus, if variance reduction techniques are applied then the choice of the midway surface can be correlated with the difference in forward and adjoint histories simulation times due to these variance reduction techniques.

Further the efficiency of the midway estimation can be affected by alterations of *the relative forward to adjoint workload*:

$$W = \frac{N_f}{N_a} \quad (3.1.13)$$

which is the second user-defined parameter of the midway Monte Carlo method. Running different numbers of forward N_f and adjoint N_a histories will influence the FOM through all three parameters τ_a , τ_f and $r[R_m]$.

3.2 A New Midway Option in the MCNP Monte Carlo Code

The MCNP code (Briesmeister, 1993) is one of the best general purpose Monte Carlo codes. It is widely used to solve many radiation transport problems: reactor design (both fission and fusion), nuclear criticality safety, radiation shielding, nuclear safeguards, detector design and analysis, nuclear well logging, personal dosimetry and health physics, accelerator target design, medical physics and radiotherapy, aerospace applications, defense applications, radiography, waste disposal, and decontamination and decommissioning. The documentation for MCNP is a 600-page manual (Briesmeister, 1993) describing the Monte-Carlo theory, geometry, physics, cross sections, variance reduction techniques, tallies, errors, input, and output.

Both neutron and photon transport problems in three-dimensional geometries can be solved by MCNP. Both fixed (external) source and eigenvalue

criticality problems can be solved by MCNP. Representations of the energy dependent data can be fully or partially continuous or multigroup. It is well-known (Hoogenboom, 1981) and accepted, that adjoint Monte Carlo calculations with a continuous energy dependence are difficult to perform. As a result, only the multigroup adjoint option is available in MCNP. The utilization of the multigroup/adjoint capability is extensively described in the report of Wagner *et al.* (1994).

The user can instruct MCNP to make various tallies (estimators for quantities of interest) related to particle current and particle flux. Currents can be tallied as a function of direction across any set of surfaces, surface segments, or unions of surfaces in the problem. Fluxes across any set of surfaces, surfaces segments, unions of surfaces, and in cells, cell segments, or unions of cells are also available. Similarly, the fluxes at designated detectors (points or rings) are standard tallies. Tallies may be made for segments of cells and surfaces without having to build the desired segments into the actual problem geometry.

MCNP's generalized user-input source capability allows the user to specify a wide variety of source conditions without having to make a code modifications. Independent probability distributions may be specified for the source variables of energy, time, position and direction, and for other parameters such as starting cell(s) or surface(s). In addition to input probability distributions for source variables, certain built-in functions are available. These include various analytic functions for fission and fusion energy spectra such as Watt, Maxwellian and Gaussian spectra; and isotropic, cosine, and mono-directional for direction.

The code is rich in variance reduction techniques that improve the efficiency of difficult calculations that range from trivial to the esoteric: energy cutoff, geometry splitting with Russian roulette, energy splitting with Russian roulette; weight cutoff with Russian roulette, weight window, exponential transformation, implicit capture, forced collisions, source variable biasing, point and ring detectors, DXTRAN (deterministic transport), and correlated sampling.

The midway Monte Carlo method described in the previous section is implemented at the Interfaculty Reactor Institute of the Delft University of Technology in the local version of MCNP. A special new type of tally - midway tally - is built into the code. Two calculations - forward and adjoint - are to be performed in arbitrary order to obtain an estimate of the midway tally. The first (forward or adjoint) calculation is used to accumulate detailed information about the forward current density or the adjoint function, respectively at the midway surface using the surface crossing estimator segmented in space, direction and energy. The second function is estimated similarly in the second (correspondingly adjoint or forward) calculation and coupled with the function of the first calculation in accordance with Eq.(3.6.1). The estimated quantity is called the midway tally. The

relative standard deviation and the FOM number of the midway tally as defined by Eq.(3.6.9) and Eq.(3.6.10) are also estimated in the second calculation. Responses of neutron detectors from neutron sources and photon detectors from neutron or photon sources can be estimated by the midway option of MCNP.

Eight MCNP subroutines were modified for the midway option to be implemented. There were no new subroutines incorporated into the code for this purpose. Only one new common block statement is added to some of these subroutines. It contains one memory word for every midway tally. All the other new variables are local and their total number does not exceed 20.

The forward calculation should be set up in accordance with the input requirements of MCNP described in the MCNP manual (Briesmeister, 1993). The adjoint calculation should be set up according to the requirements of Wagner's report (1994). Generally, it requires treatment of adjoint collisions and interchange of the source and tally regions. The tally characteristics in a forward calculation are associated with the source input cards in the adjoint run. Likewise, the source characteristics in the forward calculation are defined by the tally cards in the adjoint calculation. Hence, the adjoint problem is essentially a turned around forward problem, which in a sense can be interpreted as a backward Monte Carlo calculation with adjoint treatment of particle collisions. Special attention should be given to the proper normalization of the adjoint calculation (Wagner, 1994). In accordance with Collins (1987), the product of the source densities and the response function in the opposite direction problem should be the same as the product of the source densities times the response functions in the original problem. In order to satisfy this requirement, adjustments to the initial weight of the particles must be made to correct for the automatic normalization of the source densities by MCNP (Wagner, 1994).

In the midway calculation the surface crossing tallies are specified at the midway surface in both forward and adjoint calculation. The characteristics of the forward particle source are used as the source description in the midway forward calculation. The tally characteristics of the forward calculation are used to define the source of the midway adjoint calculation.

A number of special tally features are available in MCNP using a "special treatment" input card. The midway option is a new special feature and is called by using the special treatment card with 4 parameters in both forward and adjoint calculations. The first parameter determines the midway tally number in the current calculation. The second parameter determines the midway special feature itself and whether the current (forward or adjoint) calculation is the first or the second in the coupling sequence. This parameter has two possible values: f+a and a+f. The first and the second "item" in the "sum" designate the first and the second calculation correspondingly. Using, for example, f+a in an adjoint calculation implicates that the forward calculation is the first one (there also f+a is used) and that

the midway tally results are obtained in the adjoint calculation. Non-zero third parameter determines that simulated in the current calculation particles are only to be scored at the first crossing of the midway surface. This feature is used in calculations with the black absorber technique. The fourth parameter is non-zero only in the second midway calculation and determines the number of the midway tally of the first calculation. The tally determined by the first parameter of the second calculation is coupled with the tally determined by the fourth parameter of the first calculation.

Almost all the other aspects of the input for midway tallies are identical to these of the standard MCNP tallies. Both forward and adjoint midway tallies are called as standard "flux averaged over a surface" tallies. The angular, energy and spatial coupling at a midway surface is made using standard binning features of MCNP. The following extensions were necessary, however, and implemented:

- utilization of cosine angular bins for "flux averaged over a surface" tallies (this feature is normally available only for "currents averaged over a surface");
- utilization of the so called "user" bins for azimuthal angle binning.

Additionally a special surface segmenting technique is developed to allow accurate spatial coupling on a midway surface in unsymmetric systems. Essentially, the technique allows to cover practically any MCNP tallying surface by a number of small segments determined by overlapping cylindrical and spherical surfaces using only standard MCNP input cards. Because the segments resembles fish-scales, the technique is referred further in the text as the scaling technique.

The requirement is that the binning structures in the midway calculation are the same in the corresponding forward and adjoint midway tallies.

Some other features of MCNP can be particularly interesting in the midway calculations. The black absorber technique, for example, can be employed not only by using an non-zero value for the third parameter of the midway special treatment card, but also by setting importances of the MCNP model geometry cells to zero at the side of the midway surface away from the source in one of the two calculations. Some of standard special features of MCNP can be employed together with the midway special feature. For example, scoring at the midway surface in the adjoint midway calculation in accordance with the bins of the adjoint source energy distribution allows to estimate the spectral dependence of the midway tally.

Because only the multigroup adjoint treatment is available in MCNP, adjoint MCNP calculations for the midway coupling can only be performed in multigroup mode. The forward calculations for the midway coupling can be performed in either continuous energy or multigroup mode. The energy bin structure used for the continuous mode forward calculations should be the same as the multigroup bin boundaries in the adjoint calculation. Simi-

larly, estimation of responses for multiple detectors can be performed in a single pair of the forward and adjoint calculation. In a single pair of calculations it is possible to couple using different midway surfaces. Finally, in a single pair of calculations it is possible to couple at various relative workloads by coupling results at intermediate numbers of simulated forward and adjoint particles. This possibility can be used in a short preliminary run to evaluate the midway surface and the relative workload corresponding to the highest midway FOM. These best values can be used in the subsequent production pair of calculations to ensure maximum efficiency of the Monte Carlo estimation.

Chapter 4

Analytical and Numerical Optimization of Midway Monte Carlo

"The golden rule is that there are no golden rules."

George Bernard Shaw

Man and Superman (1903)

4.1 Introduction

Preliminary analytical and numerical studies of new Monte Carlo acceleration methods are usually performed for some simplified systems (Booth, 1996; Sarkar *et al.*, 1979; Clark, 1996, Spanier, 1970; Lux and Koblinger, 1991). This helps to draw more or less general conclusions about the applicability and relative efficiency gain provided by the new method and about the optimal values of the method parameters, which can be influenced by a user of the new method. These conclusions form the basis of the user expertise and can often be applied to rough optimization of a real system. In this case the global characteristics of the real system are used as input characteristics to the simplified optimization model. Conclusions drawn about the best values of optimized parameters of the model can be applied to the real systems. After that these rough values can be fine-tuned by short preliminary calculations for the real system to find out the conditions for the highest FOM number in the long production run.

In this Chapter attention is given to the optimization of the midway Monte Carlo method parameters using various modifications of a self-adjoint problem. For some cases, the conclusions drawn are based on analytical considerations. For a number of other cases, the author was unable to obtain a general closed-form solution and suggests recursive solutions. Other intriguing cases were not considered here and left for future study.

Conclusions, drawn in this Chapter and formulated in the form of the so called Statements should by no means be considered as general ones, simply because the number and the scope of the considered problems are very limited. The suggested Statements should be treated as rules of thumb,

rather than theorems. They are based on a number very simplified problems, which are approached either analytically or numerically. An attempt is made to share the combination of experience, intuition and scientific expertise formed after almost two years of solving different problems by the midway Monte Carlo method to an interested user of the method. We believe, that the presented results and the drawn conclusions can provide this user with guidelines for practical selection of user-defined parameters of the midway Monte Carlo method and the black absorber technique.

4.2 The Symmetric Problem with δ -scattering; Analog Midway Monte Carlo

Consider an artificial one-dimensional homogeneous particle transport problem in finite slab geometry as pictured in Figure (4.2.1). At one end the particles are introduced into the system perpendicular to the slab. A detector counting all the outcoming particles is placed at the other end of the system. Particles can be absorbed by the material or scattered along the original direction towards the detector. The parameter α is the *absorption probability*: on average α particles get absorbed and $(1-\alpha)$ are scattered per interacting particle. Physically this problem contains a pure absorbing material and analytical study of the problem becomes possible. Differently, Monte Carlo calculations of this system, preserve properties of the scattering media, because particles are not absorbed at every collision.

The problem possesses all the main features of so-called forward- or δ -scattering problems (here and further in the text we refer to scattering in the laboratory coordinate system). Compton scattering of photons, which is an important process of their interaction with a medium at energies between 100 eV and 1 MeV, is one of the typical examples of the forward-scattering problems. Another example involves interactions of intermediate (0.2 eV~ 10^5 eV) and thermal (< 0.2 eV) neutrons with light materials and fast (0.1~10 MeV) neutrons with heavy materials. In addition to the above systems with sharply expressed forward-scattering in systems with intermediate and low values of α , the considered model can be applicable to systems where the absorption probability α is high and the role of the scattering process is not of much importance for the optimization of the particle transport simulation. Evidently, in these systems, the degree of anisotropy is not of importance as well. Therefore the model can be applied to systems with high absorption and correspondingly low isotropic or anisotropic scattering. Neutron transport in shielding materials is a typical example of this type of problems.

The systems of this class can be generally characterized by rough values for the absorption probability α averaged over energy and space and the distance between the source and the detector along some line connecting them. In this sense the optimization problem can be considered monoenergetic and spatially one-dimensional.

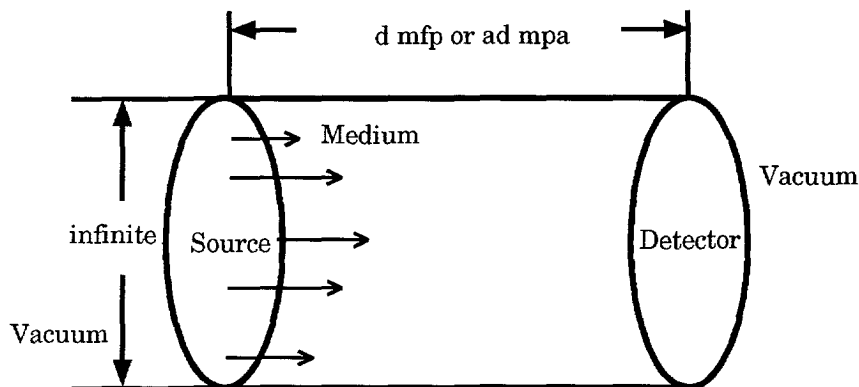


Figure 4.2.1. Symmetric Self-Adjoint Problem in a Finite Slab Geometry.

The considered problem is not only self-adjoint, but also fully symmetric. The quantity ad will be called *the system attenuation width* and will be measured in *mean free paths to absorption (mpa)*. Alternatively, the same homogeneous system can be characterized by the *system optical width* d , which is measured in *mean free paths to collision (mpc)* or equivalently in *mean free paths (mfp)*. One mean free path equals α mean paths to absorption. In the following discussion we will also use the terms of optical and attenuation distances and optical and attenuation positions which are measured in mfp and mpa, respectively. If not specified otherwise, both distances and positions are defined with respect to the position of the forward source.

The number of forward particles n_f or adjoint particles n_a registered at the forward or adjoint detector per forward or adjoint source particle respectively, exhibits an exponential behavior as a function of *the system attenuation width* ad between the source and the detector:

$$n_f = n_a = \exp(-\alpha d). \quad (4.2.1)$$

It follows then from Eqs.(3.1.5) and (3.1.6), that the relative variances of the analog forward and adjoint estimates become:

$$r_f^2 = \frac{\exp(\alpha d)}{N_f} ; \quad r_a^2 = \frac{\exp(\alpha d)}{N_a} ; \quad (4.2.2)$$

and differ only if different number of forward N_f and adjoint N_a particles are run.

From Eq.(3.1.10) and Eq.(3.1.11) it follows then, that the analog forward and adjoint Monte Carlo efficiencies are correspondingly expressed by:

$$FOM_f = \frac{1}{\tau_f \exp(\alpha d)} ; \quad FOM_a = \frac{1}{\tau_a \exp(\alpha d)} . \quad (4.2.3)$$

It becomes clear, that the substitution of the forward calculation mode with the adjoint one for this problem delivers no advantages for the efficiency of the Monte Carlo calculation, unless the times τ_f and τ_a are very different.

Consider now the midway coupling of the forward and adjoint simulation processes at a midway plane, which is placed at the attenuation distance αx mpa from the source and correspondingly at the attenuation distance width $\alpha(d-x)$ mpa from the detector. The midway estimate of the relative detector response is then calculated by a reduced form of Eq.(3.1.1) and equals the forward and adjoint responses:

$$n_m = \exp(-\alpha x) \cdot \exp(-\alpha(d-x)) , \quad (4.2.4)$$

and equals the numbers of forward particles n_f or adjoint particles n_a determined by Eq.(4.2.1).

The relative variance of the midway estimate is determined by the adapted form of Eq.(3.1.7)

$$r^2(R_m) = \frac{\exp(\alpha x)}{N_f} + \frac{\exp(\alpha(d-x))}{N_a} . \quad (4.2.5)$$

The FOM number of the analog midway Monte Carlo estimate becomes

$$FOM_m = \frac{W}{(W\tau_f + \tau_a) (\exp(\alpha x) + W \exp(\alpha(d-x)))} , \quad (4.2.6)$$

where W is the relative forward to adjoint workload defined by Eq.(3.1.13).

Generally, even if the transport problem is fully self-adjoint, one can experience differences between the estimates of the times τ_f and τ_a . The simplest examples are when forward and adjoint calculations are performed at different computers or using different algorithms. In practice, the differences are observed due to essentially different treatments of forward and adjoint collisions. For these examples the times τ_f and τ_a are pre-given, do not differ from the ones of the autonomous (uncoupled) forward and adjoint calculations and are not influenced by the user-defined parameters of the midway Monte Carlo method. More sophisticated examples include utilization of different types of variance reduction techniques, such as truncation, population control, modified sampling or partially-deterministic methods (Briesmeister, 1993). In this case as we will see, for example, in the next Section in connection with the black absorber technique, the times τ_f and τ_a may depend on the variance reduction, what makes optimization of Eq.(4.2.6) more cumbersome.

The following general analytical formulation of this Section is limited to the first analog case: the times τ_f and τ_a can be different, but fixed. They can be estimated by short preliminary runs and used as constant parameters in Eq.(4.2.6). For simplicity of notation, any midway estimation performed by coupling of analog forward and analog adjoint calculations will be further referred to as *the analog midway estimation*.

Setting the partial derivatives with respect to W and the optical distance x of Eq.(4.2.6) to zero, we easily come to the following expressions for the optimal attenuation distance of the midway plane from the source:

$$\alpha x_{opt} = \frac{\alpha d}{2} + \frac{\ln \frac{\tau_a}{\tau_f}}{2} . \quad (4.2.7)$$

and the optimal forward to adjoint workload:

$$W = \frac{\tau_a}{\tau_f} \quad (4.2.8)$$

It immediately follows from Eq.(4.2.8), that the computer time resources should be equally divided between the forward and adjoint calculations:

$$T_{f_{opt}} = T_{a_{opt}} . \quad (4.2.9)$$

The considered model is a homogenous one and there is no difference between the optimal attenuation position and the optimal optical position determined by Eq.(4.2.7). Returning to Eq.(4.2.4) we recognize, that the attenuation and not the optical position of the midway surface is essential for the optimal positioning of the midway surface by Eq.(4.2.7). Intuitively we

tend to believe, that this essential property remains also valid for heterogeneous systems. Additionally, we will see in the next Sections, that the results of the above considerations can also be applied for optimization of calculations with variance reduction, isotropic scattering and unsymmetric systems.

Therefore, they are summarized into the following

Statement of the Optimal Relative Workload

For the optimal midway Monte Carlo coupling the computer time spent in an adjoint calculation should equal the computer time spent in the forward calculation

or, in other words

for the optimal midway Monte Carlo coupling the relative forward to adjoint workload should be determined in a preliminary run as the ratio of the average adjoint to forward history simulation times.

and

Statement of the Optimal Midway Surface Position

For the optimal midway Monte Carlo coupling the midway surface should be placed in the middle of the attenuation distance between the source and the detector if simulation of the forward and adjoint histories takes in average the same time. If the time required to simulate an average forward history does not equal the time required to simulate an average adjoint history then this position should be adjusted. The value of the attenuation position adjustment equals half of the value of natural logarithm of the optimal forward to adjoint workload. The direction of the adjustment is from the (forward or adjoint) source, which particles are simulated faster and more frequently.

In the following reduced formulation, we make use of the fact that the analog simulation of our self-adjoint problem is fully symmetric and the times per forward and adjoint history are equal:

$$\tau_f = \tau_a, \quad (4.2.10)$$

For this case the optimal analog midway FOM is expressed by:

$$FOM_{m\ opt} = \frac{1}{4\tau_f \exp(\frac{ad}{2})} \quad (4.2.11)$$

It is easy to see by comparing Eq.(4.2.3) and Eq.(4.2.11), that starting already from the attenuation width

$$ad = 4 \ln 2 \sim 2.77 \quad (4.2.12)$$

between the source and the detector, the midway Monte Carlo calculation demonstrates higher efficiency than the autonomous forward one.

As a matter of fact, the relative gain in the efficiency due to utilization of the midway method grows as an exponential function of the attenuation penetration half-width:

$$\frac{FOM_{m\ opt}}{FOM_f} = \frac{\exp(\frac{ad}{2})}{4} \quad (4.2.13)$$

To demonstrate these conclusions in practice, numerical studies of this problem were performed by the MCNP code for the fully absorbing medium ($\alpha = 1$). MCNP calculation of self-adjoint, fully symmetric problems will generally show slight differences between the estimates of the mean value, its relative error, which are attributed to the statistical uncertainty of the Monte Carlo modeling. Besides that, the differences in average time per history and the FOM number can be additionally attributed to algorithmic differences in the forward and adjoint coding as is the case for a general non-symmetric and non-adjoint case. To preserve the theoretical self-adjointness and symmetry of the problem in practice, we make use of these properties and couple *two forward* MCNP calculations. One of them is called forward, because it models forward particle transport from the source to the detector. The other one is called adjoint, because it models adjoint particle transport from the detector to the source. This approach was used for the coupling calculations for all the self-adjoint problems described in this Chapter.

The studied problem is one-dimensional, mono-directional, monoenergetic and fully symmetric and the midway coupling does not require any binning of the midway phase space and the MCNP results are unbiased.

The results of the autonomous forward and midway coupling calculations together with the corresponding analytical results are presented in Table (4.2.1) as a function of the optical system width d . First of all, it is demonstrated by these calculations that the midway coupling is possible in practice. All the observed discrepancies between the analytical and numerical models have statistical nature. The mean values perfectly agree within the confidence intervals corresponding to the normal distribution. In case of the fully absorbing medium $\alpha = 1$ it is numerically confirmed that starting from about 2-3 mfp of the optical distance between the source and the detector the midway method demonstrates higher efficiency than the forward one, which agrees with Eq.(4.2.12).

	Thickness (mfp)	2	4	8	16
	Total Number of Histories	10^5	10^5	10^6	$2 \cdot 10^7$
Analytical	n_f	$1.353 \cdot 10^{-1}$	$1.832 \cdot 10^{-2}$	$3.355 \cdot 10^{-4}$	$1.125 \cdot 10^{-7}$
	$r(R_f)$	0.0080	0.0232	0.0546	0.6666
	$r(R_m)$	0.0083	0.0160	0.0146	0.0244
	FOM_m/FOM_f	0.930	2.097	13.900	745
MCNP	n_f	$1.357 \cdot 10^{-1}$	$1.808 \cdot 10^{-2}$	$3.260 \cdot 10^{-4}$	$5.000 \cdot 10^{-7}$
	$r(R_f)$	0.0080	0.0233	0.0554	1.0000
	n_m	$1.342 \cdot 10^{-1}$	$1.811 \cdot 10^{-2}$	$3.344 \cdot 10^{-4}$	$1.129 \cdot 10^{-7}$
	$r(R_m)$	0.0083	0.0160	0.0147	0.0244
	FOM_m/FOM_f	0.81	1.76	14.9	1314

Table 4.2.1. Results of the optimal analytical and MCNP midway and autonomous forward estimation for a self-adjoint symmetric problem.

To address the optimization problem for this example numerically, the optical distance between the source and the detector was chosen to be 4 mfp. The midway coupling was performed at 9 midway planes positioned every 0.4 mfp between the source and detector. The dependences of the FOM number as a function of the midway plane position at different relative forward to adjoint workloads are shown in Fig.(4.2.1). It is seen that the FOM number is the highest in the middle of the system at the relative workload of unity, which agrees with Eq.(4.2.7) and Eq.(4.2.8) under the symmetry condition Eq.(4.2.10).

We observe, that if the midway coupling is performed at a midway surface, which is closer to the detector than to the source due to practical reasons, for example, than the relative forward to adjoint workload should be less than unity. Indeed, much less forward particles would penetrate up to the midway surface, which results in higher statistical uncertainty of their number. It is to be compensated by running more adjoint particle which are transported to the shorter distances.

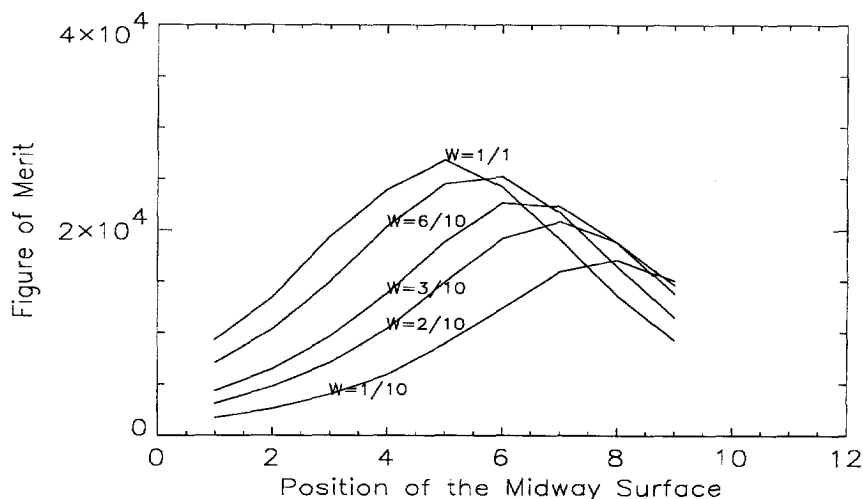


Figure 4.2.1 Midway MCNP calculation efficiency as a function of the midway plane position at different forward to adjoint workloads for a symmetric self-adjoint problem.

4.3 Symmetric Forward-scattering Problem; The Black Absorber Technique

It was mentioned in Chapter 3, that the choice of the midway surface in an analog midway Monte Carlo calculation will not influence the average time

per history of the forward and adjoint calculations. Indeed, particles of both types originate at points of the corresponding sources and followed until they get absorbed or leak out of the system. Truncating part of the geometry at the side of the midway surface away from the source in one of the two calculations will speed up the calculation, because the corresponding particles need not to be followed in the truncated part. The average computer time required to simulate this particle will reduce and the magnitude of the time reduction can depend on the midway surface choice.

Applying the black absorber technique in the scope of the midway Monte Carlo method is by definition the above truncation of the geometry. Such truncation is the only deviation from the analog midway Monte Carlo and Eq.(4.2.1) remains valid for the FOM number of our symmetric forward-scattering problem solved by midway Monte Carlo supplemented by the black absorber technique. Possible dependence of the computer time per history on the user-defined midway surface should be considered in Eq.(4.2.1), when the problem of the optimal midway surface and optimal relative workload is solved. In case of the adjoint black absorber technique, for example, the relative reduction g_a of the computer time, required to simulate a single adjoint history is proportional to the ratio of collision numbers in the truncated and original systems and depends on the attenuation position of the midway plane:

$$g_a = \frac{1 - \exp(-\alpha(d-x))}{1 - \exp(-\alpha d)} . \quad (4.3.1)$$

Attempts to optimize Eq.(4.2.6) supplemented by Eq.(4.3.1) analytically lead to a cubic equation, which solutions are difficult to interpret in the general form. Therefore, we apply here a recursive approach for the utilization of the analog Eq.(4.2.7) and Eq.(4.2.8) for optimization of the midway Monte Carlo calculations reinforced by one of the black absorber techniques. Iteratively found approximate solutions of the optimization problem can be considered as separate optimization models. For the reasons, which become evident from the following discussion, only two iterations were used.

The optimal parameters for the original analog problem are determined by the Statements of the optimal relative workload and the midway surface position from Section (4.2).

In our case the original problem is fully symmetric and the computer times per history τ_f and τ_a are equal. This results in an optimal relative workload of unity and the midway plane optically equidistant between the source and the detector midway plane in accordance with Eq.(4.2.7) and Eq.(4.2.8).

This optimal for the analog case surface is by definition used for *the first optimization model* in case with the black absorber. In this case, the ge-

ometry is truncated at the source side of the midway surface and the relative reduction in the adjoint history time is evaluated by means of Eq.(4.3.1). In accordance with the first optimization model the midway surface position is estimated to be at $x = d/2$. The estimated relative time reduction is used to re-optimize the relative forward to adjoint workload by Eq.(4.2.8) in accordance with the Statement of the optimal relative workload.

This relative time reduction is also employed by the *second optimization model*, where it is used in the second term of the right-hand side of Eq.(4.2.7) for the adjustment of the optical position of the midway surface. The correspondingly adjusted attenuation position is then used in Eq.(4.3.1) to account for the extra history time ratio adjustment, which by definition equals the relative workload of the second optimization model.

As it is seen, both models are based on the recursive utilization of the Statements of the optimal relative workload and the midway surface position from Section (4.2), which were developed for the analog case.

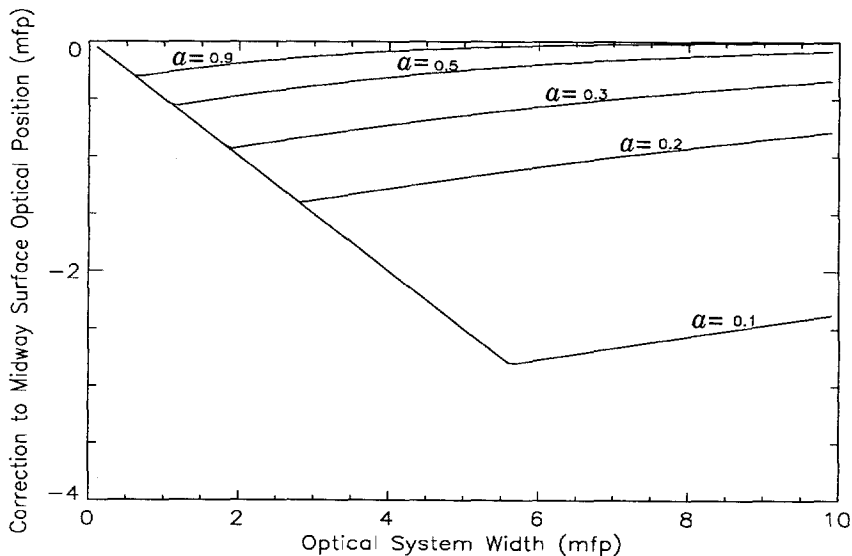


Figure 4.3.1. Corrections to the optical penetration distance between the midway surface and the source as a function of the optical system width due to adjoint history simulation time reduction effected by the adjoint black absorber technique at different absorption probabilities (2nd optimization model).

The attenuation position of the midway surface in accordance with the first optimization model is equidistant between the source and the detector. It is convenient to express the corrections to this position due to the second opti-

mization model in terms of optical distances to distinguish the dependencies from the absorption probability α . These corrections are shown in Fig.(4.3.1) as a function of the optical system width d at different absorption probabilities α .

The correction is seen to be negative, forcing the adjoint particles to be transported to larger distances than forward ones. The intrinsic constraint of the second model is that the correction may not exceed the optical half-width of the system. This constraint produces the diagonal line, which cuts off the left-hand side of the formal second model trends. However, this constraint is not a limitation of the second model approach for the black absorber technique optimization. It is rather a controversial demonstration of the important role of the black absorber technique for the midway Monte Carlo efficiency judgment. Indeed, utilization of the adjoint black absorber technique was directed on reduction of the adjoint workload by truncating part of the adjoint geometry. We recognize, however, that the smaller the optical width of the system, the lesser the part of the adjoint geometry that should be truncated and the more adjoint particles should be simulated, leading to degeneration of the midway Monte Carlo into the autonomous adjoint calculation.

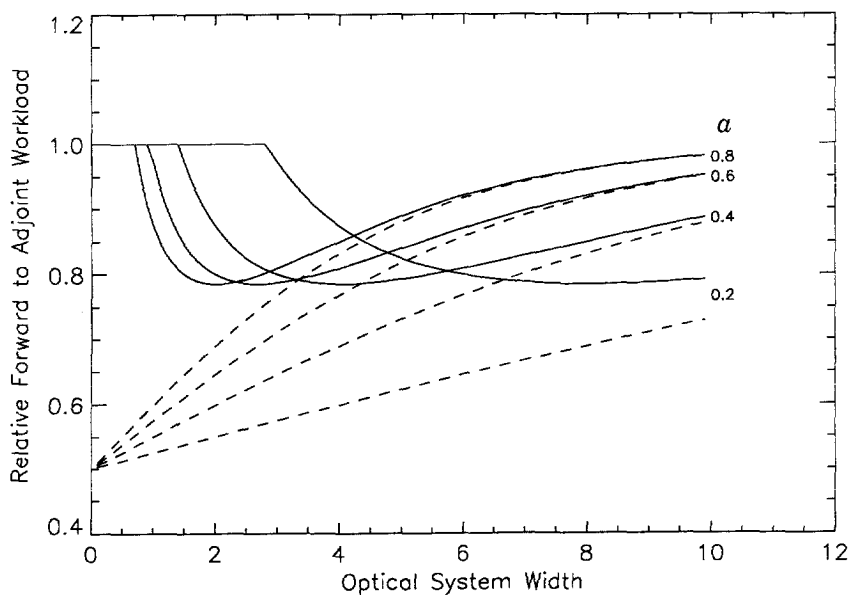


Figure 4.3.2. Reduction of the relative forward to adjoint workload as a function of the optical system width due to adjoint history simulation time reduction by 1st (- -) and the 2nd (—) optimization model.

In other words, in a system with a given absorption probability a , the position of the midway surface estimated by the second optimization model moves towards the source as the optical system width becomes smaller. At a certain moment the midway surface merges into the source surface and the forward calculation dies out of the consideration. Thus, using the black absorber technique we have demonstrated, that the midway coupling should not be applied in optically small systems.

The value of the constraint (minimum optical size of the system) depends on the absorption probability a . In systems with low absorption probability ($a \sim 0.1$) it is about 5-6 mfp. In systems with high absorption ($a \sim 0.9$) it is much less than 1 mfp. These problems are not difficult and should be solved by autonomous Monte Carlo.

Looking at Fig.(4.3.1) from another side, we realize that the larger the optical width of the system the smaller is the correction to be applied if the black absorber technique is used. In other words: the more difficult the problem is, the less we should bother about the correction of the midway surface position. If the absorption is sufficiently high, then the correction is small and there is little dependence of the correction on the system optical width itself - the correction can be ignored. This is explained by the fact, that the relative history time reduction in the systems with high absorption can be very small in accordance with Eq.(4.3.1).

Dependencies of the relative history time adjustments from the optical system width in media with different absorption probabilities a are evaluated by the first and the second optimization models and shown in Fig.(4.3.2).

The differences between the results of the two models in optically small systems are sharp. Actually, the first model directly suggests to increase the number of adjoint histories. In a limit of zero system optical width it suggests to run twice as much adjoint particles than forward ones. This is based on the fact, that the history of the forward particle is twice as long as the adjoint one (because even in this very small system adjoint geometry is truncated in the middle of the system), but the contributions of both particles are equal to each other (because they are counted at the same midway surface equidistant from the source and detector). In accordance with this model the time saved from running truncated adjoint histories is used to run more of them. The drawback of the model is, that there is no attention given to the fact that the saved time from running truncated adjoint histories can be used to transport them further towards the source.

By contrast the second model does consider this possibility and generally calls for less truncation. In optically small systems it does not promote any truncation at all, so that the midway surface merges into the source (bounding) surface. There is no sense to perform the forward calculation in this case, which in terms of the midway method results in zero relative forward to adjoint workload. Again, we come to the conclusion, that in optically small systems the midway calculation can degenerate into the

autonomous adjoint calculation by force of the adjoint black absorber technique applied in correspondence with the second optimization model. This degeneration takes place at an optical system width which is a decreasing function of the absorption probability α as mentioned earlier.

In a limit of infinitely large optical width of the system the two optimization models agree with each other and suggest, that equal numbers of forward and adjoint histories should be run. This is because of the strong (in our case - exponential) decrease of the particle flux in the optically thick system. The difference between the times, required for a particle to penetrate half of the distance and the whole distance becomes very small (see Eq.(4.3.1)).

At this moment it is interesting to look at the relative gain, provided by the midway Monte Carlo and the black absorber techniques with the parameters of the first and the second optimization model. The dependencies are shown in Fig.(4.3.3) as a function of the system optical width d at different absorption probabilities α .

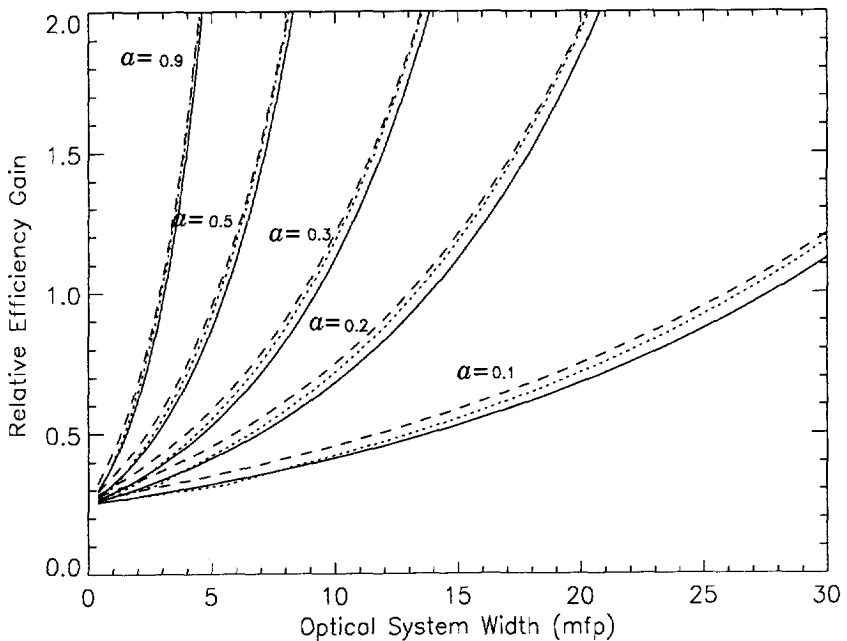


Figure 4.3.3. Relative efficiency gain as a function of the optical system width at different absorption probabilities α due to midway Monte Carlo: analog (—); adjoint black absorber truncation with the 1st (---) and 2nd (...) optimization model parameters.

It is seen that for highly absorbing systems the midway Monte Carlo method becomes very efficient in comparison with the autonomous calculation already at system optical widths of about 3 mfp. Additionally, the degree of scattering anisotropy in these systems does not play an important role. Therefore, the requirement of the forward-scattering can be ignored in systems with high absorption and the above analytical model can be applied for optimization of the midway method independently of the anisotropy.

For systems with high forward scattering and low absorption ($\alpha \sim 0.1$) the system should be as wide as 30 mfp. These optical widths correspond to the system attenuation width of about 2.77 in correspondence with Eq.(4.3.1). We observe also, that the supplementary black absorption technique does not help much to improve the FOM in the considered system and that the provided gain does not depend much on the optimization model chosen. The first optimization model is the easiest to apply, it shows the best gain and may be preferred in practice to the analog midway and, anyway, to the 2nd model optimization. The 2nd model served only as a mean to observe the tendency of the midway Monte Carlo method to degenerate into the autonomous Monte Carlo calculation in optically small systems.

Statement of the Midway Monte Carlo Applicability

The midway Monte Carlo method can serve as an efficient tool of Monte Carlo acceleration. The optimal parameters of the method can be determined by the Statements of the optimal relative workload and the midway surface position. Then the second optimization model should be applied to test the midway method applicability. If no degeneration into autonomous Monte Carlo is observed, the position of the midway surface remains unadjusted, but the relative workload is determined again by the Statement of the optimal relative workload for the case with the reduced computer history time due to black-absorber geometry truncation.

As it is seen, these conclusions emphasize the importance of the Statements of the optimal relative workload and the midway surface position not only for the analog midway calculations, but also for the calculations where the black absorber technique is used.

Besides that, we can formulate

First Statement of the Midway Monte Carlo Gain Essentials

Midway Monte Carlo is efficient in difficult penetration problems,

where difficult penetration problems stand for problems in optically large systems with high attenuation, or, in other words, for problems in systems with large attenuation width ($\alpha d \gg 1$).

4.4 Unsymmetric Problem with Isotropic Scattering

The analytical model considered above includes only mono-directional - forward - treatment of scattering. Applicability of this model to the isotropic case is justified only for systems with high absorption probability. The model does not allow any simple, for example tridirectional (Booth, 1996), form for the general case of anisotropic scattering. It does not also allow for isotropical scattering. It is also interesting to investigate the dependencies of the optimal midway and black absorber truncation parameters in presence of implicit capture and other variance reduction techniques such as, for example, exponential transform. These, in general, remain subjects for future research..

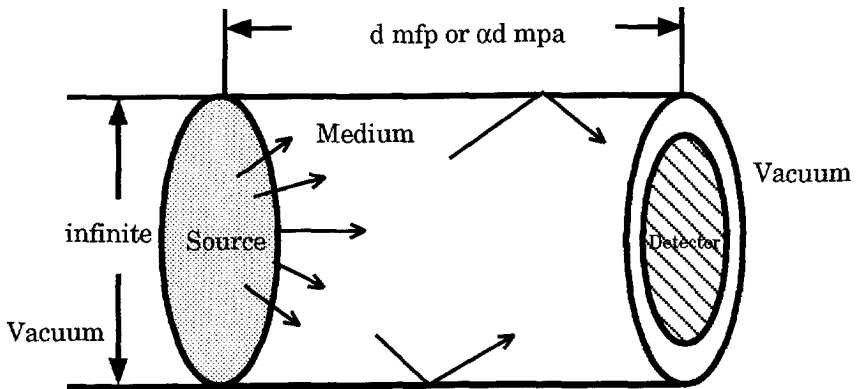


Figure 4.4.1. Unsymmetric Self-Adjoint Problem in a Finite Slab Geometry.

The next Chapters of this thesis are devoted to application of the midway Monte Carlo method to some realistic systems. These systems can be generally characterized by various degrees of scattering anisotropy, standard utilization of an implicit capture variance reduction technique in the corresponding Monte Carlo calculations and usually quite different sizes of the source and the detector domains. This Section is devoted to a *numerical* study of optimal parameters of the midway method and the black absorber

technique and the corresponding efficiency gain in the simplified systems. Since in the previous Section consideration was given to the case of the highly forward-scattering, here we consider only another extreme - isotropic scattering. The idea behind it is that the reality of other practical cases should be in between the conclusions drawn in the previous Section for the forward-scattering case and in this Section for the isotropic case.

The following example is aimed to demonstrate the dependence of the optimal FOM number on the midway surface position and the relative workload for a problem where the source and the detector have different sizes. We consider a practical case where the detector is smaller than the source. The source has 10 times larger area than the detector. The optical width of the considered system was chosen to be 8 mfp. The particles are now emitted isotropically. The sketch of the considered system is drawn at Fig.(4.4.1). The angular distributions of the functions to be coupled at the midway surface are highly anisotropic and 10 cosine bins are used to describe them. The surface binning is generally not required if at least one of the coupled functions does not show any spatial dependency at the midway surface. In this problem there is no spatial dependency of the forward current density at the midway surface and no surface binning is required. The transport operator of the problem does not change and the problem remains self-adjoint. The numerical simulations are performed using the autonomous forward and the midway options of MCNP. Capture is treated implicitly, which is the default feature of MCNP. The black absorber technique is not applied.

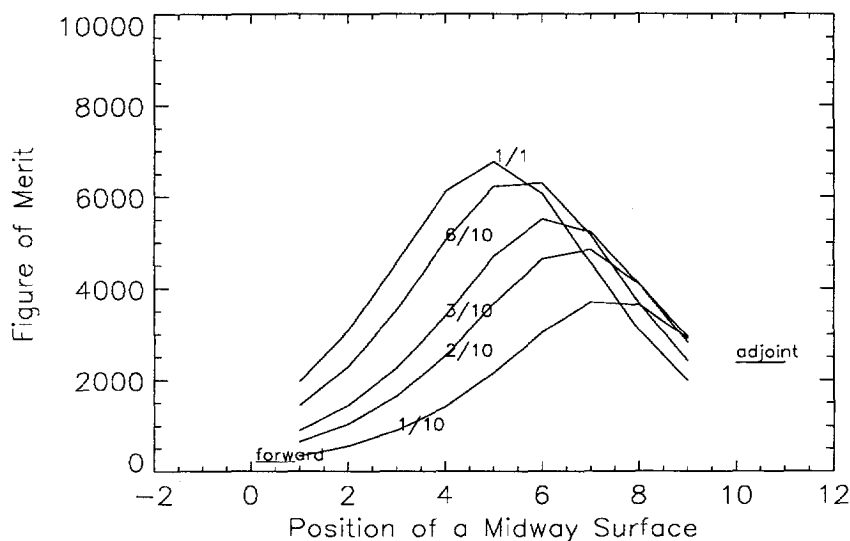


Figure 4.4.2 Midway MCNP calculation efficiency as a function of the midway plane position at different forward to adjoint workloads for a self-adjoint problem in case of the detector smaller than the source ($\alpha=1$).

The most important observation from the calculational results is that the position of the global FOM optimum is not affected by the fact that the detector size was considerably reduced. Indeed, the dependences of the FOM number on the midway plane position at various relative workloads for the case of unity absorption probability pictured in Fig.(4.4.2) demonstrate that the midway plane, positioned at equal distances from the source and the detector and relative workload of unity still provide optimal efficiency of the midway estimation. At the same time, the efficiency of the forward calculation is much lower than that of the adjoint one.

Actually, we have observed that

if the difference between the forward and adjoint source sizes is the only difference between the forward and adjoint calculations, then the optimal midway Monte Carlo calculation is the one which is performed at unity relative workload and which involves coupling at a midway surface placed equidistantly between the source and detector.

It is generally accepted (Lux and Koblinger, 1991; Wagner, 1994), that the adjoint Monte Carlo transport can be preferred to the forward one if the size of the detector region is smaller than that of the source. For this reason, one may tend to think, that for more efficient midway coupling in the problem with a smaller detector it is more favorable to run more adjoint particles and to transport them to larger distances than forward particles. It is, however, important to understand, that

if the detector is smaller than the source, then autonomous adjoint Monte Carlo calculation will have better efficiency than the autonomous forward Monte Carlo calculation not because the adjoint source is smaller than the forward source, but because the adjoint detector is larger, than the forward detector.

In the scope of the midway calculation, the reason for the observed preservation of the optimum position of the midway surface is that in both the forward and adjoint calculations the scoring takes place at the same midway plane and the size of the forward detector equals the size of the adjoint one. This brings us to an important conclusion, which can be formulated as in the following

Statement of the Midway Monte Carlo Optimal Parameter Essentials

Optimal parameters of the midway Monte Carlo calculation are not directly determined by the source and detector sizes. They are rather determined by the effective optical distance between the source and the detector.

In other words, variations of the source or detector sizes do not directly call for reoptimization of the midway surface and the relative workload of an optimal midway calculation.

Absorption Probability	Forward	Midway				
		without black absorber	with black absorber			
	FOM		Optimal Relative Midway Surface Position	Relative Forward to Adjoint Workload		FOM
				Preliminary Calculation	1st optimization model	
0.01	8787	3621	0.5	0.55	0.54	13245
0.1	2458	2312	0.5	0.8	0.85	8826
0.3	447	3143	0.5	1.0	0.95	3288

Table 4.4.1. Results of the autonomous forward, midway and black absorber MCNP estimates in systems with isotropic scattering (optical width 8 mfp).

The calculational efficiency for the above example can be further improved with the help of the adjoint black absorber technique. As it was already mentioned in the previous Section, in systems with high absorption probabilities a the degree of anisotropy should not strongly influence much the choice of the optimal parameters of the midway calculation improved by the black absorber technique. At the same time we have learnt, that the utilization of the midway method for highly absorbing systems can be of much support to enhance the efficiency of the Monte Carlo modeling. Additional utilization of the black absorber techniques does not provide a basis

for significant improvements. Here, therefore, we consider a system with low absorption probability and correspondingly high degree of isotropic scattering, where backscattering effects play a significant role. The values of a chosen for the example calculations are 0.01, 0.1 and 0.3.

The optical width of the investigated systems was chosen first to be 8 mfp. For all the three values of a the position of the midway surface and the relative workload were optimized. The parameters and results of the optimal calculations are presented in Table (4.4.1).

We observe, that in these isotropic highly-scattering problems utilization of the black absorber technique leads to much better efficiency, than the usual midway Monte Carlo calculation. Actually, for the cases of very low absorption probability $\alpha = 0.01$ and $\alpha = 0.1$, the usual midway method is not worth considering. At the same time if the black absorber technique is applied, the gain in FOM is in the first case about 1.5 and in the second case about 3.5 times. In the third case of considerable absorption the midway method runs well by, increasing the efficiency in 7.0 times, with only small improvement by the black absorber technique up to 7.3 times.

We note, that in all three cases it becomes more advantageous to run more adjoint particles. The position of the midway surface remains in the middle of the system. It seems to be insensitive to the presence of the black absorber. These qualities of the estimated optimal parameters look very much similar to those recommended by the Statement of the midway Monte Carlo applicability and the Statements of the optimal relative workload and the midway surface position, which were confirmed to work optimally in the case of highly forward-scattering systems. Moreover, the values presented in Table (4.4.1) on the optimal parameters obtained in accordance with these Statements almost coincide with the ones optimized by the midway option of MCNP.

To see, how the attractiveness of the midway Monte Carlo method and the black absorber technique behave as a function of the optical distance of the system we rerun the above problems for the systems with optical thickness of 16 mfp. The corresponding results are presented in Table (4.4.2).

Again we observe, that the above referenced Statements work well for optimization of the midway Monte Carlo method, not only in systems with strong forward-scattering anisotropy, but also in systems with isotropic scattering.

Since the considered system is optically very large, the pure midway Monte Carlo method loses only in the first case of very low absorption. The black absorber technique is a worthy supporter - it more than doubles the original FOM. In the second case ($\alpha = 0.1$), the midway method works very well - the gain is almost 16 times, which is again improved by the black absorber technique, so that the total gain is 26 times as large. The third case of considerable absorption with $\alpha = 0.3$ shows quite low autonomous FOM

of 0.64, which is improved by the midway by the factor of 190 and by the black absorber technique by 214.

The black absorber technique showed here considerable support of the analog midway Monte Carlo method in systems where back-scattering plays a significant role. Even in systems, where the analog midway method does not work, we are able to get significant gains in the Monte Carlo efficiency by utilizing this method.

Absorption Probability	Forward	Midway							
		without black absorber	with black absorber						
			FOM	Relative Midway Surface Position		Relative Forward to Adjoint Workload		FOM	
				Optimization					
				Trial and Error	Optimization Statement	Trial and Error	Optimization Statement or 1st optimization model		
0.01	2341	595	0.5	0.5	0.5	0.59	5446		
0.1	54	857	0.5	0.5	0.85	0.89	1414		
0.3	0.64	122	0.5	0.5	0.75	0.73	137		

Table 4.4.2. Results of the autonomous forward, midway and black absorber MCNP estimates in systems with isotropic scattering (optical width 16 mfp).

Generally, utilization of the forward and adjoint black absorber techniques can be governed by the following

Statement of the Black Absorber Technique Applicability

Utilization of the midway Monte Carlo method should normally be supported by one of the black absorber techniques to secure better efficiency. If the system happens to be highly absorbing, then the black absorber technique does not help much, but the midway method is advantageous itself. If the system happens to be highly scattering, then the midway method itself may be weak, but the black absorber technique helps so much, that the combination gives considerable gain. The decision whether the midway Monte Carlo should be used can be taken in accordance with the Statement of the midway Monte Carlo applicability. If applicable, the optimal parameters can be estimated in accordance with the Statement of the midway Monte Carlo applicability and the Statements of the optimal relative workload and the midway surface position.

The last question, which we study in this Section is a question of the midway method relative efficiency as a function of the differences between the size of the midway surface and the sizes of the source and the detector. We have seen earlier in this Section, that the large size of the scoring domain promotes utilization of the adjoint Monte Carlo in systems with large sources and small detectors. The principle of high Monte Carlo efficiency in systems with large scoring domains is also applicable to midway Monte Carlo calculations in systems with small sources and detectors. Actually, this principle forms the basis for

The Second Statement of the Midway Monte Carlo Gain Essentials

The midway Monte Carlo method is efficient in systems, where both the source and the detector are small.

We tested this statement by MCNP calculations for two systems with the absorption probability $\alpha = 0.5$. The optical system width for this calculations was 8 mfp. In both systems the source size equals the size of the detector, but they differ from problem to problem. In the second problem the areas of the source and the detector are 1000 times smaller than in the forward problem. In the first problem the source and detector sizes equal the size of the midway surface. No black absorber technique is used, i.e. the systems are fully symmetric.

The relative gain due to midway Monte Carlo for these two problems is shown in Table (4.4.3).

We recognize, that the efficiency of the FOM calculations almost does not depend on the source/detector size, which agrees with the expectations. Indeed, the scoring domain remains the same for all midway calculations,

and the size of the forward and adjoint source domains do not influence the efficiency. It is also observed, that the relative efficiency of the midway Monte Carlo method quickly grows as source/detector size decreases. It is important to understand, however, that

in problems where only one of the two (forward or adjoint) detector is small and the other one (adjoint or forward) is comparable in size with the midway surface, the midway Monte Carlo calculation will not show any specific advantages over the autonomous (adjoint or forward) Monte Carlo calculation, unless it is a difficult penetration problem or a problem with a complicated streaming path.

Relative Source/Detector to Midway Surface Area	1	0.001
Forward FOM	91	0.39
Midway FOM	1552	1307
Relative Efficiency Gain	17	3351

Table 4.4.3. Comparison of autonomous and midway Monte Carlo efficiencies as a function of the relative source/detector to midway surface area (optical width 8 mfp; $\alpha = 0.5$)

Problems with complicated streaming paths, just mentioned above, constitute the third class of problems, where the midway Monte Carlo method can be efficiently used. These are the problems with complicated streaming paths, which particles must follow from the source to reach the detector. Think, for example, of a system consisting of a scattering material, where the source and the detector are separated by a piece of black absorber of limited volume, so that particles must stream along side this volume. Detector responses are usually difficult to estimate in these systems, because the contributions require a chain of scattering events eventually leading to scattering towards the detector. The midway method provides a large scoring area, which can be reached much easier by both the forward and adjoint particles. We conclude this Chapter by distinguishing this class of problems in

Third Statement of the Midway Monte Carlo Gain Essentials

Midway Monte Carlo method is efficient in systems with complicated streaming paths from the source to the detector.

Chapter 5

Examples of Applicability and Efficiency of the Midway Monte Carlo Methods

*"Few things are harder to put up with than
the annoyance of a good example."*

Mark Twain (Samuel Langhorne Clemens)

Pudd'nhead Wilson (1894)

5.1 Introduction

The main purpose of this Chapter is to enhance the utilization of the midway forward-adjoint coupling capability in MCNP for different types of problems. To this end we provide examples demonstrating the usage, applicability, and validity and efficiency of the midway option in MCNP. We present a number of MCNP multigroup neutron and photon calculations to compare the forward, adjoint and the midway results with each other. All the calculations described in this Chapter were performed on an DEC Alpha Workstation 600 5/266.

5.2. A Difficult Neutron Problem

The following example has been used in a MCNP report (Wagner *et al.*, 1994) to demonstrate advantages of an adjoint importance generator (Wagner *et al.*, 1994) in the MCNP code. Neutrons are transported from a 25 cm radius disk source incident on a 60 cm thick slab of lead. The source has a

cosine angular density and a multigroup energy spectrum corresponding to the continuous density function

$$S_g = \int_{E_g}^{E_{g+1}} (E_{up} - E) dE, \quad (5.2.1)$$

over the range from 0.01 MeV to $E_{up} = 10.0$ MeV. The next-event estimator is used in the original problem at the detector placed 5 cm from the opposite side of the lead slab with an energy response $R_g = (E_g + E_{g+1}) / 2$ over the range from 0.01 to 10.0 MeV. Here E_g and E_{g+1} are the boundaries of the multigroup structure, corresponding to the 30-group MENDF5 library (Wagner *et al.*, 1994). A drawing of this configuration is provided in Fig.(5.2.1).

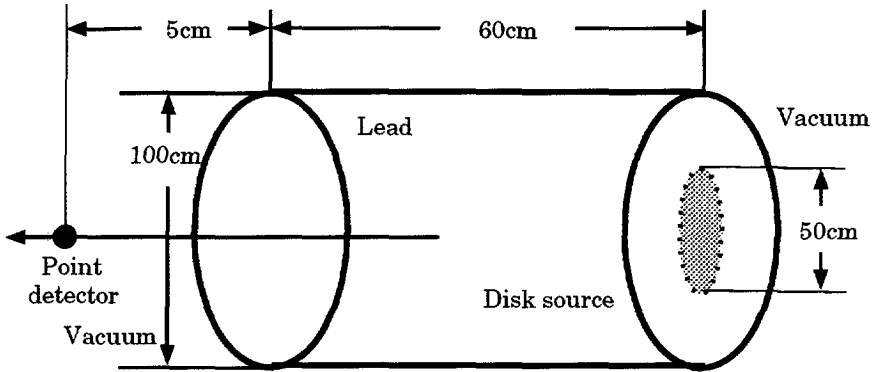


Figure 5.2.1 Configuration for a Reference Neutron Deep Penetration Problem

To perform this calculation in the adjoint mode, the user must first change the disk source into a surface current tally with energy response S_g and change the point detector into a point source with a spectrum defined by R_g . Due to the cosine angular density of the forward source, the disk source is replaced by a surface current tally, rather than by a surface flux tally.

This problem simulates deep penetration and therefore is rather computationally intensive in both forward and adjoint modes. The average over energy mean free path of lead was estimated by MCNP to be 3.72 cm as an

average over all the histories with the flux, so that the optical width of the system equals to 16.13 mfp.

The midway calculation is the combination of the above two calculations, with surface crossing tallies placed at a midway plane placed orthogonally to the problem axis between the source and the detector. The surface coupling was performed using 50 ring segments of 1 cm width each, described by 50 concentric cylinders along the problem symmetry axis. The number of cosine bins was set to 20 and the number of azimuthal bins to 10. The energy coupling was performed using the multigroup structure of the MENDF5 library. The adjoint black absorption technique was used.

The estimate for the absorption probability a can easily be determined by MCNP as the relative capture rate in an infinite system containing lead and an arbitrary source with density S_g . This estimated value equals 0.19. The estimated value of the adjoint to forward history computer times ratio τ_a/τ_f for the original problem was estimated by MCNP to be about 0.22. These two values were used for rough estimation of the optimal parameters of the midway method in accordance with Eq.(4.2.7) and Eq.(4.2.8). The relative workload was set to 0.22. The midway plane, placed originally at equal distances from the source and the detector was shifted towards the detector by $\text{abs}(\ln 0.22 / (2 \cdot 0.19)) \sim 3.98$ mfp or ~ 14.8 cm.

The optimized parameters were also obtained from a preliminary calculation with coupling at different distances at different workloads. The optimal position of the midway surface was found to be at 15 cm from the detector, which perfectly agrees with the analytical estimation. The optimal value for the relative workload was found to be 0.4, which is different from the analytical result. Still, the analytical value is a good estimate, since the relative difference in the FOM numbers due to these different estimates is only about 10 %. This comparison confirms once more the applicability of the Statements of the optimal relative workload and the midway surface position of the previous Chapter.

The first set of calculations were performed using only default variance reduction of MCNP. These calculations will be called analog in contrast with the calculations optimized by an importance function. The results of the forward, adjoint and midway analog simulation are compared in Table (5.2.1). The midway method shows a significant increase of the calculational efficiency: the midway FOM is 6 time higher than the FOM of the forward next-event estimation and almost 9 times higher than the analog adjoint estimation.

Additional increase of efficiency can be achieved by further optimization of importance functions, which is very often a cumbersome task to perform. The simulation efficiency of this deep penetration problem is increased in the report of Wagner *et al.* (1994) by utilizing an iterative procedure, which involves subsequent forward and adjoint generation of an optimal importance function. For comparison purposes we have used some intermediate

approximation of this importance function assigned by the authors of the reference report to be inversely proportional to a number of tracks crossing differentiated layers of the penetration medium. Midway importances in corresponding forward and adjoint calculations were set the same values except for the layers at the detector sides of the midway surface. Since the forward particles need not to penetrate up to the detector in the midway calculation, the importances in the regions were set decreasing from the midway surface to the detector. Utilization of the black-box technique automatically leads to zero adjoint importances in the layers at the source side of the midway surface.

	Midway Surface Crossing Estimator	Forward Next Event Estimator	Adjoint Surface Crossing Estimator
Flux $\times 10^6$, per history	9.8792	9.9427	10.032
Number of Forward Histories	4 000 000	1 000 000	-
Number of Adjoint Histories	10 000 000	-	10 000 000
Relative Error, r [R]	0.0039	0.0147	0.0160
CPU Time, T (min)	55.3	23.77	29.46
FOM $(r^2 [R] T)^{-1}$, min^{-1}	1162	186	132

Table 5.2.1 Comparison of Analog Monte Carlo Simulation Results obtained by different methods for a Difficult Neutron Problem.

	Midway Surface Crossing Estimator	Forward Next Event Estimator	Adjoint Surface Crossing Estimator
Flux $\times 10^6$, per history	9.8444	9.8248	9.8346
Number of Forward Histories	300 000	500 000	-
Number of Adjoint Histories	1 000 000	-	1 000 000
Relative Error, r [R]	0.0074	0.0103	0.0177
CPU Time, T (min)	9.77	32.47	11.71
FOM, $(r^2 [R] T)^{-1}$, min^{-1}	1857	282	272

Table 5.2.2 Comparison of Non-analog Monte Carlo Simulation Results obtained by different methods for a Difficult Neutron Problem.

The results of these improved calculations are presented in the Table (5.2.2). Optimization through an importance function improved the efficiency by roughly a factor of 2. However, the efficiencies of the optimized forward and adjoint simulation are still about 6 á 7 times lower than that of the analog midway method. The authors of the reference report used successive iterations to generate the importance function. It required some manual adjustments of the function inherited from the preceding iterations and allowed an additional efficiency gain of about a factor of 2.

So far, the much more straightforward and easy-to-implement midway method applied to the difficult neutron penetration and streaming to a small detector problem without any further optimization ensured an immediate and valuable gain in efficiency. This gain is impossible to achieve by means of other variance reduction techniques including a next event estimator and importances, which generation required also time, patience and experience.

5.3 A Difficult Photon Problem

This example involves photon transport through lead. The problem consists of a 20 cm radius spherical volume source, centered at the origin, enclosed in a 30 cm thick (~19.6 mfp; 1 mfp is about 1.53 cm) spherical shell of lead. The material of the source volume is also lead. The source spectrum extends over the energy range 0.50 to 20.0 MeV and is described by a given function. Two different setups of the problem are used. For the first setup the spherical symmetry of the problem is essential - the detector response is estimated in the forward mode as a flux crossing a 45 cm radius spherical surface. In the adjoint mode the detector response is estimated using the track length estimator in the volume of the spherical forward source domain. The problem is fully symmetrical and has only one coordinate. For the second setup there is no spherical symmetry, but a symmetry around an axis towards a point detector positioned on the axis, 45 cm from the origin. A drawing of both configurations is given in Fig.(5.3.1). The problem is adopted from the report of Wagner *et al.* (1994), where it has been used to illustrate the applicability of the adjoint mode in MCNP. Both setups describe the same problem and the detector responses are the same. It is interesting to distinguish between these two setups, because they have common features with applications of different nature. The first setup is an example of the calculation about a global radiation flow out of a "nuclear reactor" and represents a pure penetration problem. The second setup is an example of transport along various paths towards a small detector isolated from the source by an attenuating material.

Efficiencies of the forward Monte-Carlo calculations are different in this example due to the different estimators. The midway calculations for the

two setups will also have different efficiencies due to different midway surfaces, different surface segmentation, different angular dependences, and different sources in both forward and adjoint calculation. As a result the relative gains will also be different.

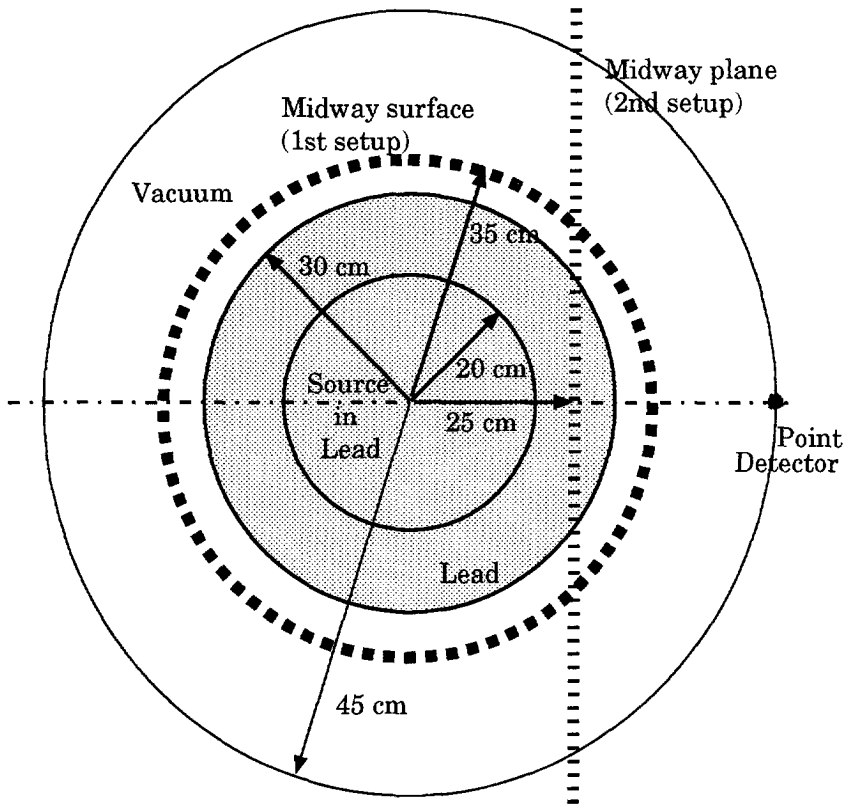


Figure 5.3.1 Configuration of the Reference Photon Problem

Starting from the first setup we immediately recognize, that the midway coupling does require neither surface segmenting nor azimuthal angle binning. The number of cosine bins was set to 10. The midway surface is simply a sphere with radius of 30 cm, which corresponds to the half-thickness of lead. The relative workload was set to unity, and no further optimization was performed as the gain due to the midway problem was sharp enough for this demonstration problem. The results are presented in Table (5.3.1).

The difference between the forward and adjoint efficiencies for this setup of the problem is not much pronounced. Despite the fact, that the adjoint detector is smaller (20 cm radius spherical volume) than the forward one (45 cm radius spherical surface), adjoint Monte Carlo works better, because a large number of forward photons is captured in the forward source volume itself. The rest of the forward photons pass quite easily through the

intermediate midway spherical surface of a considerable large radius of 36 cm, but only part of them are able to pass the optically remote detector surface.

Estimator	Midway Surface Crossing	Forward Surface Crossing	Adjoint Track Length
Flux $\times 10^{10}$, per history	4.60067	4.5260	4.5623
Number of Forward Histories	10 000 000	400 000 000	-
Number of Adjoint Histories	10 000 000	-	190 000 000
Relative Error, r [R]	0.0165	0.0167	0.0173
CPU Time, T (min)	31	480	270
FOM, $(r^2 [R] T)^{-1}$, min^{-1}	118	7.5	12

Table 5.3.1 Comparison of Monte Carlo Simulation Results for a Difficult Photon Deep Penetration Problem with Spherical Symmetry.

Upper Energy Bounds, MeV	Flux ₁ (n/cm ²)	Relative Error	Flux ₂ (n/cm ²)	Relative Error	Relative Difference between Midway and
	Forward		Midway		
1.0	8.69213 x 10 ⁻¹¹	0.0413	9.09912 x 10 ⁻¹¹	0.0256	4.68
2.0	1.38931 x 10 ⁻¹⁰	0.0297	1.45602 x 10 ⁻¹⁰	0.0219	4.80
3.0	1.08284 x 10 ⁻¹⁰	0.0325	1.09099 x 10 ⁻¹⁰	0.0266	0.75
4.0	5.33943 x 10 ⁻¹¹	0.0455	5.11846 x 10 ⁻¹¹	0.0339	-4.13
5.0	2.50305 x 10 ⁻¹¹	0.0664	2.55039 x 10 ⁻¹¹	0.0426	1.89
6.0	1.64393 x 10 ⁻¹¹	0.0814	1.67835 x 10 ⁻¹¹	0.0536	2.09
7.0	1.23290 x 10 ⁻¹¹	0.0941	9.78208 x 10 ⁻¹²	0.0646	-20.66
8.0	7.02305 x 10 ⁻¹²	0.1241	6.53382 x 10 ⁻¹²	0.0762	-6.90
9.0	2.95930 x 10 ⁻¹²	0.1925	3.48358 x 10 ⁻¹²	0.0941	17.72
10.0	1.28681 x 10 ⁻¹²	0.2887	1.10304 x 10 ⁻¹²	0.1284	-6.5
Total	4.52598 x 10 ⁻¹⁰	0.0167	4.60067 x 10 ⁻¹⁰	0.0165	1.65

Table 5.3.2 Comparison of Energy Spectra for a Difficult Photon Deep Penetration Problem with Spherical Symmetry.

Utilization of midway Monte Carlo results immediately in an increase of the FOM by almost a factor of 10 compared to the adjoint solution and more than 15 compared to the forward one.

The energy spectrum of the detector response was also determined in the forward and midway modes and the results are presented in Table (5.3.2). All but one (the seventh) of the relative differences listed in Table (5.3.2) are shown to be within the limits of one standard deviation of the statistical uncertainties. Turning to the second setup of the problem, we recognize that it appears to be quite difficult in all three Monte Carlo modes. The next-event estimation is employed in the forward calculation, but is not efficient enough, because of the large optical thickness of the problem.

Acceleration is provided by the midway Monte Carlo method, which is almost 50 times more efficient than the forward one and slightly more efficient than the adjoint one, as can be seen from Table (5.3.3). The midway surface is a plane orthogonal to the axis of the system, placed quite close to the forward source - at a distance of 22.5 cm from the center of the system - in order to allow the forward photons to contribute before they are absorbed. The surface is segmented using 100 concentric cylinders along the problem symmetry axis to ensure against biases. The numbers of cosine and azimuthal bins were both set to 5.

	Midway Surface Crossing Estimator	Forward Next Event Estimator	Adjoint Track Length Estimator
Flux x 10^{10} , per history	4.53585	2.8241	4.5615
Number of Forward Histories	4 000 000	100 000 000	-
Number of Adjoint Histories	10 000 000	-	10 000 000
Relative Error, r [R]	0.0695	0.1233	0.0326
CPU Time, T (min)	13.17	200.57	66.21
FOM, $(r^2 [R] T)^{-1}$, min^{-1}	16	0.33	14

Table 5.3.3 Comparison of Monte Carlo Simulation Results for a Difficult Photon Deep Penetration and Streaming to a Small Detector Problem with Axial Symmetry.

We observe, that the next event estimator traditionally employed in problems of this type does not promise any good - after running the problem for three and a half hours we still have a very unreliable estimate, which is almost two times lower than the expected value. The adjoint calculation works quite well and introducing the midway method helps only very little.

The optimal midway surface is found to be close to the surface of the source - at a distance of 22.5 cm from the center of the system - in order to allow the forward photons to contribute before they are absorbed and to transport the adjoint particles over longer distances. We recognize, that utilization of adjoint Monte Carlo for this problem is quite sufficient. Setting up and execution of one adjoint calculation is more simple than setting up, execution and coupling of the two adjoint and forward ones. Unfortunately for the adjoint approach, its utilization is not always as straightforward as in the above example. The difficulties associated with the autonomous utilization of adjoint Monte Carlo are almost unbearable in calculations which involve nuclear reactors. The midway method appears then to be an efficient remedy against these difficulties. These problems are discussed in Chapter 7.

5.4 Two Point Detectors

In this section we would like to illuminate the attractiveness of the midway Monte Carlo method in systems with multiple detectors.

		Midway Surface Crossing Estimator	Forward Next Event Estimator	Adjoint Surface Crossing Estimator
Total Number of Forward Histories		300 000	200 000	-
Total Number of Adjoint Histories		1 000 000	-	1 000 000
Total CPU Time, T (min)		15.49	15.51	22.88
First Detector	Flux $\times 10^6$, per history	9.84444	9.7288	9.8346
	Relative Error, r [R]	0.0074	0.0164	0.0177
	FOM $(r^2 [R] T)^{-1}$, min^{-1}	1179	238	140
Second Detector	Flux $\times 10^6$, per history	9.13175	9.0113	9.0651
	Relative Error, r [R]	0.0074	0.0153	0.0179
	FOM $(r^2 [R] T)^{-1}$, min^{-1}	1179	274	136

Table 5.4.1 Comparison of Non-analog Monte Carlo Simulation Results Obtained "Simultaneously" at Two Point Detectors by Different Methods for a Difficult Neutron Problem.

The sample problem is based on the neutron penetration problem of Section (5.2). The only difference in the problem setup is that the response should be determined at two detector positions. The first detector is placed at the original position - 65 cm from the source disk and the second detector 2 cm further away.

In order to accelerate all the calculations we use the importance function used in the non-analog calculations of Section (5.2). As we have seen, utilization of this importance function increased the efficiencies of the forward, adjoint and the midway calculation by about a factor of 2 and the relative efficiencies were not changed.

The efficiency of the Monte Carlo multiple response determination is defined for each detector as a FOM number by Eq.(3.1.10). Here $r[R]$ is the relative standard deviation of each Monte Carlo estimate and T is the total computer time required for determination of *both* responses. This definition of efficiency models simultaneous determination of the responses.

The obtained results are presented in Table (5.3.1). As it is shown in this Table the relative forward to adjoint workload used to generate the presented results is 3/10. The number of adjoint histories used for each detector was set to 500 000. The total computer time used to run the adjoint particles for the two detectors is approximately the same as the computer time in the forward part of the midway calculation. Here the Statement of the Optimal Relative Workload was applied, but it was also seen by running preliminary jobs, that the chosen value for the workload is the optimal one. The conclusion is that increasing the number of detectors does not necessarily mean increasing the time spent to run the adjoint particles. The optimal computer time used to run adjoint particles was preserved by running less adjoint particles for each detector and the total computer time spent in the midway calculation did not grow. Of course, the uncertainty associated with the modeled adjoint function for each detector at the midway surface is larger in case when less adjoint particles are run. However, this uncertainty is inversely proportional to the square of the number of particles, which is run for each detector. Generally, the midway FOM numbers will reduce slowly as a function of the inverse number of detectors. At the same time, the efficiency of the next-event estimates also slows down as the number of estimators grows, because tracking of the pseudo-particles associated with each estimator consumes much computer time. Efficiency of track length estimates does not generally depend on the number of estimators used in the problem and the midway method may loose in efficiency if the number of detectors is large. At the same time it is very important to note, that determination of a single detector response remains a difficult variance reduction problem in most applications of the Monte Carlo method and that problems of multiple response determination have secondary significance.

Chapter 6

Validation of the Midway MCNP Option against Neutron and Photon Benchmarks

*"Mr. Tunrbull had predicted evil consequences...
and was now doing the best in his power
to bring about the verification of his own prophecies."*

Anthony Trollope
Phineas Finn (1869)

6.1 Introduction

In this Chapter the midway Monte Carlo method and its realization in the MCNP code is validated against established benchmark problems. In our attempts to test the method we chose two of the most difficult neutron and photon benchmarks. Making this choice we also tried to cover a broad spectrum of applications. The sky shine benchmark problems, discussed in Section (6.2) is of concern for nuclear engineers dealing with the design of nuclear installations (Nason *et al.*, 1981). The oil well logging problems, as studied in Section (6.3) is of great importance for the oil and gas exploration engineering community.

6.2 The Skyshine MCNP Benchmark

To validate the applicability and demonstrate the high efficiency of the midway method, the method was applied to model the dose rates for the MCNP photon skyshine benchmark (Whalen *et al.*, 1991). Interest in the computation of gamma-ray exposure rates in air at large distances from concentrated gamma sources has arisen because air-scattered photon radiation (commonly referred to as "skyshine") arouses concern in the design of nuclear installations (Nason *et al.*, 1981). Until 1980, most skyshine

studies were concerned with fallout fields or involved complicated geometries that were difficult to model (Nason *et al.*, 1981). As a result, it was difficult to assess the accuracy of transport code models of skyshine fields from concentrated gamma-sources. Concern over the adequacy of such models prompted to conduct a skyshine benchmark experiment at a shielding research facility in the Kansas plains in 1980 (Nason *et al.*, 1981). In this experiment, a collimated gamma source was placed in an open field at ground level (see Fig.(6.2.1)). Dose rates of sky-scattered gamma rays were measured by detectors on the ground at different distances from the source.

In accordance with the MCNP benchmark (Whalen *et al.*, 1991), the photon dose rates of sky-scattered gamma rays from a collimated gamma source at ground level are subject to estimation at detector positions. This benchmark was chosen for study because it involves a combination of point detectors and complicated streaming paths and poses a difficult variance reduction problem. It was also chosen because of its relevance to the nuclear engineering shielding community. In the original Los Alamos report on the benchmark (Whalen *et al.*, 1991), the MCNP results for the dose rates were compared to the measured data.

Here, the reference autonomous forward and the coupled forward-adjoint midway calculations were performed and compared with each other. Because only the multigroup adjoint option is available in MCNP, all the calculations were performed in the multigroup mode of MCNP. The default MCNP multigroup library MGXSNP, which contains 30 neutron and 12 photon groups was used. The results of the autonomous adjoint calculation are not presented here because they appeared to be much less efficient than the results of the reference autonomous forward calculations. All the calculations were performed on an Dec Alpha Workstation 600 5/266.

6.2.1 The reference MCNP model

The reference MCNP model is a multigroup analog of the original continuous energy MCNP model for the benchmark described in the MCNP benchmark report (Whalen *et al.*, 1991). The report contains the MCNP input file for the reference calculation. Using the multigroup mode is the only difference of the reference model from the original MCNP model.

Above the ground the modeled system was bounded by a 1 km radius hemisphere placed at the origin of a cartesian coordinate system. A ^{60}Co point gamma source (1.33 and 1.17 MeV) was modeled about the center of origin. The source geometry guaranteed that the source photons would leave the source silo isotropically within a certain cone.

The next-event estimator was used to ensure sufficient statistics of the result. Eight concentric ring detectors centered at the origin were placed 1.0 m above and parallel to the air-ground interface. The radii of the ring detectors were 50 m and 100 m to 700 m at 100 m intervals. A single forward MCNP calculation was performed to estimate the responses of all 8 detectors.

Additionally, to improve the efficiency this model was strongly optimized by an importance function, which improves sampling. Generation of the proper importance function required further subdivision of the geometrical model into cells (see Fig.(6.2.1.1)). The regions that were directly irradiated by the source (i.e. within the source cone - the closest to the source) were partitioned into spherical-shell layer cells bounded by the source cone. The regions above the ground that received only scattered radiation were partitioned into segmented conical shell cells which were parallel to radiated out from the source cone. The regions beneath the ground were sliced into three flat disk cells. In total 19 cells and 20 surfaces were used in the model. This approach requires deep insight into the geometry and physics of the problem. Optimizing the importances was done by trial and error and required substantial effort and expertise.

Calculations were performed with and without importances.

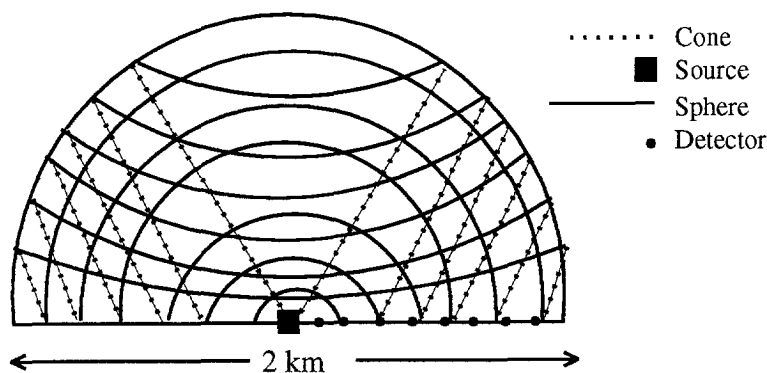


Figure 6.2.1.1 The gamma-ray skyshine benchmark: reference model setup (sketch above ground).

6.2.2 The Midway MCNP model

One forward and 8 adjoint calculations were performed to estimate responses of all 8 detectors. The adjoint input files for the 8 calculations differ from each other only by one value - the radius of the adjoint source ring corresponding to the 8 detectors of the reference forward model. Neither

the shape nor the position of the midway surface was optimized: the source cone used in the reference calculation was used as the midway coupling surface in all midway calculations. This cone was chosen because it separates all 8 detectors from the source (see Fig.(6.2.2.1)). This midway surface was segmented by 90 surfaces every 50 cm above the ground and 9 surfaces every 1 cm below the ground. The segmenting surfaces were planes orthogonal to the system axis. Sixteen angle cosines and sixteen azimuthal angles were used to model the angular dependencies of the coupled functions. Energy coupling was performed using the multigroup energy boundaries. The importance map was not used and there was no need for complex cell subdivision used in the reference model. The number of geometry cells used in the midway model was 7. Because the adjoint black absorber technique was applied, the importances of the cells which belong to the part of the model at the side of the midway surface away from the detector were set to zero in the adjoint calculation. The Statement of Optimal Relative Workload was used to estimate the optimal relative forward to adjoint workload. The estimated value appeared to be about 10/6 for all the detectors. Then short preliminary calculations were performed and proved that the chosen value is indeed the best one.

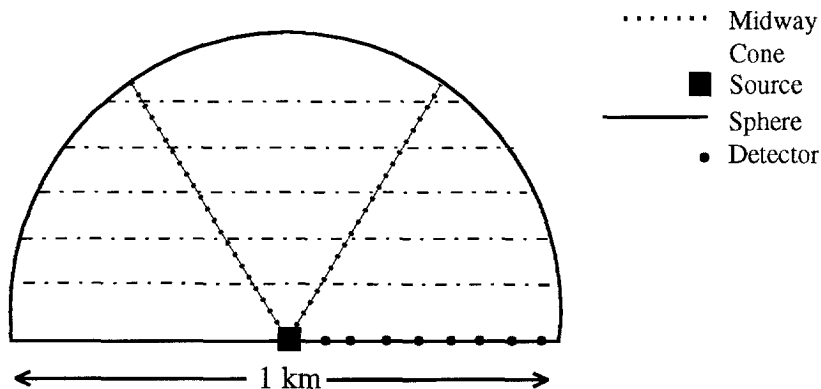


Figure 6.2.2.1 The gamma-ray skyshine benchmark: midway model setup (sketch above ground).

6.2.3 Comparison of Results and Discussion

The results of the calculations are presented in Table (6.2.3.1). It is observed, that all the midway estimates for each but the second (at 100 m distance from the origin) detector agrees with at least one of the two (default MCNP calculation or optimized by importances) within the estimated standard deviations. For the second detector it agrees with the other two estimates within the two estimated standard deviations. These results

Method	Optimization	Detector Position	Number of Histories Forward Adjoint		Dose Rate, MeV / cm ² / history	Relative Error, r[R]	CPU Time, T(min)	Figure of Merit, (R ² T) ⁻¹ , min ⁻¹
Forward Next Event	No	50 m	1 000 000	-	4.9363*10 ⁻¹⁵	0.0100	21.76	464
	Importances		1 000 000	-	4.8607*10 ⁻¹⁵	0.0070	63.23	320
Midway	Inferior		1 000 000	600 000	5.0430*10 ⁻¹⁵	0.0124	10.25	634
Forward Next Event	No	100 m	1 000 000	-	1.9985*10 ⁻¹⁵	0.0084	21.76	646
	Importances		1 000 000	-	1.9967*10 ⁻¹⁵	0.0063	63.23	394
Midway	Inferior		1 000 000	600 000	2.0705*10 ⁻¹⁵	0.0114	10.25	751
Forward Next Event	No	200 m	1 000 000	-	6.1701*10 ⁻¹⁶	0.0109	21.76	389
	Importances		1 000 000	-	6.1677*10 ⁻¹⁶	0.0073	63.23	295
Midway	Default		1 000 000	600 000	6.0689*10 ⁻¹⁶	0.0115	10.25	737
Forward Next Event	No	300 m	1 000 000	-	2.3147*10 ⁻¹⁶	0.0125	21.76	292
	Importances		1 000 000	-	2.3905*10 ⁻¹⁶	0.0091	63.23	192
Midway	Inferior		1 000 000	600 000	2.3642*10 ⁻¹⁶	0.0133	10.25	552
Forward Next Event	No	400 m	1 000 000	-	1.0069*10 ⁻¹⁶	0.0159	21.76	183
	Importances		1 000 000	-	1.0070*10 ⁻¹⁶	0.0093	63.23	183
Midway	Inferior		1 000 000	600 000	1.0123*10 ⁻¹⁶	0.0195	10.25	256
Forward Next Event	No	500 m	1 000 000	-	4.5112*10 ⁻¹⁷	0.0252	21.76	72
	Importances		1 000 000	-	4.5368*10 ⁻¹⁷	0.00125	63.23	102
Midway	Inferior		1 000 000	600 000	4.6203*10 ⁻¹⁷	0.0237	10.25	174
Forward Next Event	No	600 m	1 000 000	-	2.0877*10 ⁻¹⁷	0.0280	21.76	59
	Importances		1 000 000	-	2.1089*10 ⁻¹⁷	0.0138	63.23	83
Midway	Inferior				2.0318*10 ⁻¹⁷	0.0215	10.25	211
Forward Next Event	No	700 m	1 000 000	-	1.0181*10 ⁻¹⁷	0.0353	21.76	37
	Importances		1 000 000	-	1.0536*10 ⁻¹⁷	0.0208	63.23	37
Midway	Inferior		1 000 000	600 000	1.0245*10 ⁻¹⁷	0.0392	10.25	63
	Minor		1 000 000	600 000	1.0203*10 ⁻¹⁷	0.0220	10.39	199

Table 6.2.3.1. Comparison of Monte Carlo Simulation Efficiencies for the Skyshine Benchmark.

agree with the 1σ (68%) and 2σ (95%) confidence intervals (Briesmeister, 1993) obtained from the standard tables for the normal distribution function and demonstrates the unbiased nature of the midway estimate.

In accordance with the setup of the original benchmark problem the efficiency comparison was made for the problem when all the 8 detector responses were to be determined in as short as possible CPU time. In a sense this is an unfair approach for both the forward next-event and the midway methods. Indeed, in the forward autonomous calculation 8 different next-event pseudo-particles are tracked simultaneously, which considerably slows down the calculation. The computer time used for the adjoint part of the midway calculation is proportional to the number of the detectors, which also reduces the FOM. From another point of view, the autonomous forward problem was optimized by a single importances set for an "average" detector. Similarly, a single midway surface was used for coupling for all the 8 detectors. In contrast, however, the position of this surface was not optimized at all. Optimization of the relative workload did not require any expertise, but only one set of short preliminary forward and adjoint runs.

The gain provided by the importance function suggested in the MCNP report (Whalen, 1991) is very unclear. For 4 detectors the optimized calculation is worse than the unoptimized one, for 2 detectors the FOMs are equal and only for 2 detectors the optimized calculation is more efficient. In accordance with the authors of the original MCNP model for this skyshine benchmark problem, it required considerable insight into the problem and expertise to develop the complex setup of the geometry in order to set up the importance function. These results show, that after all utilization of the recommended importance function leads to an average gain of less than unity (0.94).

In contrast, the midway calculations show that a significantly higher efficiency can be achieved with the help of the easy-to-implement midway calculation to ensure sufficient statistics of the result with significantly less calculational and preparatory workload and experience. Indeed, we observe, that the midway FOM numbers are always higher, than the corresponding unoptimized and optimized autonomous forward ones. Compared to the unoptimized calculation the average gain due to the midway calculation is about 1.9 times and compared to the optimized one 2.1 times. Coupling at the first reasonable midway surface after very simple relative workload optimization gave significant FOM improvement for this problem. It is clear that coupling at different, optimally chosen midway surfaces for each of the detectors, can lead to further improvement of the FOM behavior. To demonstrate this we have included the fourth cone (counted from the source) of the reference problem into the midway model and rerun the problem to determine the response of the most remote detector by midway coupling at this surface. The results of this calculation are shown in the last row of the Table (6.2.3.1). The FOM number of this calculation is

more than 3 times higher than in the unoptimized midway calculation and more than 5 times higher than in the calculation optimized by the importances.

If the efficiency increase provided by the midway method is not sufficient, it is still possible to apply other variance reduction techniques (including an importance function) resulting in a corresponding additional gain.

The midway estimates of the detector responses have higher efficiencies than the autonomous forward and adjoint calculations because both forward and adjoint particles need to penetrate only about half the optical distance. Additionally, the scoring domain in the midway calculation is much larger than that in the autonomous forward and adjoint calculations. Despite the complexity of the streaming paths between the source and the detector, most of them cross the midway surface, contribute to the midway response and to the efficiency increase.

6.3 The Nuclear Oil Well Logging Tool MCNP Benchmark

Nuclear well logging is used to determine the lithology and fluid characteristics of the rock formation surrounding the borehole by using neutron or photon radiation sources. The radiation interacts with the materials in and around the borehole. Sensitive detectors are used to measure the scattered radiation. Interpretation of these measurements is required to assess the properties of the surrounding material. These interpretations are usually made based on benchmark measurements with the tool in a series of known borehole configurations, information from other logging tools, and detailed radiation transport calculations of the tool in the benchmark and downhole environments.

The purposes of the calculations are to predict and understand the measured results in as much detail as possible. In addition calculations can be used to provide tool responses where measurement standards do not exist. Consequently, environmental corrections to the tool response resulting from changes in downhole conditions can be modeled using accurate radiation transport calculations. These calculations can provide detailed insight into the response of the tool, which is crucial to designing new or improved nuclear tools.

Radiation transport calculations in nuclear well logging problems are rather difficult to perform. They are inherently three dimensional and represent medium to deep radiation penetration. Extremely accurate calculational results are needed to extract as much information as possible from the measurements.

Modeling these problems requires sophisticated multidimensional radiation transport techniques. To address the complexity of these problems both Monte Carlo and deterministic methods are widely used (Ullo, 1986; Soran, 1987). For many applications, however, Monte Carlo is the only choice (Ullo, 1986). Both general purpose and specific Monte Carlo codes have been used or developed for modeling well logging responses (Briesmeister, 1993; Chucas *et al.*, 1996; Ao, 1994). Particularly, the MCNP code (Briesmeister, 1993) is widely used for oil well logging calculations (Foster *et al.*, 1990).

Unfortunately, Monte Carlo calculations require long computer times to generate statistically converged results to sufficient precision in nuclear well logging problems, because

- the detectors involved have relatively small sizes compared to the sizes of the modeled formation
- they are basically medium to deep penetration problems for which adequate scoring statistics at particular detector locations can be difficult to obtain.

The requirement for small statistical uncertainty is very severe in logging calculations because small changes in a detector response, often no larger than a few percent, are important for evaluation of environmental variations. Therefore, Monte Carlo methods would not be practical for well logging applications unless variance reduction methods (Briesmeister, 1993; Chucas *et al.*, 1994; Mickael, 1995; Hendricks and Carter, 1985; Ao *et al.*, 1995) that enhance the sampling laws of those particles that have a high probability to contribute to a detector response are applied. The sampling laws are modified in such a way that the statistical uncertainty in the desired quantity is reduced. At the same time the estimation is also altered as to remove any bias from the estimator.

To demonstrate the applicability and high efficiency of the midway method in difficult oil well logging calculations, the method was applied to analyze the oil well porosity tool benchmark, which is one of the most difficult MCNP variance reduction tests (Brockhoff and Hendricks, 1994). It presents a model of a typical nuclear well logging tool and was chosen for this study to demonstrate the usefulness of the midway method for nuclear well logging calculations.

The problem configuration is shown in Fig.(6.3.1.1), which depicts a typical well logging configuration. The formation consists of limestone with 20% porosity. The generic tool is pushed up against the wall of the water borehole.

The tool sonde consists of solid iron and contains an Americium-Beryllium neutron source. Two detectors with different sizes contain ^3He at a pressure of 4 atm, and are placed at different distances from the source along the axis of the tool. The direction distribution of the source neutrons is de-

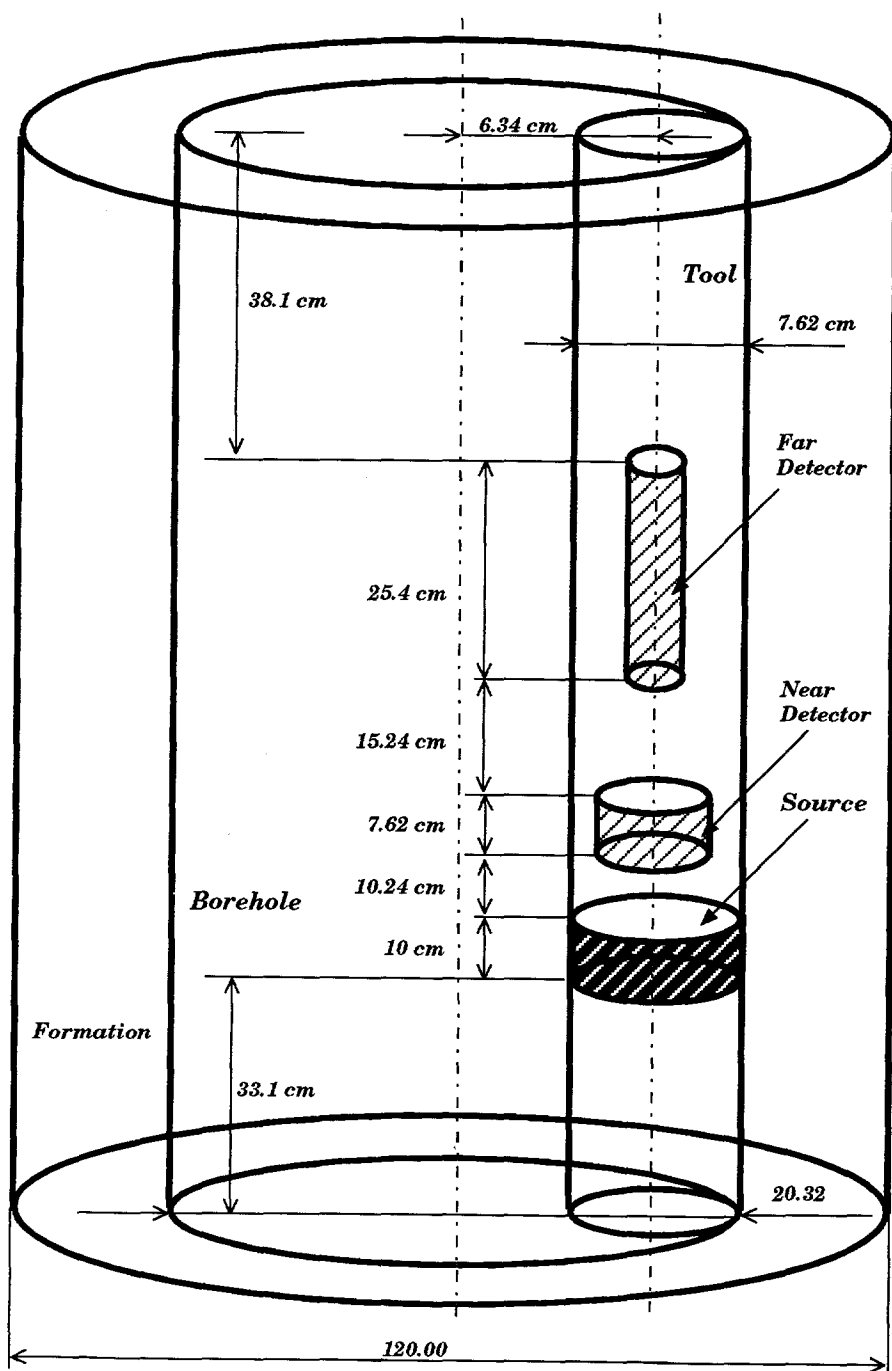


Figure 6.3.1.1. Benchmarking Oil Well Logging Porosity Tool Model

defined as proportional to $\exp(0.5\mu)$, where μ is the cosine between the direction of the emitted neutrons and the tool axis in the direction of the detectors. Neutron fluxes are to be determined in the detectors. The model contains no shielding.

6.3.1 The Reference MCNP model

The reference MCNP test model (Brockhoff and Hendricks, 1994) of the porosity tool required variance reduction to ensure sufficient statistics of the result. The original simulation was optimized with a set of weight windows (Briesmeister, 1993) to improve the efficiency of the results, generation of which required substantial effort. The medium was divided into small cells where average weight window values are assigned. Currently, there is no systematic way suggested for determining the number or the size of these cells (Mickael, 1994).

In order to represent sufficiently the importance function map, the problem was described by means of 231 cells and 24 surfaces, whereas for the analog model we used only 7 cells bounded by 13 surfaces. In the last case the cells and the surfaces are required to describe the geometry of the model. The weight windows were generated for the 231 cells by means of an adjoint diffusion code. The energy dependence of the importance function was described by 5 ranges. The generated weight windows are only applicable for the continuous energy calculations. Therefore both the analog and optimized calculations were performed in the continuous mode. One of the standard continuous energy MCNP libraries was used. All calculations were performed on a Dec Alpha Workstation 600 5/266.

6.3.2 The Midway MCNP Model

The midway calculations of the problem were performed without any variance reduction. Therefore, no cell subdivision for the importance map description was required for the original model geometry. The number of geometry cells used in the forward run is 10. Because the adjoint black absorber technique was applied for the midway adjoint calculation, the part of the model at the side of the midway surface away from the detector was ignored. Therefore in the adjoint calculation we used 6 geometrical cells.

Short preliminary midway runs were performed to optimize the midway plane position and the relative forward to adjoint workload. As a result, two different midway planes were chosen at positions 4 cm above the upper source surface for the near detector and 10 cm above the upper source sur-

face for the far detector. The same preliminary runs were used to determine the optimal forward to adjoint Monte Carlo workload by means of midway coupling at different intermediate forward and adjoint number of histories. The optimal ratio appeared to be about 1/8 for both detectors. Because the problem is essentially non-symmetric, the midway surface was segmented using 500 overlapping cylinders of 3 cm radius with their centers distributed on the midway surface. The number of cosine bins and azimuthal angle bins used for the midway coupling were 18 and 3, respectively. Both forward and adjoint midway calculations were performed in multigroup mode. The standard multigroup MCNP library MGXSNP (Wagner *et al.*, 1994) was used.

6.3.3 Comparison of Results

The reference and the midway calculations were performed in different - continuous and multigroup - modes using different data libraries. Therefore, it is generally difficult to expect a perfect agreement between these two types of calculations. Hence, comparison of the detector responses were made between the analog and optimized calculations for both (continuous energy and multigroup) modes independently. The requirement is that the estimated means of the detector responses agree with each other within the limits of the estimated standard deviations. For each mode the gain in efficiency due to the utilization of the corresponding optimization method (weight-windows or midway) were estimated. These relative efficiencies of the optimization methods were compared with each other.

The results of the calculations are presented in Table (6.3.4.1). It is observed, that the estimated detector responses for each mode perfectly agree with each other within the estimated standard deviations, which demonstrates the unbiased nature of both optimized results. The differences between the results of the continuous energy and multigroup calculational modes are attributed to the differences in the data libraries and are ignored for our purpose of efficiency comparison. For the near detector the gain in efficiency due to the midway optimization is about 8 times, whereas the corresponding gain due to the weight windows is only 1.4 times. For the far detector the efficiency gain due to the weight windows is about 8, but due to the midway method it is about 15.

6.3.4 Discussion

Weight-window optimization as performed by the authors of the original MCNP model for the benchmark problem required considerable insight into the problem and development of a complex setup of the geometry.

Detector Position			forward reference		forward	midway
			analog	weight windows	analog	analog
			continuous		multigroup	
near	Number of Histories	forward + adjoint	5 000 000	1 000 000	2 500 000	100 000 + 800 000
	Flux $\times 10^4$, $(\text{cm}^2 \text{ sec source particle})^{-1}$		5.1588	5.0604	4.7046	4.64810
	Relative Error, $r[R]$		0.0064	0.0140	0.0095	0.0116
	CPU Time, T (min)		689.50	105.68	171.9	15.19
	FOM, $(r^2 [R] T)^{-1}, \text{min}^{-1}$		35	48	63	491
far	Number of Histories	forward + adjoint	5 000 000	1 000 000	2 500 000	1 000 000 + 8 000 000
	Flux $\times 10^4$, $(\text{cm}^2 \text{ sec source particle})^{-1}$		6.2822	6.3027	4.2633	4.3289
	Relative Error, $r[R]$		0.0249	0.0230	0.0389	0.0014
	CPU Time, T (min)		689.50	105.68	171.9	143.41
	FOM, $(r^2 [R] T)^{-1}, \text{min}^{-1}$		2.3	18	3.7	56

Table 6.3.4.1. Comparison of Monte Carlo Simulation Efficiencies for the Oil Well Benchmarking Porosity Tool Model.

Then, it also required utilization of the weight-windows generator code, which often requires substantial effort and expertise. In contrast, the midway calculations show that a significantly higher efficiency can be achieved with the help of the easy-to-implement midway calculation to ensure sufficient statistics of the result with significantly less calculational and preparatory workload and experience.

Another attractive feature of the midway method utilization for nuclear well logging problems is that many practical modifications of the geometry and composition of the tool, borehole or formation models do not require adjustments of the midway model. In the case of a shifted detector in the tool or different porosity of the limestone, for example, there is no need to adjust the midway mesh structure. Often there will be also no need to adjust the relative forward to adjoint workload ratio or the position of the midway plane. We have considered two different midway planes only to ensure the maximum FOM for each of the two detectors separately, but in practice one coupling surface will often suffice. Thus, no additional expertise is required to obtain the efficient midway result for the adjusted problem. To utilize the weight windows additional expertise and time investments will be generally needed to change the cell map of the model and to generate the weight windows.

Further, in cases when the efficiency increase provided by the midway method is not sufficient, it is still possible to apply other variance reduction techniques (including weight windows) resulting in a corresponding additional gain. Just as in other deep penetration problems, the midway estimates of the detector responses in this oil well logging benchmark have higher efficiencies than the autonomous calculations because both forward and adjoint particles need to penetrate only about half the optical distance. Additionally, the midway surface is considerably larger than the sizes of the source and the detector, resulting in more probable scoring in the midway calculation, than in the autonomous forward and adjoint calculations. Despite the complexity of the streaming paths between the source and the detector, most of them cross the midway surface. Because the computer times are comparable with the ones of the autonomous calculations and the number of scores is much larger, the efficiency of the midway calculation is higher.

Chapter 7

Midway Applications to Interpretation of Experimental Data

"You know my methods. Apply them."

Sir Arthur Conan Doyle

Sign of Four (1890)

7.1 Introduction

This Chapter is devoted to applications of the midway Monte Carlo method to interpretation of experimental data. Two types of typical problems are considered.

The first type involves determination of the local neutron flux and activation rates in a core of a real nuclear reactor system. The core of the HOR research reactor of the Delft University of Technology in the Netherlands is considered. For these problems the attractiveness and applicability of Monte Carlo methods in general and of the efficient midway Monte Carlo method in particular for realistic in-core power and flux distribution determination are discussed.

The second type involves response determination of detectors, which are located outside of and relatively remote from the core of a nuclear reactor. Problems of this type are solved for two different reactor systems - the HOR reactor and the LFR reactor of the Netherlands Energy Research Foundation. Responses of both neutron and photon detectors are calculated for the Boron Neutron Capture Therapy facility of the LFR reactor. Consideration is given not only to the total neutron flux, but also to its energy dependence.

Wherever possible, calculational results obtained by the midway Monte Carlo method are not only compared with results obtained in the autonomous forward Monte Carlo calculation, but also with measured data.

7.2 Motivation for utilization of the midway Monte Carlo method for power distribution determination in a nuclear reactor

Accurate determination of the power distribution is important for reactor design and safety inspection. Lack of accurate knowledge about the power production and the conditions of heat transfer, i.e. uncertainties in determination of the power distribution together with thermal-hydraulic uncertainties leads to a situation where the reliable and safe operation of the fuel elements is possible only when the reactor is operated at a lower power level. Underloading of a power station leads to a considerable increase of the production costs.

The demand of high cost savings motivates developments of accurate power management systems. A modern management system includes experimental devices and computers for measurements and processing of in-core neutron reaction rate and coolant temperature data. It also includes computers employing physical models, nuclear and design data to perform flux, power and temperature distribution calculations. A trustworthy control system justifies the corresponding expenses by allowing to operate the reactor at the optimum power level.

Informational sources of the control system have associated errors. Different informational sources give different estimates of the same quantity. Calculations, in particular, have random errors associated with initial data (e.g. cross sections, number densities). Besides that, calculations have associated random methodical errors. They are methodical because they arise out of the deficiencies of the utilized calculational method. These deficiencies are to be found in the formulae of the mathematical method, discretization schemes, computer round off, truncations, etc. They can be treated as random (Fröhner, 1994), because only their average in a phase space of different methods or in a phase space of different reactor models behavior can, in principle, be predicted. In contrast to the random methodical errors of the calculation, experimental data have inherently associated random statistical errors. The randomness of these errors has a statistical nature: repeating the experiment several times will lead to different outcomes.

In a comprehensive data system the informational sources could be correlated with each other. If the average characteristics of the random uncertainty of each particular informational source and the degree of the correlation with the other sources are known, then better estimates for the desired quantities can be derived through informational *confluence* founded on Bayesian conditioning (Koroluk, 1985).

Properties of these approaches have been studied recently (Bryson *et al.*, 1993; Serov and Hoogenboom, 1996a). It is possible to describe how any

number of different correlated sources can be used in confluence and show how insight into the nature of the given source can help to obtain better estimates for different types of data associated with the source.

For example, the formulae for the case of two independent informational sources - calculation and experiment - were presented and employed by the author (Serov and Hoogenboom, 1994) for power distribution determination. An example of an integrated code system, based on this approach is the CONHOR system (Serov, 1993; Serov *et al.*, 1996f), which was developed for the HOR research reactor of the Delft University of Technology in the Netherlands to match the calculational results with the in-core experimental data through confluence.

The confluence approach is applicable if the random uncertainties associated with the calculation are known. Random methodical errors in flux and power distributions in nuclear reactors calculated by deterministic diffusion or transport codes and the degree of correlation between these errors are practically impossible to determine, because of the deterministic nature of the computer code. Indeed, use of initial data perturbation methods leads to estimation of the errors associated with these data. It is difficult to imagine how to perturb the method itself. This was, for example, the major difficulty of utilization of the confluence procedure in the CONHOR system, where the diffusion code CITATION (Fowler *et al.*, 1971) was employed for the neutron is calculations. In this respect, calculations based on Monte Carlo methods resemble experiments due to the statistical nature of these methods. The nature of the Monte Carlo method provides the basis for estimation of statistical uncertainties of a quantity side by side with the mean value of the quantity itself. Estimation of the degree of correlation between different quantities can be easily performed as well.

For this reason, the results of a Monte Carlo calculation can be used easily in confluence with the experimental data (Serov and Hoogenboom, 1994). More to that, the Monte Carlo method is known as inherently the most accurate: the uncertainties of the results can be reduced to zero if the Monte Carlo calculation lasts infinitely long.

However, in the usual procedure for flux determination in nuclear reactors, the experimental data consists of activation measurement results of very thin foils. For confluence with the calculation, the foil activation rates are to be computed. In contrast with deterministic calculations of detector responses in small volumes, utilization of Monte Carlo methods does not require any special approximations or additional discretization of the geometry around the foil.

From another point of view, analog Monte Carlo calculations of small detector responses in large reactor systems can be associated with a problem of taking very large computer time to generate statistically converged results to sufficient precision. In addition, the problem of a flux distribution determination requires response estimation in many foils located at differ-

ent positions in the core. The variance reduction techniques most suitable for the local response determination, namely the importance function and the next-event estimator may be associated with serious difficulties in problems of this type. Indeed, it is not possible to use more than one importance function in one calculation and one needs to solve a complicated problem of a multifunctional optimization. Use of a separate next-event estimator for every foil is possible, but may be very inefficient since tracking of the pseudo-particles associated with each of the foils consumes much computer time.

In these circumstances the efficiency of the Monte Carlo calculations can be improved by solving the adjoint transport problem instead of the forward one, because the size of each foil is much less than the size of the fission source domain (Hoogenboom, 1977).

For reactor systems which contain a multiplying medium, as it was already mentioned in the Introduction to this thesis, detector responses can in principle be determined by adjoint Monte Carlo as some functional of the adjoint function (Hoogenboom, 1977), but the method was shown to be associated with a practical disadvantage. Therefore, the detector response can be calculated in the adjoint mode by integrating the adjoint function, weighted with the fission source density over energy, direction and space in the source domain. However, the fission source in a Monte Carlo reactor calculation is not a pre-given analytical function, but rather a statistical distribution available from a prior forward eigenfunction Monte Carlo calculation at discrete values of space coordinates, energies, directions and weights of particles created at fission events. It is practically impossible to use it as a scoring function in case of an adjoint simulation and one needs to step towards deterministic discretization of the scoring (fission source) domain into a number of energy, position and direction meshes. The average source density and the adjoint flux can be accumulated for each mesh. If the reactor system is large, however, it can be very unwieldy and may require much computer and human resources to subdivide the whole volume of the source domain into small meshes in space, direction and energy. Additionally, the scores in such small meshes can be prone to large variances. Moreover, a large number of meshes can seriously decelerate the Monte Carlo calculation and the gain in efficiency expected from substituting the forward simulation by the adjoint one, may turn into a loss. From this we conclude, that the typically large fission source domain in the reactor system cannot be as efficient as expected, when the adjoint Monte Carlo method is preferred to the forward one because of the small detector size.

The midway method combines the beneficial features of the analog forward and adjoint Monte Carlo simulation:

- the fission source is replaced by virtual sources at surfaces surrounding every foil somewhere in its vicinity;
- the forward transport from the surfaces to the detectors is beneficially replaced by adjoint transport from the detector to the surface;
- if the surrounding material compositions of each of the foils up to the midway coupling surface are identical, then only one adjoint calculation is necessary to determine the responses of all the foils if the black absorbed technique is used.

These are the considerations in favor of using the midway Monte Carlo method for problems of power and flux distribution determination in nuclear reactors. The midway method can be used for efficient simultaneous determination of many detector responses. It also preserves all the main advantageous features of Monte Carlo: it is very accurate and provides information about the statistical uncertainties of its estimates. These features are of importance if the confluence with the experimental data is needed to obtain the best estimates of the desired quantities and the data of the calculation.

The problem discussed in the following Section deals with the application of the midway method to a real case of a foil activation rate determination.

7.3 HOR research reactor

HOR (Hoger Onderwijs Reactor) is a 2 MWth swimming pool type research reactor situated at the Interfaculty Reactor Institute in Delft, The Netherlands. It has plate type fuel elements made up of Al-U alloy with aluminium cladding. There are 19 plates in a fuel assembly separated by 3 mm of light water which acts as coolant and moderator. In the fuel assemblies containing a control element the central 9 plates are replaced by a single boron carbide powder plate of 1.25 cm thickness, which is surrounded by an aluminium clad. Horizontal cross sections of a fuel assembly and a control assembly as modeled for MCNP simulation are shown in Fig.(7.3.1).

The reactor is controlled by means of four control elements. The core grid plate has 43 positions, normally loaded with fuel elements including several reflector elements, containing BeO or Be-metal. In some positions of the grid outside the core there are experimental facilities. The MCNP model of the reactor horizontal cross section is shown in Fig.(7.3.2).

This model was developed recently (John *et al.*, 1996) and was used to act as reference for calculations with deterministic codes. For this purpose

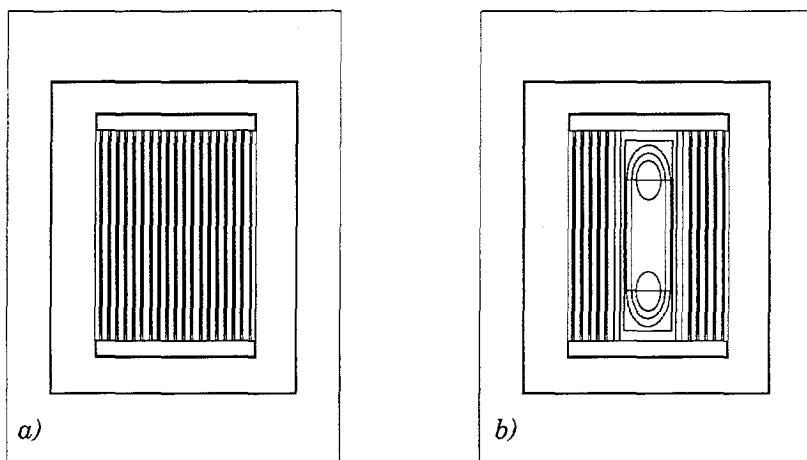


Figure. 7.3.1 Horizontal cross section of the HOR fuel (a) and control (b) assembly.

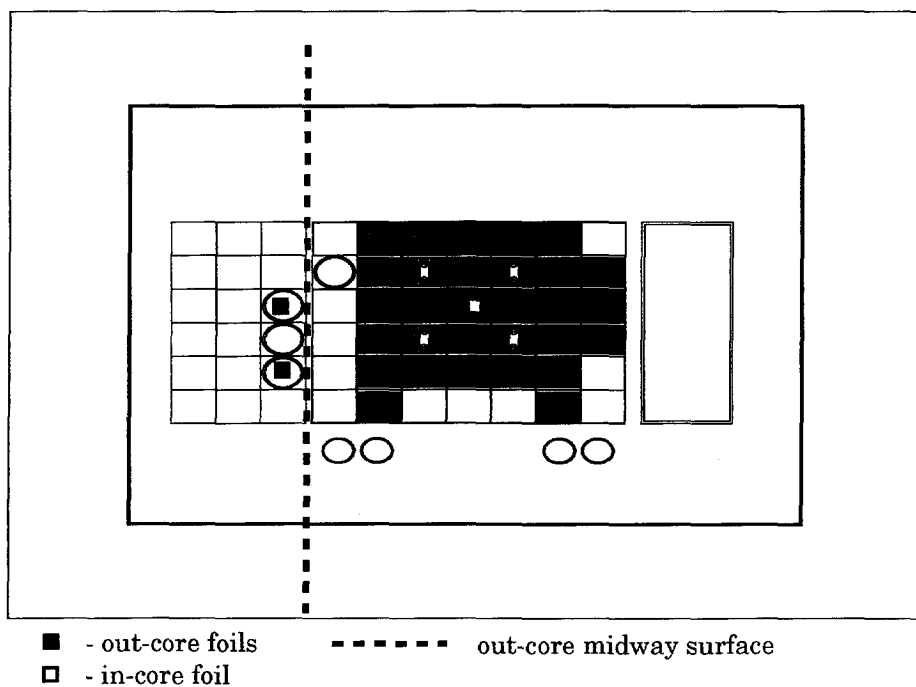


Figure 7.3.2. Horizontal model of the MCNP HOR model.

both continuous MCNPHOR_c and multigroup MCNPHOR_m libraries of cross sections based on JEF2.2 were generated (John *et al.*, 1996). This reference MCNP model of the HOR reactor was also used to predict responses of a number of activation detectors.

The actual value of a measured activity (counts) can be converted into the averaged experimental foil activation rate A_e . Calculational activation rates can be computed by MCNP (Briesmeister, 1993) as

$$A_c = \int_E \Sigma_\gamma(E) \phi(E) dE. \quad (7.3.1)$$

where $\Sigma_\gamma(E)$ is the (n, γ) reaction cross section of the detector material and $\phi(E)$ is the energy-dependent fluence (cm⁻² per source particle). The total number of neutrons N originating per second in the core at the nominal power of the HOR of 2 MW with the neutron yield $\nu=2.4$ and the energy release $E_f = 200$ MeV per fission equals to:

$$N = \frac{2.4 \cdot 2 \cdot 10^6}{200 \cdot 10^6 \cdot 1.602 \cdot 10^{-19}} = 1.5 \cdot 10^{17} \text{ s}^{-1} \quad (7.3.2)$$

The criticality calculations were performed by John (1996) with MCNP to generate a criticality fission volume-distributed source file (Briesmeister, 1993) for use in a subsequent MCNP calculation. In all the forward autonomous and midway calculations this file was used as the fission neutron source file.

7.3.1 In-core foil activation rate determination

Firstly we consider one of the in-core activation detectors, which are normally placed into the core in the beginning of each fuel cycle of the HOR reactor. Generally, aluminium stringers containing 6 detectors each are placed vertically into each fuel assembly in the water gap between the fuel plates in the beginning of every cycle. The detectors are gold foils of 10 mm diameter and a thickness of 0.05 mm. They are irradiated at the low power level of 10 Watt. Their responses are used to determine the neutron flux density in the reactor core (Brand *et al.*, 1971; Serov and Hoogenboom, 1994, Serov and Hoogenboom, 1996a).

For this study we considered a particular loading of the core with the reference number 9503 and the problem of a single foil response determination. The chosen foil is the one placed into the central fuel assembly 5 cm above the middle line of the core.

The reference MCNP model was extended to model the stringer containing the foil and the foil itself. To perform the midway calculation an ellipsoid surface was incorporated into the model. The ellipsoid enclosed the foil and was fenced by the water channel containing the foil, because it may not include any points containing fission materials. The diameter of the foil in the direction corresponding to the width of the water channel is 0.125 cm. In this direction the ellipsoid is segmented by 25 planes every 0.01 cm. The diameters of the ellipsoid in the other two directions were chosen to be 1 cm. For angular coupling 7 cosine and 7 azimuthal direction bins were used. The 172 multigroup structure of the MCNPHOR_m library was used for coupling of energy dependences. The adjoint black absorber technique was applied, so that the adjoint midway model includes only the foil and the ellipsoid as shown in Fig.(7.3.1.1).

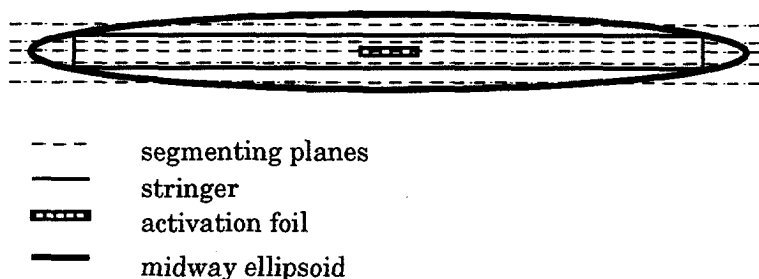


Figure 7.3.1.1. Adjoint midway MCNP model used for response determination of an in-core foil in the HOR reactor.

The forward autonomous and the midway calculations were performed to determine the neutron fluxes in the foils and the activation rates. The track length estimator was used in the forward autonomous calculation. An attempt to use the next-event estimator was not successful. The reason is that the core presents a relatively large highly-scattering medium with the fission source points in all the fuel plates including points remote from the detector position. It takes a very long time to track pseudo-particles originated in the vicinity of these remote source points towards the detector domain.

The diameters of the midway ellipsoid used in the midway calculations were not optimized. We attempted to optimize the relative forward to adjoint workload using the Statement of the Optimal Relative Workload, but it appeared not to work in this case. The Statement suggests that the computer time consumed in the midway adjoint calculation equals the computer time consumed in the midway forward calculation. The forward calculation which was performed first, took quite a long time - 324 min², because the fission source was to be sampled properly. Even after running the forward problem for so long, the virtual forward source at the midway surface is still associated with non-zero statistical uncertainty. Running the adjoint problem as long as the forward one appears to be unnecessary, because the adjoint problem is very simple and the distribution of the adjoint function at the midway surface converges quite quickly. After a certain moment, it is not worthy to run more adjoint histories: the adjoint function is converged, but the convergence of the forward one is fixed. Therefore, a short preliminary adjoint run was performed to optimize the relative forward to adjoint workload, which appeared to be about 2. Finally, the optimal adjoint calculation took about 6 min or less than 2% of the total computer time required for the midway calculation. The Statement of the Optimal Relative Workload does not work, because the size of the midway ellipsoid is limited by the width of the water channel surrounding the foil.

Method	Number of Histories		Total Flux, cm ⁻² s ⁻¹	Relative Error, r[R]	CPU Time, T(min)	Figure of Merit (r[R] ² T) ⁻¹ , min ⁻¹
	Forward	Adjoint				
Forward	2 000 000	-	3.7973*10 ¹³	0.0909	324	0.37
Midway	2 500 000	5 000 000	4.0136*10 ¹³	0.0495	330	1.2

Table 7.3.1.1. Neutron Fluxes in the In-core Activation Foil in the HOR Reactor obtained in the Forward Autonomous and Midway MCNP Calculations.

The calculated foil fluxes are presented in Table (7.3.1.1). The calculated and measured activation rates are shown in Table (7.3.1.2). The agreement

² All the calculations described in this Chapter are performed on a Dec Alpha Workstation 600 5/266.

between the forward, midway and experimental data is very good - the results agree with each other within the limits of the statistical uncertainties. We observe, that the efficiency of the performed midway calculation is more than 40 times higher than the efficiency of the corresponding forward calculation. This gain is expected to be even better if the diameters of the midway ellipsoid are optimized.

Method	Number of Histories		Activation Rate, s^{-1}	Relative Error, $r[R]$	CPU Time, $T(\text{min})$	Figure of Merit $(r[R]^2 T)^{-1}$, min^{-1}
	Forward	Adjoint				
Experiment	-	-	$1.70 \cdot 10^{-10}$	0.10	-	-
Forward	2 000 000	-	$1.982 \cdot 10^{-10}$	0.2109	324	0.07
Midway	2 500 000	5 000 000	$1.957 \cdot 10^{-10}$	0.031	340	3.1

Table 7.3.1.2. Activation Rates in the In-Core Gold Foil in the HOR Reactor obtained in the Activation Measurement and in the Forward Autonomous and Midway MCNP Calculations.

The fact, that running the adjoint problem is very cheap favors utilization of the midway method for calculation of accurate flux and power distributions. Indeed, one can place as many midway ellipsoids in the MCNP model of the HOR reactor as there are experimental foils. Only one forward calculation is necessary to accumulate the virtual surface source at all the ellipsoids. The time necessary to run adjoint problems to determine the response of each foil is proportional to the number of foils, but since every single adjoint run is very short, the total computer time necessary to run the adjoint histories originated at all the foils will not be high. Additionally, it is important to note, that the employed relative workload of 2 is optimal only for the case of one detector response. In the problem with multiple detectors it is likely to be higher (less adjoint histories will be "recommended" to run per each detector) so that the total computer time spent on adjoint histories will remain limited.

Application of the midway method to determination of the entire flux distribution does not make up a part of this research. Yet, in this Section we studied a real case of foil activation rate determination and proved in case of the HOR reactor, that the Monte Carlo calculations accelerated by the midway method can be beneficially used for flux and power determination

just by repeating the above calculations for every foil. The confluence with the experimental data (see Section (7.2)) can then be performed to obtain the best estimates if the coefficients of correlation between the estimated foil responses are estimated next to their mean values and relative errors. This can be a subject for future research.

7.3.2 Out-of-core foil activation rate determination

Activation measurements are regularly performed outside the core of the HOR reactor. Detectors are placed at positions in the grid specially reserved for experimental facilities. The grid positions, where the activation responses and fluxes were calculated are marked in Fig.(7.3.2). These positions are separated from the core by a considerably thick layer of water, resulting in a detector response determination problems of medium to deep penetration. The detectors are very small gold foils - 10 mm in diameter and a thickness of 0.05 mm, which makes the problem even more complicated.

Method	Foil	Number of Histories		Total Flux, $\text{cm}^{-2}\text{s}^{-1}$	Relative Error, $r[R]$	CPU Time, T (min)	FOM $(r[R]^2T)^{-1}$, (min)
		Forward	Adjoint				
Track Length	1	2 000 000	-	$3.559 \cdot 10^{12}$	0.0375	327	2.2
Next Event		2 000 000	-	$3.548 \cdot 10^{12}$	0.0089	1137	11.1
Midway		2 000 000	1 000 000	$3.515 \cdot 10^{12}$	0.0097	397	27
Track Length	2	2 000 000	-	$3.455 \cdot 10^{12}$	0.0376	327	2.2
Next Event		2 000 000	-	$3.281 \cdot 10^{12}$	0.0099	1137	8.9
Midway		2 000 000	1 000 000	$3.354 \cdot 10^{12}$	0.0091	408	29

Table 7.3.2.1. Neutron Fluxes in the Out-of-core Activation Foil in the HOR Reactor obtained in the Autonomous Forward and Midway MCNP Calculations.

The original MCNP model described in Section (7.3.1) was used in calculations to predict the fluxes and activation rates at the positions of two out-of-core detectors. The track length and the next-event estimators were used in separate runs of the reference calculations in order not to influence each other efficiencies. Also, a midway plane was placed between the core and detectors and the virtual forward source at this surface was modeled by performing the forward midway calculation. The midway plane is shown in Fig.(7.3.2). For the midway coupling, the midway plane was segmented using the fish scales technique. One hundred thirty seven overlapping cylinders with a radius of 5 cm and centers shifted with respect to each other centers were used to cover the area of about 2500 cm^2 . The number of direction cosine bins used for directional coupling were 7. The 172 multi-group structure of the MCNPHOR_m library was used for coupling of energy dependences. The normalization factor of Eq.(7.3.2) was used in all the calculations.

Autonomous forward and midway forward calculations were performed with the fission volume source prepared in a preliminary criticality run. A short preliminary adjoint run was used to determine the optimal forward to adjoint Monte Carlo workload by means of midway coupling at different intermediate forward and adjoint numbers of histories. The optimal ratio appeared to be about 1/2. This ratio was also obtained by the Statement of the Optimal Relative Workload.

Method	Neutron Detector	Activation, s^{-1}	Relative Error, $r[R]$
Experiment	1	$1.50 \cdot 10^{-13}$	0.10
Forward Track Length		$1.6109 \cdot 10^{-11}$	0.032
Midway		$1.5518 \cdot 10^{-11}$	0.003
Experiment	2	$1.42 \cdot 10^{-11}$	0.10
Forward Track Length		$1.4729 \cdot 10^{-11}$	0.033
Midway		$1.3201 \cdot 10^{-11}$	0.004

Table 7.3.2.2 Comparison of foil Activation Rates in the Out-of-core HOR Activation Detectors.

The fluxes at the detectors were calculated and are presented in Table (7.3.2.1) together with the relevant data for the efficiency comparisons. MCNP is able to calculate the neutron activation rates in the foils auto-

matically using Eq.(7.3.1). Experimental activation rates were also computed based on the measured numbers of counts. The calculational and experimental results are presented in Table (7.3.2.2). First of all, it is observed, that the midway estimates for both detectors agree with the results of the reference calculations within the estimated standard deviation. Secondly, both the autonomous forward and the midway results agree with the experiment within 2 standard deviations. The latter proves, that both the reference and the midway models of the HOR reactor including input data as number densities and cross sections from the multigroup library MCNPHOR_g can be successfully used for accurate modeling of experiments external to the core.

7.4 A Boron Neutron Capture Therapy Facility

7.4.1 Introduction

Boron Neutron Capture Therapy (BNCT) is a potentially effective therapeutic method for malignant tumors. This therapy is based on introduction of boron nuclei into malignant tissue and subsequent irradiation of these nuclei by thermal neutrons, which results in killing the tumor cells by the energetic ^4He and ^7Li particles produced in the $^{10}\text{B}(n,\alpha)$ reactions. Calculations of radiation dose distributions are required for neutron beam design and performance analysis, for various radiobiological and biochemical studies and eventual human clinical trials of BNCT.

Radiation transport calculations of physically realistic neutron and photon radiation dose distributions for BNCT are rather difficult to perform. They are inherently three dimensional and represent deep radiation penetration. The results of these calculations should be very accurate and provide a reliable link with the real world.

Modeling these problems requires sophisticated multidimensional radiation transport techniques. To address the complexities of these problems both Monte Carlo and deterministic methods are widely used (Wheeler and Nigg, 1992). In many BNCT design projects Monte Carlo methods are preferred to the deterministic ones (Liu en Brugger, 1994; Liu, 1995; Vroegindeweij *et al.*, 1996). Unfortunately, the following characteristics of BNCT calculations make them difficult to perform:

- the detectors involved have relatively small sizes compared to the sizes of the modeled system

- they are basically deep penetration problems for which adequate scoring statistics at particular detector locations can be difficult to obtain.

At the same time the requirement for statistically reliable estimates is very severe in BNCT calculations because small changes of composition and position of the irradiated material are important for proper preparation and application of BNCT. Therefore, Monte Carlo methods would not be practical for BNCT applications, unless variance reduction methods (see, for example, Booth, 1985) are used.

Both general purpose and specific Monte Carlo codes have been used or developed for modeling BNCT problems (Briesmeister, 1993; Wheeler and Nigg, 1992). The MCNP code is one of the most commonly used codes for BNCT applications (Liu and Brugger, 1994; Liu, 1995; Vroegindeweij *et al.*, 1996).

Responses of neutron and photon detectors in the BNCT facility at the Low Flux Reactor (LFR) of the Netherlands Energy Research Foundation (ECN) were determined by the midway option of MCNP. The setup and the results of these calculations are described in this thesis and elsewhere (Serov *et al.*, 1996e) and compared to the experimental data and the reference calculation (Vroegindeweij *et al.*, 1996).

7.4.2 Application

The Low Flux Reactor of the Netherlands Energy Research Foundation ECN in Petten is a thermal research reactor of the Argonaut type with a nominal power of 30 kW. The reactor consists roughly of a ring-shaped core, an inner cylindrical graphite reflector and an outer graphite reflector. Recently, the thermal neutron BNCT facility was developed and constructed at the LFR. The development study of the thermal facility was performed by the Monte Carlo code MCNP and described by Vroegindeweij (1996).

Because only the multigroup adjoint option is available in MCNP, the reference autonomous forward and the coupled forward-adjoint midway calculations were performed in the multigroup mode of MCNP. The default MCNP multigroup library MGXSNP, which contains 30 neutron and 12 photon groups was used. The reference MCNP model of the LFR reactor at the BNCT facility used in our calculations is a multigroup analog of the original continuous energy MCNP model. To demonstrate the applicability and high efficiency of the midway method in the difficult BNCT calcula-

tions, the midway method was used to predict the neutron and photon detector responses of the thermal neutron facility.

A horizontal cross section of the MCNP model used in the autonomous forward reference calculation and in the forward midway calculation is presented in Fig.(7.4.2.1). The dotted line indicates the midway coupling surface, which was used in the midway calculations. This is one of the planes between the core and the thermal facility already present in the reference models. Because the adjoint black absorber technique was applied, the geometry in the adjoint midway model was cut by the midway plane as shown in Fig.(7.4.2.2).

Autonomous forward and midway forward calculations are performed in the neutron-photon coupling mode with an external neutron source, which was taken from fluence rate measurements (Kraakman, 1982). The track length estimator is used in the reference calculation to determine the total and group neutron fluxes and total photon fluxes at 4 detector positions. The detectors are Au, Cu, Mn and Ni foils, which were placed and irradiated in the facility. Neutron activation rates in these foils were also calculated.

The reference MCNP model required variance reduction to ensure sufficient statistics of the result. The original simulation was optimized with a set of weight windows for an "average" neutron detector to improve the efficiency of the results. Generation of the weight windows was performed by the MCNP weight-windows generator (Briesmeister, 1993). The use of this generator is not straightforward and requires considerable expertise and insight into the problem.

A short preliminary adjoint run was used to determine the optimal forward to adjoint Monte Carlo workload by means of midway coupling at different intermediate forward and adjoint numbers of histories. The optimal ratio appeared to be about 1/2. Because the neutron and photon flux and current distributions are essentially non-symmetric at the midway plane, the midway surface was segmented using 136 overlapping cylinders of 5 cm radius³ with their centers distributed on the midway surface around its center. It is interesting to note, that the midway surface segmenting structure is the same as used for the HOR out-of-core foil calculations (see Section (7.3.2)). The rest of the midway plane was not subdivided into segments. The number of cosine bins used for the midway coupling was 10. Energy coupling was performed using the multigroup energy boundaries. All the calculations were performed on a Dec Alpha Workstation 600 5/266.

³ The neutron mean free path in graphite surrounding the midway plane is about 2.5 cm

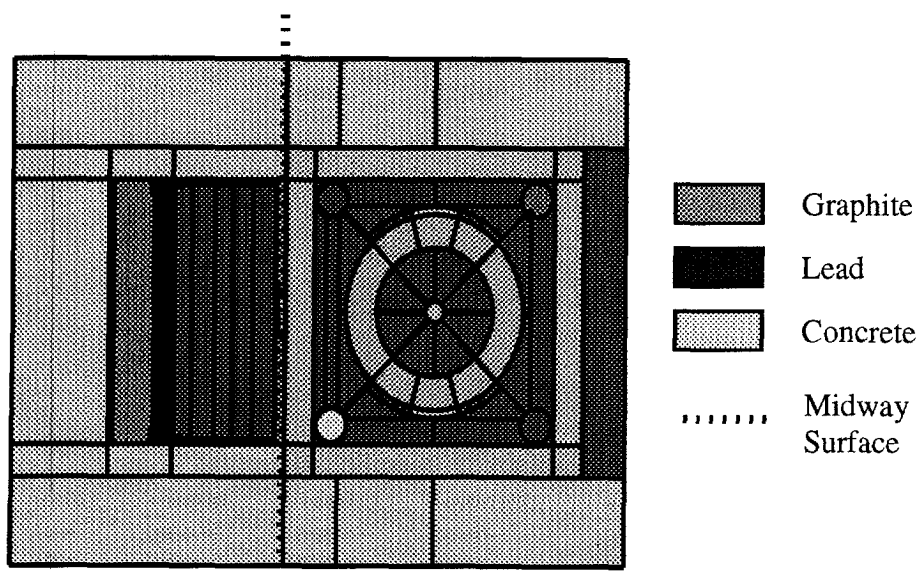


Fig.7.4.2.1 Horizontal cross section of the reference and the midway forward MCNP model

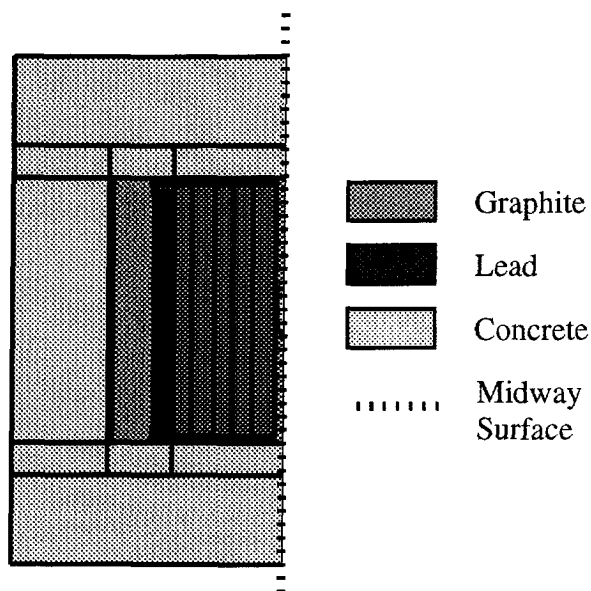


Fig.7.4.2.2 Horizontal cross section of the midway adjoint MCNP model

7.4.3 Comparison of Results and Discussion

The results of the neutron foil activation calculations and the corresponding experimental data are presented in Table (7.4.3.1).

Method	Neutron Detector	Activation, s^{-1}	Relative Error, $r[R]$
Experiment	Au	$1.02 \cdot 10^{-13}$	0.02
Forward		$1.1769 \cdot 10^{-13}$	0.0168
Midway		$1.1027 \cdot 10^{-13}$	0.0128
Experiment	Cu	$4.05 \cdot 10^{-15}$	0.12
Forward		$4.3877 \cdot 10^{-15}$	0.0173
Midway		$3.9923 \cdot 10^{-15}$	0.0069
Experiment	Mn	$1.27 \cdot 10^{-14}$	0.04
Forward		$1.4241 \cdot 10^{-14}$	0.0135
Midway		$1.3526 \cdot 10^{-14}$	0.0067
Experiment	Ni	$2.00 \cdot 10^{-19}$	0.10
Forward		$8.2234 \cdot 10^{-20}$	0.6596
Midway		$1.1591 \cdot 10^{-19}$	0.05

Table 7.4.3.1. Foil Activation Rates in the BNCT Facility.

The results of the reference calculations differ from the results of the original study (Vroegindeweij, 1996), because a different cross section library was used. The purpose of the current study was rather to compare calculational results due to different methods for the same problem, but we still expected reasonable agreement with the experimental data. Still, the differences between both autonomous forward or the midway results and the experimental data are in general of the same order of magnitude as in the original study. Further, it is observed, that all 4 midway estimates agree with the results of the reference calculations within the estimated standard deviation.

Neutron energy distributions calculated for the Ni detector in autonomous forward and midway MCNP modes in 5 energy groups were also compared. The results are presented in Table (7.4.3.2). It is observed, that the results in the thermal and two following intermediate groups well agree within the

limits of two standard deviations. At the same time, the results cannot be compared for the two fast groups: the autonomous forward estimates remain unreliable after running for almost 50 CPU hours. For these two groups the midway method provides the estimates with statistical uncertainties lower than 10% already after running the problem for 2 CPU hours. These relatively small uncertainties and the agreement between the results for the thermal and intermediate three groups form the basis for confidence in the reliability of the midway results for the fast two groups as well.

Method	Group Flux, $\text{cm}^{-2}\text{s}^{-1}$ (Relative Error, $r[R]$)					CPU Time, min
Group Energy Boundaries, MeV	$139 \cdot 10^{-10}$	$4.13 \cdot 10^{-7}$	0.0248	0.823	1.35	
	- $4.13 \cdot 10^{-10}$	- 0.00248	- 0.823	- 1.35	- 17	
Forward	$1.094 \cdot 10^9$ (0.013)	$1.24 \cdot 10^7$ (0.068)	$2.11 \cdot 10^6$ (0.14)	$4.63 \cdot 10^5$ (0.38)	$2.11 \cdot 10^5$ (0.80)	2837
Midway	$1.109 \cdot 10^9$ (0.021)	$1.43 \cdot 10^7$ (0.017)	$2.94 \cdot 10^6$ (0.040)	$5.60 \cdot 10^5$ (0.096)	$6.55 \cdot 10^5$ (0.080)	316

Table 7.4.3.2. Group Neutron Fluxes in a Ni Neutron Detector in the BNCT facility.

The efficiencies of the autonomous forward and midway calculations of total neutron flux at the positions of the Ni and Au detectors and the total photon flux at the positions of Au and Mn detectors were compared. The results of the comparison are presented in Tables (7.4.3.3), (7.4.3.4), (7.4.3.5) and (7.4.3.6), respectively.

Method	Number of Histories		Total Flux, $\text{cm}^{-2}\text{s}^{-1}$	Relative Error, $r[R]$	CPU Time, T (min)	FOM (r^2T) ⁻¹ , min^{-1}
	Forward	Adjoint				
Forward	14 500 000	-	$1.1096 \cdot 10^9$	0.0116	3745	2.0
Midway	2 500 000	5 000 000	$1.1088 \cdot 10^9$	0.035	325	8.0

Table 7.4.3.3. Monte Carlo Efficiencies for Ni Neutron Flux Detector

Method	Number of Histories		Total Flux, $\text{cm}^{-2}\text{s}^{-1}$	Relative Error, $r[R]$	CPU Time, T (min)	FOM $(r^2T)^{-1}$, min^{-1}
	Forward	Adjoint				
Forward	14 500 000	-	1.2955×10^9	0.0170	3745	0.93
Midway	2 500 000	5 000 000	1.3241×10^9	0.0157	325	12.48

Table 7.4.3.4. Monte Carlo Efficiencies for Au Neutron Flux Detector

Method	Number of Histories		Total Flux, $\text{cm}^{-2}\text{s}^{-1}$	Relative Error, $r[R]$	CPU Time, T (min)	FOM $(r^2T)^{-1}$, min^{-1}
	Forward	Adjoint				
Forward	14 500 000	-	9.7469×10^7	0.0574	4771	0.064
Midway	2 500 000	5 000 000	1.0271×10^7	0.0328	274	3.39

Table 7.4.3.5. Monte Carlo Efficiencies for Photon Flux Detector at the position of the Au foil.

Method	Number of Histories		Total Flux, $\text{cm}^{-2}\text{s}^{-1}$	Relative Error, $r[R]$	CPU Time, T (min)	FOM $(r^2T)^{-1}$, min^{-1}
	Forward	Adjoint				
Forward	14 500 000	-	2.9576×10^7	0.0133	4771	0.11
Midway	2 500 000	5 000 000	2.6118×10^7	0.0492	278	1.49

Table 7.4.3.6. Monte Carlo efficiencies for Photon Flux Detector at the position of the Mn Foil.

Optimization of the reference problem with weight windows required considerable insight into the problem and expertise to use the MCNP weight-windows generator. In contrast, the midway calculations show that a significantly higher efficiency can be achieved with the help of the easy-to-implement midway calculation to ensure sufficient statistics of the results with significantly less calculational and preparatory workload and experience. Indeed, we observe, that the FOM numbers of the unoptimized midway calculations are 4 times higher for the neutron and 5 times higher for the photon detector than the numbers corresponding to the reference calculation optimized by weight windows. Coupling at the first reasonable midway surface after very simple relative workload optimization gave significant FOM improvement.

Chapter 8

General Conclusions

*"Life is the art of drawing sufficient conclusions
from insufficient premises."*

Samuel Butler

Notebooks (1912)

In this thesis the midway method for radiation detector response determination is developed, analyzed, applied to the Monte Carlo method of radiation transport, implemented in the general purpose Monte Carlo code MCNP, tested, validated against established benchmarks and applied to interpretation of experimental data.

The midway method is based on the general reciprocity theorem of the transport theory and on coupling of the forward and adjoint functions of particle densities at an intermediate surface between the source and detector domains. The midway formalism is ultimately tied together with the generalized contribution response theory. According to the midway response method the forward problem with the virtual forward surface source is replaced by the corresponding adjoint problem and subsequent adjoint response determination with this virtual source. The fundamental interconnection between the midway response determination form and the virtual boundary conditions is sufficiently demonstrated in the previous Chapters. The proven Statement of two exact solution redundancy is used to develop the supplementary to the midway method black absorber techniques. The formula of the midway response determination is developed within the transport theory with external sources and within the criticality theory. The theory is also developed for photons, which are generated at inelastic or capture neutron interactions. The midway surface is an arbitrary surface, which encloses either the source or the detector domain but never both. The latter condition is the only essential restriction of the midway theory, which limits midway surface choice possibilities in geometrical spaces of practical problems.

The attention was further drawn to development of the midway Monte Carlo method for radiation transport calculations. The discretization ap-

proximation was used to make Monte Carlo coupling workable. It is questionable whether this approach is the only one. The next-event surface estimator (Kawai and Hayashida, 1986) can appear to be a sufficient tool against theoretical singularities of the midway scoring. Another possible direction of research directed to overcome this problem is to turn to a randomization principle (Ermakov and Michailov, 1982). Additionally, future studies can be devoted to simultaneous utilization of the midway method with other variance reduction techniques.

The variance of the estimated detector response is derived and used in this research, but no attention is paid to variance of variance and other supplementary characteristics of the statistical simulation convergence.

The midway Monte Carlo method is implemented in the general purpose MCNP Monte Carlo code with relative ease. Many fruitful features of MCNP can be used together with the midway option, which confirms the artlessness of the midway Monte Carlo method.

The discussions also deal with the questions of optimal positioning of the midway surface and optimal ratio of forward to adjoint histories numbers. A number of useful Statements are developed, which can provide a user of the midway Monte Carlo method with guidelines for practical selection of these parameters. As it is also stressed earlier in the text, these Statements should by no means be considered as theorems, but rather as expressions of scientific expertise, intuition and familiarity of the author with the midway method. Still the Statements clarify the nature of the applicability and efficiency of the midway Monte Carlo method and the black absorber technique. Future research can be directed to study optimal sizes of the energy, position and direction meshes used for the midway coupling.

The midway Monte Carlo method is demonstrated to be very efficient in problems with deep penetration, problems with small source and detector domains and problems with complicated streaming paths, because both forward and adjoint particles need to penetrate only about half of the penetration distance and score at the large midway surface. Besides that, the midway calculations are usually additionally accelerated by one of the developed black absorber techniques, which allow to truncate a considerable part of the geometrical model in one (forward or adjoint) of the calculations.

The research included wide-ranging testing, benchmarking and application of the midway Monte Carlo method and the corresponding MCNP option against a number of problems aiming to verify the method and to promote it in the community of nuclear Monte Carlo users. The chosen tests cover different areas of the Monte Carlo method utilization: nuclear well logging, photon skyshine, boron neutron capture therapy, power distribution in a

nuclear reactor and reactor shielding. All the considered problems pose a difficult variance reduction challenge. The calculations were performed using existing variance reduction methods of MCNP and the midway method. The performed comparative analyses showed, that the midway method appears to be much more efficient than the standard techniques in overwhelming majority of the studied cases and can be recommended for use in many difficult variance reduction problems of neutral particle transport.

References

- Ao Q., "McLDL - A specific purpose Monte Carlo Code for Modelling the Response of Dual Spaced Gamma-Gamma Logging Tools," User's Guide, North Carolina State University, (1994).
- Ao Q., R.P. Gardner and K.Vergheze, "A Combined Weight Window and Biasing Approach Based on a Subspace Importance Map in the Monte Carlo Simulation of Gamma-Gamma Lithodensity Logging Tool Responses with the Revised McLDL Code," *Nucl.Sci.Symp. and Medical Imaging Conference*, IEEE Conference Record, **2**, (1995).
- Bell G.I. and S.Glasstone, "Nuclear Reactor Theory," Litton Educational Publishing, New York, (1970).
- Booth T.E., "A Weight Window/Importance Generator for Monte Carlo Streaming Problems," *Proc. of the Sixth International Conference on Radiation Shielding*, (1983).
- Booth T.E., "A Sample Problem for Variance Reduction in MCNP," LA-10363-MS, Los Alamos National Laboratory (1985).
- Booth T.E., "The Intelligent Random Number Technique in MCNP," *Nucl. Sci. Eng.*, **100**, (1988).
- Booth T.E., "Analytic Score Distributions for a Spatially Continuous Tridirectional Monte Carlo Transport Problem," *Nucl. Sci. Eng.*, **122**, (1996).
- Brand P. H.van Dam, J.W. de Vries *et al.*, "Flux-, Power- and Butnrup Determination for Pool-Type Reactors," IRI-INT-130/131-71-01, Interuniversitair Reactor Institute, Delft, (1971).
- Briesmeister J.F., "MCNP - A General Monte Carlo Code for Neutron and Photon Transport, Version 4A," Los Alamos National Laboratory, LA-12625-M (1993).
- Bryson J.W., J.C.Lee and J.A.Hassberger, "Optimal Flux Map Generation Through Parameter Estimation Techniques", *Nucl. Sci. Eng.*, **114**, (1993).
- Brockhoff R.C. and J.S.Hendricks, "A New MCNP-TM Test Set," Los Alamos National Laboratory, LA-12839, (1994).
- Burn K.W., "Complete Optimization of Space/Energy Cell Importances with the DSA Cell Importance Model," *Ann. Nucl. Energy*, **19**, (1992).
- Case K.M. and P.F.Zweifel, " *Linear Transport Theory*," Addison-Wesley Publishing Co., Inc., (1967).

- Chucas S.J., M.Grimstone "The Acceleration Tehcniques Used in the Monte Carlo Code MCBEND," *Eight International Conference on Radiation Shielding*, Arlington, Texas, (1994).
- Chucas S., M.Grimstone, T.Shuttelworth, "Advances in the Monte Carlo Code MCBEND," *Topical Meeting on Radiation Protection & Shielding*, No. Flamouth, Massachusetts, (1996).
- Collins D.G., "Normalization of Forward and Adjoint MCNP Runs," Los Alamos National Laboratory internal memorandum, DGC-87-187 (1987).
- Ermakov S.M. and Michailov G.A., "*Statistical Modeling*", Science, Moscow, (1982).
- Foster R.A., R.C.Little, J.F. Briesmeister, J.S.Hendricks, "MCNP Capabilities for Nuclear Well Logging Calculations," *IEEE Transactions on Nuclear Science*, **37**, (1990).
- Fowler T.B., D.R.Vondy, G.W.Cunningham, "CITATION - Nuclear Reactor Analysis Code," TM-2469, Rev.2, Oak Ridge National Laboratory, Reactor Division (1971).
- Fröhner T.B., "Assignment of Uncertainties to scientific Data", *Proc. Inter. Conf. on the Reactor Physics and Reactor Computations*, Tel-Aviv, January 23-26, (1994).
- GertsI S.A.W., "A New Concept of Deep-Penetration Transport Calculations and Two New Forms of the Neutron Transport Equation," LA-6628-MS, Los Alamos Scientific Laboratory, (1976).
- GertsI S.A.W., "Comments on "The spatial channel theory applied tp reactor shielding analysis," *Nucl. Sci. Eng.*, **64**, (1977).
- Clark F.H., "The Exponential Transform as an Importance Sampling Device - A Review," ORNL-RSIC-14, Oak Ridge National Laboratory, (1966).
- Harrington B.V. and G.Constantine, "Analysis of Epithermal Neutron Beam Experiments at the HOFAR Reactor," *Nuclear Technology*, **109**, (1995).
- Hendricks J.S. and L.L.Carter, "Anisotropic Angle Biasing of Photons," *Nucl. Sci. Eng.*, **89**, (1985).
- Hensen G.E. and H.A.Sandmeier, "Neutron Penetration Factors Obtain by Using Adjoint Transport Calculations," *Nucl. Sci. Eng.*, **22**, (1965).
- Hoogenboom J.E., "*Adjoint Monte Carlo Methods In Neutron Transport Calculations*," Delft University Of Technology, Thesis, (1977).

Hoogenboom J.E., "A Practical Adjoint Monte Carlo Tehcnique for Fixed-Source and Eigenfunction Neutron Transport Problems," *Nucl. Sci. Eng.*, **79**, (1981).

John T.M. P.F.A. de Leege and J.E. Hoogenboom, "Resolving the Reactivity Discrepancy for the HOR Research Reactor," *Jahrestagung Kerntechnik'96*, Rosengarten, 21-23 May, (1996).

Kawai M., Y.Hayashida and H.Nishi, "Application of Forward and Adjoint Monte Carlo coupling Technique to Detector System Designs," *Progress in Nuclear Energy*, **24**, (1990).

Kawai M. and Y.Hayashida, "Development of General Next Event Surface Crossing Estimators for Monte Carlo Method," *Journal of Nuclear Science and Technology*, **23**, (1986).

Korobeinokov V.V. and V.I.Usanov, "*Coupling Methods in Problems of Radiation Transport*," Energoizdat, Moscow, (in Russian) (1994).

Koroluk B.S., "*Reference Book on Prability Theory and Mathematical Statistics*," Science, Moscow, (1985).

Kraakman R.W.A. and W.P.Voorbraak, "Power calibration and Fluence Rate Measurements," unpublished laboratory note FYS/RASA-83/03, ECN-Petten, (1982).

Laky P.G. and M.Tsoufanidis, "Neutron Fluence at the Pressure Vessel of a Pressurized Water Reactor Determined by the MCNP code," *Nucl. Sci. Eng.*, **121**, (1995).

Lee J.B., B.W.Lee and B.C.Lee, "Radiation Streaming Analysis in the Radial and Tangential Beam Tubes of a TRIGA Research Reactor Using MCNP and Comparison with Measurement," *Nucl. Sci. Eng.*, **121**, (1995).

Lewins J., "*Importance: The Adjoint Function*," Pergamon Press, New York, (1970).

Liu H.B. and R.M.Brugger, "Conceptual Designs of Epithermal Neutron Beams for Boron Neutron Capture Therapy from Low-Power Reactors," *Nucleare Technology*, **108**, (1994).

Liu H.B., "Design of Neutron Beams for Neutron Capture Therapy Using a 300-kW Slab TRIGA Reactor," *Nuclear Technology*, **109**, (1995).

Lux I. and L.Koblinger, *Monte Carlo Particle Transport Methods: Neutron and Photon Calculations*, CRC Press, Boca Ration, Florida, (1991).

Marcuk G.I. and V.V.Orlov, "*On Theory of Adjoint Functions*," *Neutron Physics*, Moscow, Gosatomisdat, (in Russian) (1961).

- Mickael M.W., " A Fast, Automated, Semideterministic Weight Windows Generator for MCNP," *Nucl. Sci. Eng.*, **119**, (1995).
- Nason R.R., J.K. Shultis, R.E.Faw and C.E. Clifford, "A Benchmark Gamma-Ray Skyshine Experiment," *Nucl. Sci. Eng.*, **79**, (1981).
- Redmond E.L., J.C.Yanch and O.K.Harling, "Monte Carlo Simulation of The Massachusetts Institute of Technology Research Reactor," *Nuclear Technology*, **106**, (1994).
- Sarkar P.K. and M.A.Prasad, "Prediction of statistical Error and Optimization of Biased Monte Carlo Transport calculations," *Nucl. Sci. Eng.*, **70**, (1979).
- Serov I.V. and J.E.Hoogenboom, "CONHOR code System for Determination of Power Distribution and Burnup for the HOR Reactor," IRI-131-93-008, Interfacultair Reactor Institute, Delft, (1993).
- Serov I.V. and J.E.Hoogenboom, "A General Technique for Confluence of Calculational and Experimental Information with Application to Power Distribution Determination," *Proc. Inter. Conf. on the Reactor Physics and Reactor Computations*, Tel-Aviv, January 23-26, (1994).
- Serov I.V. and J.E.Hoogenboom, "A Forward-Adjoint Midway Coupling Method in MCNP," *Proc. of the 9th Topical Meeting*, Moscow, MEPhI, h/c "Volga", September 4-8, (1995).
- Serov I.V. and J.E.Hoogenboom, "Confluence of Calculational and Experimental Information for Determination of Power Distribution and Burnup," *Ann. Nucl. Energy*, **23**, (1996a).
- Serov I.V., T.M. John and J.E. Hoogenboom, "Midway Forward-Adjoint Coupling Method in MCNP Neutron and Photon Monte Carlo Detection," *submitted to Nucl. Sci. Eng.*, (1996b).
- Serov I.V., T.M. John and J.E.Hoogenboom, "Validation of a New Midway Forward-adjoint Coupling Option in MCNP against the Sky-Shine Benchmark," *Proc. Inter. Conf. on the Physics of Reactors PHYSOR96*, Mito, (1996c).
- Serov I.V., T.M. John and J.E.Hoogenboom, "Midway against Oil Well Porosity Tool Model Benchmark," *submitted to Applied Radiation and Isotopes (incorporating Nuclear Geophysics)*, (1996d).
- Serov I.V., C. Vroegindewij, T.M. John and J.E. Hoogenboom, " Efficient Calculation of a BNCT facility by a Midway Coupling Option in MCNP," *submitted to Ann.Nucl. Energy*, (1996e).

Serov I.V., P.F.A de Leege, H. Gibcus, "Improved HOR fuel management by flux measurement data feedback, " *Proc. ENS-conference on Research Reactor Fuel Management RRFM*, Brugge (1996f).

Soran P.D., "Nuclear Modeling Tehcniques and Nuclear Data," *IEEE Trans. Nucl. Sci.*, **35**, (1987).

Spanier J., "An Analytic Approach to Variance Reduction," *SIAM J. Appl. Math.*, **18**, (1970).

Uhlo J.J., "Use of Multidimensional Transport Methodology on Nuclear Well Logging Problems," *Nucl. Sci. Eng.*, **92**, (1986).

Ussachoff L.M., *Int. Conf. Peaceful Uses Atomic Energy*, **5**, United Nations, New York, (1955).

Vroegindewij C., F.Stecher-Rasmussen and R. Huiskamp, "A Thermal Neutron Facility for Radiobiological Studies", *submitted to Ann.Nucl.Energy*, (1996).

Wagner J.C., E.L.Redmond II, S.P.Palmtag and J.S.Hendricks, "MCNP: Multigroup/Adjoint Capabilities", Los Alamos National Laboratory Report LA-12704, (1994).

Whalen D.J., D.E.Hollowell and J.S.Hendricks, "MCNP: Photon Benchmark Problems," Los Alamos National Laboratory, LA-12196, (1991).

Wheeler F.J. and D.W. Nigg, "Thee-Dimensional Radiation Dose Distribution Analysis for Boron Neutron Capture Therapy," *Nucl. Sci. Eng.*, **110**, (1992).

Williams M.L. and W.W. Engle, "The Concept of Spatial Channel Theory Applied to Reactor Shielding Analysis", *Nucl. Sci. Eng.*, **62**, (1977).

Williams M.L., "Response to "Comments on the concept of spatial channel theory applied to reactor shielding analysis," *Nucl. Sci. Eng.*, **35**, (1980).

Williams M.L., "Generalized Contributon Response Theory," *Nucl. Sci. Eng.*, **108**, (1991).

List of Publications

Serov I.V. and J.E.Hoogenboom, "CONHOR code System for Determination of Power Distribution and Burnup for the HOR Reactor," IRI-131-93-008, Interfacultair Reactor Institute, Delft, (1993).

Serov I.V. and J.E.Hoogenboom, "A General Technique for Confluence of Calculational and Experimental Information with Application to Power Distribution Determination," *Proc. Inter. Conf. on the Reactor Physics and Reactor Computations*, Tel-Aviv, January 23-26, (1994).

Serov I.V. and J.E.Hoogenboom, "A Forward-Adjoint Midway Coupling Method in MCNP," *Proc. of the 9th Topical Meeting*, Moscow, MEPhI, h/c "Volga", September 4-8, (1995).

Serov I.V. and J.E.Hoogenboom, "Confluence of Calculational and Experimental Information for Determination of Power Distribution and Burnup," *Ann. Nucl. Energy*, **23**, (1996a).

Serov I.V., T.M. John and J.E. Hoogenboom, "Midway Forward-Adjoint Coupling Method in MCNP Neutron and Photon Monte Carlo Detection," *submitted to Nucl. Sci. Eng.*, (1996b).

Serov I.V., T.M. John and J.E.Hoogenboom, "Validation of a New Midway Forward-adjoint Coupling Option in MCNP against the Sky-Shine Benchmark," *Proc. Inter. Conf. on the Physics of Reactors PHYSOR96*, Mito, (1996c).

Serov I.V., T.M. John and J.E.Hoogenboom, "Midway against Oil Well Porosity Tool Model Benchmark," *submitted to Applied Radiation and Isotopes (incorporating Nuclear Geophysics)*, (1996d).

Serov I.V., C. Vroegindewij, T.M. John and J.E. Hoogenboom, "Efficient Calculation of a BNCT facility by a Midway Coupling Option in MCNP," *submitted to Ann. Nucl. Energy*, (1996e).

Serov I.V., P.F.A de Leege, H. Gibcus, "Improved HOR fuel management by flux measurement data feedback," *Proc. ENS-conference on Research Reactor Fuel Management RRFM*, Brugge (1996f).

J.E.Hoogenboom, P.F. de Leege, I.V.Serov, V.A.Khotylev, "Software Support for the HOR Research Reactor Operation," *Proc. of the 9th Topical Meeting*, Moscow, MEPhI, h/c "Volga", September 4-8, (1995).

Samenvatting

In dit proefschrift is de midwaymethode voor bepaling van stralingsdetectorresponsies ontwikkeld, geanalyseerd, toegepast op de Monte-Carlomethode, geïmplementeerd in het MCNP Monte-Carloprogramma, getest, gevalideerd tegen bestaande benchmarkproblemen en toegepast voor interpretatie van experimentele gegevens.

De midwaymethode is gebaseerd op het algemene theorema van reciprociteit en op koppeling van de voorwaartse en geadjungeerde deeltjesverdelingsfuncties. De koppeling vindt plaats op een tussen de bron en detector liggend oppervlak. Het midwayformalisme is essentieel verbonden aan de algemene contributontheorie. Volgens de midwaymethode wordt het voorwaartse probleem met een virtuele bron op het midwayoppervlak door een geadjungeerd probleem vervangen. De detectorresponsie wordt dan in het geadjungeerde probleem op dit oppervlak bepaald. De fundamentele relatie tussen de midwayvorm van de responsiebepaling en virtuele randvoorwaarden wordt afdoende gedemonstreerd. De bewezen overtolligheidsstelling van twee exacte voorwaartse en geadjungeerde oplossingen wordt gebruikt om aanvullende zwarte-absorbertechnieken te ontwikkelen. De formule voor de midwayresponsiebepaling is ook voor de kritikaliteitstheorie ontwikkeld. Daarnaast is de midwayformule ontwikkeld voor het geval van detectie van fotonen, die bij inelastische verstrooiing of ontvangst van neutronen ontstaan. In alle gevallen is het midwayoppervlak een willekeurig oppervlak, dat of de bron of de detector, maar nooit beide omsluit. De laatste voorwaarde is de enige essentiële restrictie van de midwaytheorie, die de keuzen van midwayoppervlakken in de geometrische ruimte van het probleem beperkt.

Verder is aandacht gegeven aan ontwikkeling van de midway Monte Carlo methode. Een discretisatiebenadering wordt gebruikt voor de koppeling van voorwaartse en geadjungeerde Monte Carlo simulatieprocessen. De midway Monte-Carlomethode is geïmplementeerd in het MCNP Monte-Carloprogramma. De gemiddelde waarde van de midwaydetectorresponsie wordt met behulp van MCNP samen met de relatieve statistische fout en een speciaal efficiëntiemaatstafgetal - figure of merit - bepaald.

Kwesties van optimale positionering van het midwayoppervlak en optimale verhouding tussen aantallen van gesimuleerde voorwaartse en geadjungeerde deeltjes worden uitgebreid besproken. Een aantal stellingen wordt

voorgesteld, die enige leidraad aan een gebruiker van de midwaymethode kunnen geven.

In problemen met diepe penetratie, kleine bronnen en detectoren, en complexe stromingspaden is de midwaymethode om twee redenen aantrekkelijk gebleken. De eerste is dat de afstand die de gesimuleerde deeltjes moeten afleggen circa twee keer minder is dan de gehele afstand tussen de bron en de detector. De tweede reden is dat beide soorten deeltjes op een relatief groot midwayoppervlak scoren. Daarnaast worden de midwayberekeningen gewoonlijk door het gebruik van één van de zwarte-absorbertechnieken nog extra versneld. Volgens deze technieken wordt een aanzienlijke deel van de geometrie in één (voorwaartse of geadjungeerde) van de berekeningen beknot.

Het onderzoek sluit een brede scala in van testen, benchmarkproblemen en toepassingen van de midway Monte-Carlomethode en de midwayoptie van MCNP tegen een aantal problemen. De doelstelling is geweest om de methode te verifiëren en te promoten in een gemeenschap van gebruikers van de nucleaire Monte-Carlomethode. De gekozen testen bestrijken verschillende gebruiksterreinen van Monte Carlo: nucleaire oilbronlogging, fotonenskyshine-experimenten, boronneutronenvangsttherapie, vermogensverdeling in een kernreactor en reactorafscherming. Alle beschouwde problemen stellen moeilijke variantiereductie-eisen. De berekeningen werden uitgevoerd met behulp van standaard MCNP variantiereductiemethoden en eveneens met de midwaymethode. De uitgevoerde vergelijkingsanalyses laten zien dat in overgrote meerderheid van de bestudeerde gevallen de midwaymethode veel efficiënter dan de standaardtechnieken blijkt te zijn. Voor veel moeilijke variantiereductieproblemen van verspreiding van neutrale deeltjes kan de methode worden aanbevolen.

Dankwoord

Bij deze wil ik alle mensen bedanken die op één of andere wijze hebben bijgedragen aan de totstandkoming van dit proefschrift. Het verrichten van dit onderzoek valt samen met mijn eerste jaren in Nederland, het land waar ik zo ontzettend veel steun heb gekregen, die wellicht in een dubbel-zo-dik boek niet te beschrijven is. Ik zal in dit dankwoord geen namen noemen, maar wel de plaatsen in Nederland, die voor mij een bijzondere betekenis hebben: Aalten, Almelo, Amstelveen, Amsterdam, Arnhem, Barlo, Bolsward, Den Haag, Delft, Doetinchem, Harlingen, Hilversum, Lichtenvoorde, Petten, Pijnacker, Rijswijk, Rotterdam, Terborg, Utrecht, Velp, Westzaan en Winterswijk. De mensen aan wie ik dank verschuldigd ben zullen zich achter de namen van deze plaatsen gemakkelijk herkennen.

De volgende Russische plaatsen, waarvan ik de verbintenis met het proefschrift heel duidelijk zie, noem ik hier graag: Leningrad, Moskou, Shatura, Smolensk, Troitsk en "Volga". Ook plaatsen in andere werelddelen hebben een rol gespeeld, namelijk Jeruzalem, Los Alamos, Mito-city en Tel-Aviv.

In het bijzonder en in directe verbintenis met het proefschrift bedank ik mijn Nederlandse vader Ir. Klaas Joseph, mijn promotoren, leraren en begeleiders Prof.dr.ir. Hugo van Dam en Dr.ir. Eduard Hoogenboom, mijn wetenschappelijke collega Dr. John, de computerexpert Ir. Piet de Leege en de secretaresses van onze afdeling, Riny Purmer en Sonja Jobse.

Ik wil ook mijn ouders bedanken voor mijn opvoeding en opleiding. Zonder mijn geliefde Elena zou ik nooit hebben kunnen promoveren.

Curriculum Vitae

De auteur werd op 10 oktober 1966 geboren te oude russische stad Smolensk. Hij heeft in 1989 met lof afgestudeerd in de kernreactorfysica aan Moscow Engineering Physics Institute. Na twee jaar gewerkt te hebben aan een Kurchatov Institute of Atomic Energy te Moscow is hij naar Nederland geëmigreerd. In dienst van de TU Delft heeft hij zich bezig gehouden met ontwikkeling van mathematische en statistische methoden voor computermodellering en analyses van neutronen- en fotonenvelden in diverse media. Aan in dit proefschrift beschreven onderzoek heeft hij sinds het begin 1994 gewerkt.